

---

JULIUS-MAXIMILIANS-UNIVERSITÄT WÜRZBURG  
FAKULTÄT FÜR BIOLOGIE  
LEHRSTUHL FÜR MIKROBIOLOGIE

---

**Epigenetic switch induced by MYC in Non-Small-Cell Lung Cancer**

---

**Durch MYC induzierte epigenetische Veränderung im Nichtkleinzelligen  
Bronchialkarzinom**



Dissertation  
zur Erlangung des naturwissenschaftlichen Doktorgrades  
der Julius-Maximilians-Universität Würzburg

vorgelegt von  
**Inês Sofia Cardoso e Castro**  
geboren in Paredes (Portugal)

Würzburg, 2012

Eingereicht am:

Mitglieder der Prüfungskommission:

Vorsitzende:

1. Gutachter: Prof. Dr. T. Rudel

2. Gutachter: PD Dr. R. Hock

Tag des Prüfungskolloquiums:

Doktorurkunde ausgehändigt am:

I hereby declare that my thesis entitled:

**Epigenetic switch induced by MYC in Non-Small-Cell Lung Cancer**

is the result of my own work. I did not receive any help or support from commercial consultants. All sources and / or materials applied are listed and specified in the thesis.

Furthermore, I confirm that this thesis has not yet been submitted as part of another examination process neither in identical nor in similar form.

Würzburg, 12.12.2012

Inês Castro

## Acknowledgements

During the last years, many are those that in several ways stood by me and contributed to make this thesis possible. To you, maybe as much as to myself, I owe the success of this journey. Any acknowledgement list will be undoubtedly defaulted, however to make it is unavoidable.

*To Professor Ulf R. Rapp,*

Thank you for giving me the opportunity to work on this project and bring me into the fascinating world of oncobiology.

*To Professor Thomas Rudel,*

Thank you for taking over the supervision of this work. Thank you for everything else. Words cannot express how thankful I am for your support during the last 3 years.

*To Professor Robert Hock,*

Thank you for your agreement in being a part of my PhD committee.

*To Dr. Achim Breiling,*

Thank you for the fruitful collaboration in the epigenetic studies.

*To Dr. Tobias Müller,*

Thank you for the great statistical analysis of tons of data.

*To Dr. Joachim Fensterle,*

Thank you for your help with the transplantation experiments.

*To Dr. Fatih Ceteci and Simone Hausmann,*

Thank you for your help with the histological analysis.

*To Mrs. Rapp,*

Thank you for all your support!

*To all my colleagues,*

Thank you for the support and nice time at MSZ and at the Department of Microbiology. A special gratitude word goes to Birgit Bergmann.

*To Katharina Lütkenhaus and Claudia Sibilski,*

Thank you for being the colleagues that anyone wishes. Those colleagues that you bring home after closing the door of the lab!

*To Ana, Ni, Belinha and Clarinha*

Thank you girls! You make my life easier, colorful and loud, really loud.

*To my parents,*

Thank you Mum for teaching me love and also for bringing Science into my life. Thank you Dad for all your care, love, patience and wisdom.

*To my sisters Cristiana and Catarina,*

Thank you for taking over the hard job of being a Mum of a teenager, even when you were not grown up yourselves. You did it great. Thank you also for being my mates!

*To my nephews Afonso, Bernardo, Constança and Carolina,*

Thank you for making me believe that the future is a better place!

*To Peter,*

Thank you for all your love.

---

## Table of Contents

|  |           |
|--|-----------|
| <b>1. Abstract.....</b>                                | <b>5</b>  |
| <b>1. Zusammenfassung.....</b>                         | <b>6</b>  |
| <b>2. Introduction.....</b>                            | <b>8</b>  |
| 2.1. Lung development .....                            | 8         |
| 2.2. Cancer.....                                       | 10        |
| 2.3. Lung cancer – NSCLC .....                         | 11        |
| 2.4. MYC.....  | 13        |
| 2.4.1. MYC protein family .....                        | 13        |
| 2.4.2. Cooperation partners .....                      | 15        |
| 2.5. Cancer stem cell hypothesis .....                 | 16        |
| 2.6. Metastasis .....                                  | 18        |
| 2.7. GATA family.....                                  | 21        |
| 2.8. Epigenetic changes in cancer.....                 | 23        |
| 2.9. Previous work and aim of the project.....         | 26        |
| <b>3. Materials and methods .....</b>                  | <b>28</b> |
| 3.1. Materials .....                                   | 28        |
| 3.1.1. Instruments .....                               | 28        |
| 3.1.2. Chemical reagents.....                          | 29        |
| 3.1.3. Buffers and solutions .....                     | 31        |
| 3.1.4. Enzymes .....                                   | 31        |
| 3.1.5. Consumable material .....                       | 32        |
| 3.1.6. Antibodies .....                                | 32        |
| 3.1.7. Plasmids .....                                  | 33        |
| 3.1.8. Oligonucleotides for genotyping .....           | 34        |
| 3.1.9. Oligonucleotides for cloning .....              | 34        |
| 3.1.10. Oligonucleotides for Real-Time PCR.....        | 35        |
| 3.1.11. Oligonucleotides for bisulfite sequencing..... | 36        |
| 3.1.12. Kits .....                                     | 36        |

---

|  |    |
|--|----|
| 3.1.13. Bacterial strains .....                                    | 37 |
| 3.1.14. Cell lines .....   | 37 |
| 3.1.15. Mouse lines .....  | 38 |
| 3.1.16. Media and additives .....                                  | 38 |
| 3.1.17. Eukaryotic cell culture .....                              | 39 |
| 3.2. Methods .....   | 39 |
| 3.2.1. Bacterial manipulation.....                                 | 39 |
| 3.2.2. Analysis of DNA-molecules .....                             | 40 |
| 3.2.3. Polymerase Chain Reaction (PCR).....                        | 41 |
| 3.2.4. Enzymatic manipulation of DNA.....                          | 41 |
| 3.2.5. Isolation of RNA.....                                       | 42 |
| 3.2.6. Real-Time PCR .....   | 43 |
| 3.2.7. Bisulfite sequencing .....                                  | 44 |
| 3.2.8. Array-based DNA methylation profiling (Infinium-chip) ..... | 45 |
| 3.2.9. Chromatin immunoprecipitation.....                          | 46 |
| 3.2.10. Freezing cell lines .....                                  | 46 |
| 3.2.11. Transfection of eukaryotic cells using lipofectamine ..... | 47 |
| 3.2.12. Viral infection of cell lines.....                         | 47 |
| 3.2.13. Soft agar assay.....                                       | 47 |
| 3.2.14. Immunocytochemistry.....                                   | 48 |
| 3.2.15. Luciferase reporter assay .....                            | 48 |
| 3.2.16. Proliferation assessment of adherent cells .....           | 49 |
| 3.2.17. Wound healing assay.....                                   | 49 |
| 3.2.18. Animal experiments .....                                   | 49 |
| 3.2.19. Preparation of tissue-sections.....                        | 50 |
| 3.2.20. Hematoxylin and eosin (HE) staining .....                  | 50 |
| 3.2.21. Immunohistochemistry.....                                  | 50 |
| 3.2.22. Genotyping of transgenic mice .....                        | 51 |
| 3.2.23. Transplantation experiments .....                          | 51 |
| 3.2.24. In vivo bioluminescence imaging.....                       | 52 |
| 3.3. Statistical Analysis .....                                    | 52 |

---

|   |           |
|---|-----------|
| <b>4. Results</b> .....   | <b>54</b> |
| 4.1. MYC expression in NSCLC tumor cells induces cell type change and metastasis formation .....                  | 54        |
| 4.2. MYC induces GATA4 expression in NSCLC.....   | 57        |
| 4.3. GATA4 knock-down in MYC expressing NSCLC cells inhibits the metastatic potential induced by MYC .....        | 60        |
| 4.4. MYC induces changes in GATA4 promoter activity .....   | 62        |
| 4.5. MYC induces GATA4 promoter demethylation in c-MYC/KRas-mutant typeII-pneumocytes .....                       | 64        |
| 4.6. MYC induces GATA4 promoter demethylation in human NSCLC cells.....   | 65        |
| 4.7. Epigenetic landscape of the GATA4 promoter changes upon MYC expression .....                                 | 69        |
| 4.8. MYC leads to changes in protein occupancy at the GATA4 promoter region.....                                  | 71        |
| 4.9. MAZ displacement in A549 cells leads to GATA4 expression .....   | 73        |
| 4.10. Histone deacetylase inhibition in MYC expressing cells does not lead to an increase of GATA4 activity ..... | 74        |
| 4.11. Methylation profile of A549 cells changes upon MYC expression .....   | 75        |
| 4.12. Epigenetic changes induced by MYC in A549 cells alter the expression profile .....                          | 76        |
| 4.13. Overexpression of GATA4 in A549 cells changes their anchorage independent growth ability .....              | 79        |
| 4.14. GATA4 expressing A549 cells show a decrease in their migration ability.....                                 | 81        |
| 4.15. GATA4 expression in A549 cells leads to accelerated tumor growth <i>in vivo</i> .....                       | 82        |
| 4.16. A549 cells show downregulation of angiogenic factors upon GATA4 expression .....                            | 84        |
| 4.17. A549 cells show downregulation of pluripotent stem cells markers, but not of CD30.....                      | 85        |
| <b>5. Discussion</b> .....  | <b>87</b> |
| 5.1. MYC induces a phenotypic and lineage switch in NSCLC.....  | 87        |
| 5.2. MYC drives GATA4 expression in human NSCLC cells.....  | 89        |
| 5.3. MYC induces GATA4 promoter demethylation .....   | 90        |
| 5.4. MYC induces the enrichment of active histone marks and changes protein occupancy at the GATA4 promoter ..... | 93        |
| 5.5. MYC induces changes in protein occupancy at GATA4 promoter.....  | 95        |
| 5.6. Epigenetic changes induced by MYC are genome-wide.....   | 96        |
| 5.7. GATA4 alone is not enough to induce angiogenesis <i>in vitro</i> .....                                       | 103       |

|  |            |
|--|------------|
| 5.8. GATA4 induces accelerated tumor growth <i>in vivo</i> ..... | 106        |
| 5.9. GATA4 might induce pluripotency in NSCLC cells.....         | 107        |
| <b>6. References.....</b>  | <b>109</b> |
| <b>7. Appendix.....</b>  | <b>122</b> |
| 7.1. List of abbreviations .....                                 | 122        |
| <b>Curriculum Vitae.....</b>                                     | <b>125</b> |



## 1. Abstract

Non–Small-Cell Lung Cancer (NSCLC) is the most frequent human lung cancer and a major cause of death due to its high rate of metastasis<sup>1</sup>. These facts emphasize the urgent need for the investigation of new targets for anti-metastatic therapy.

Up to now a number of genes and gene products have been identified that positively or negatively affect the probability of established human tumor cell lines to metastasize<sup>2</sup>. Previously, together with the group of Professor Ulf Rapp, we have described the first conditional mouse model for metastasis of NSCLC and identified a gene, *c-MYC*, that is able to orchestrate all steps of this process. We could identify potential markers for detection of metastasis and highlighted GATA4, which is exclusively expressed during lung development, as a target for future therapeutic intervention<sup>2</sup>. However, the mechanism underlying this metastatic conversion remained to be identified, and was therefore the focus of the present work.

Here, GATA4 is identified as a MYC target in the development of metastasis and epigenetic alterations at the *GATA4* promoter level are shown after MYC expression in NSCLC *in vivo* and *in vitro*. Such alterations include site-specific demethylation that accompanies the displacement of the MYC-associated zinc finger protein (MAZ) from the *GATA4* promoter, which leads to GATA4 expression. Histone modification analysis of the *GATA4* promoter revealed a switch from repressive histone marks to active histone marks after MYC binding, which corresponds to active GATA4 expression. This work identifies a novel epigenetic mechanism by which MYC activates GATA4 leading to metastasis in NSCLC, suggesting novel potential targets for the development of anti-metastatic therapy.

## 1. Zusammenfassung

Das nichtkleinzellige Bronchialkarzinom (Non-Small-Cell Lung Cancer/NSCLC) ist die häufigste Form des Lungenkrebs und ist aufgrund seiner hohen Metastasierungsrate für die meisten krebsbedingten Todesfälle verantwortlich<sup>1</sup>.

Bisher konnte eine Vielzahl von Genen und Genprodukten identifiziert werden, die einen Einfluss auf das Metastasierungspotenzial von humanen Tumorzelllinien *in vitro* haben<sup>2</sup>. Vor kurzem gelang es uns unter der Leitung von Prof. Ulf R. Rapp das erste konditionelle Modell der Metastasierung von NSCLC zu beschreiben. Wir identifizierten u.a. das Gen c-MYC, welches in der Lage ist, in alle Schritte des Prozesses manipulierend einzugreifen. Im Rahmen dieser Arbeit konnten wir potentielle Marker zur Detektion der Metastasierung identifizieren. Unser Hauptaugenmerk lag dabei auf GATA4, ein Gen, das nur während der Lungenentwicklung exprimiert wird. Als potentielles Ziel für spätere therapeutische Eingriffe erscheint es daher besonders geeignet<sup>2</sup>. Die der Metastasierung zugrunde liegenden Mechanismen sind bisher weitestgehend ungeklärt und stellen daher einen Fokus dieser Arbeit dar.

Im Rahmen der vorliegenden Arbeit wurde GATA4 als ein von MYC regulierter Faktor identifiziert, der an der Entwicklung von Metastasen beteiligt ist. Epigenetische Veränderungen am GATA4-Promotor nach der Expression von MYC konnten sowohl *in vitro* als auch *in vivo* nachgewiesen werden. Die Veränderungen beinhalten ortsspezifische Methylierungen, die einhergehen mit der Dislokation des MYC-assoziierten zinc finger protein (MAZ), die zur Expression von GATA4 führt. Die Analyse der Histon-Modifikationen am GATA4-Promotor ergab, dass nach der Bindung von MYC ein Wechsel von reprimierenden Histon-Markierungen zu aktiven stattfindet, der mit der GATA4-Expression korreliert. Im Rahmen dieser Arbeit

konnte also ein neuartiger epigenetischer Mechanismus identifiziert werden, mit dem MYC GATA4 aktiviert und auf diese Weise zur Metastasenbildung bei NSCLC führt. Gleichzeitig wurden dadurch neue potentielle Zielstrukturen für die Entwicklung von anti-metastasierenden Therapeutika gefunden.

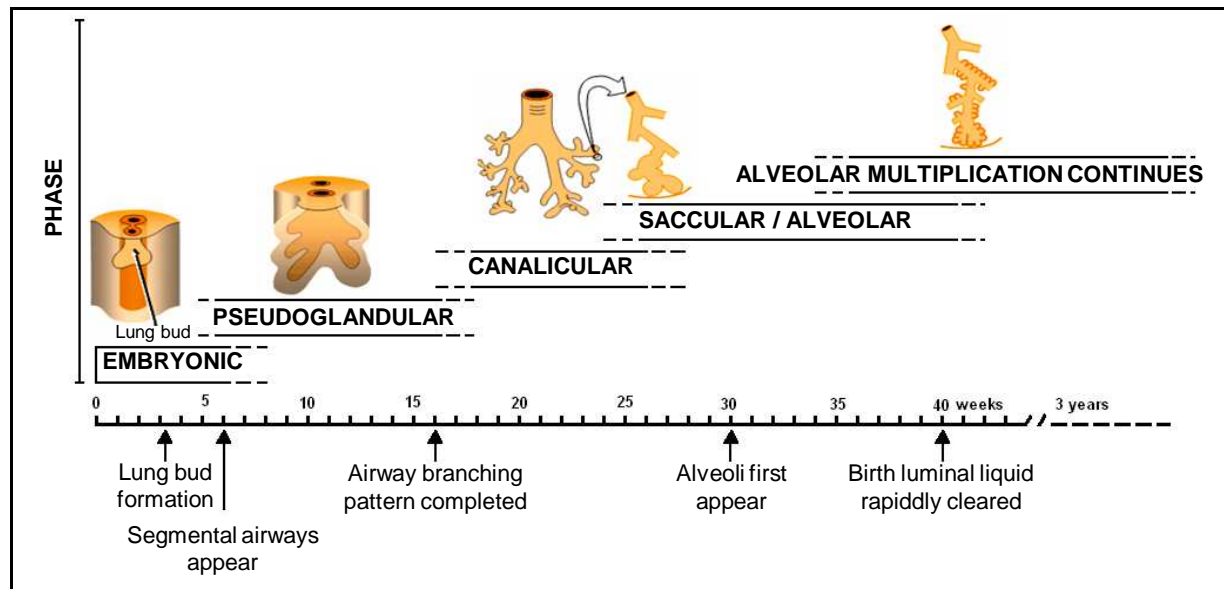
## 2. Introduction

### 2.1. Lung development

The complex process of mammalian lung development includes lung airway branching morphogenesis and alveolarization, together with angiogenesis and vasculogenesis<sup>3</sup>. This process is orchestrated by finely integrated and mutually regulated networks of transcriptional factors, growth factors, matrix components and physical forces<sup>3</sup>.

The respiratory system arises from the ventral foregut endoderm<sup>4</sup>. Following the embryonic period, which in humans corresponds to the first few weeks after fertilization, four overlapping phases of lung development are recognized: pseudoglandular, canalicular, saccular and alveolar<sup>5</sup> (Fig. 2.1). In the embryonic phase, lung appears as evaginations of the primitive gut which invade the surrounding mesenchyma. Two buds are formed on the left side and three on the right, representing the precursors of the mainstem bronchi and lobes in the adult lung<sup>6</sup>. In the pseudoglandular phase, progressive and complete division of the airways into smaller branches occurs and the diaphragm is formed<sup>6</sup>. This is followed by the canalicular phase where vascularization of peripheral mesenchyme rapidly increases the capillaries move into close contact with the surface epithelium, and connective tissue components are reduced to a minimum<sup>5</sup>. During saccular phase additional respiratory airways develop and the future respiratory units (acini) differentiate<sup>5</sup>. The epithelial cells differentiate into flat type I cells and larger type II. The latest cells secrete a mixture of lipids and proteins called surfactant during the final weeks of gestation which are essential to reduce the surface tension of the fluid, and have antimicrobial properties<sup>6</sup>. Finally in the alveolar phase, which lasts at least the first 3 years of

postnatal life alveolar formation commences, and alveoli multiply greatly in number up to a total of about 300 millions and reach a total surface area about 70 square meters<sup>6</sup>.



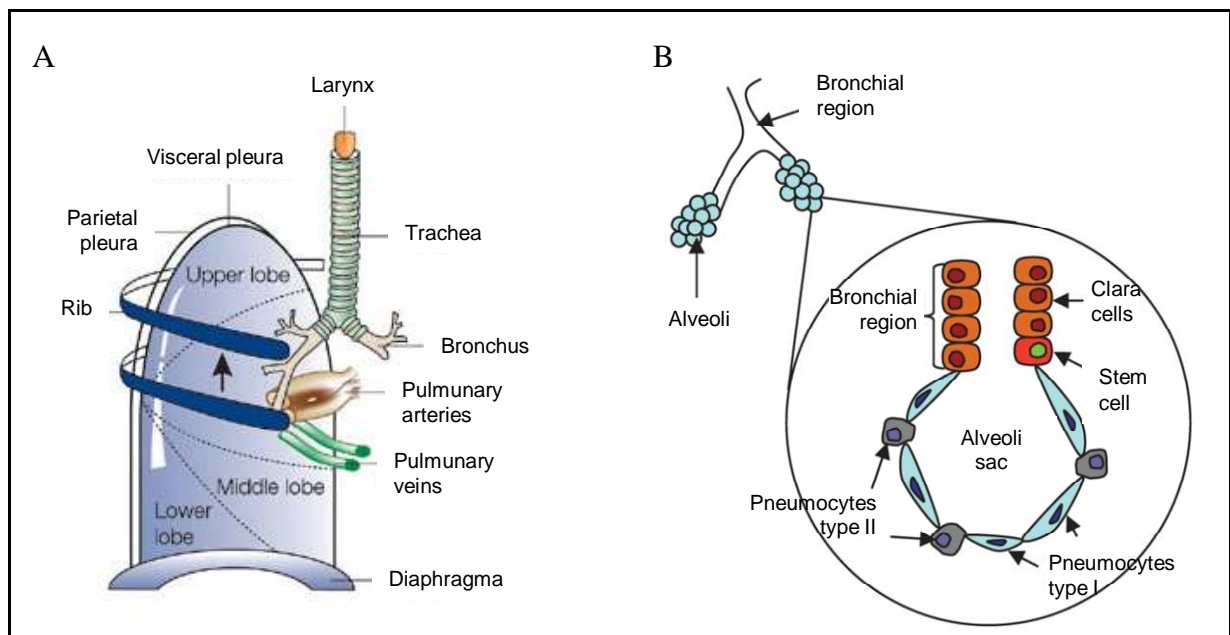
Modified from<sup>5</sup> and<sup>7</sup>

### Figure 2.1. Major events during lung development.

Lung formation starts at the third week of embryonic development and extends to at least the third year of postnatal life and is divided in 5 distinct stages: embryonic, pseudoglandular, canalicular, saccular and alveolar.

The adult lung is mainly comprised of numerous airways, alveolar ductal lumens and alveoli where the gas exchange of carbon dioxide and oxygen takes place, as well as alveolar septa and small pulmonary vessels<sup>8</sup> (Fig. 2.2.A). Nearly 50 distinct types of cells have been identified in the lungs. Endothelial and epithelial cells (pneumocytes) and an attenuated interstitial space form the barrier which separates the pulmonary capillaries from the alveolar air. Two types of pneumocytes can be found in alveoli (Fig. 2.2.B). The type I cells are very flat and cover most of the alveolar surface. The type II cells are more irregularly shaped and secrete surfactant proteins, like surfactant associated protein C, Sp-C, which are the precursors of the type I pneumocytes<sup>6,4</sup>.

Sp-C is also expressed by a rare cell population located at the bronchioalveolar duct junction, which also express CC10, a marker for clara cells. These cells are called bronchioalveolar stem cells (BASCs) and have been shown to be capable of self-renewal and differentiation and to contribute to both the alveolar and bronchiolar lineages<sup>9,10</sup>.



Modified from<sup>6</sup> and<sup>11</sup>

### Figure 2.2. Anatomy and cell populations of the lung.

(A) Gross anatomy of lung and thorax. (B) Alveolar structure and cell populations. The putative lung stem cells (BASC) are located at the junction between the branching, bronchial region and the alveolar sac, and express markers from pneumocytes type II (Sp-C) cells and clara cells (CC10).

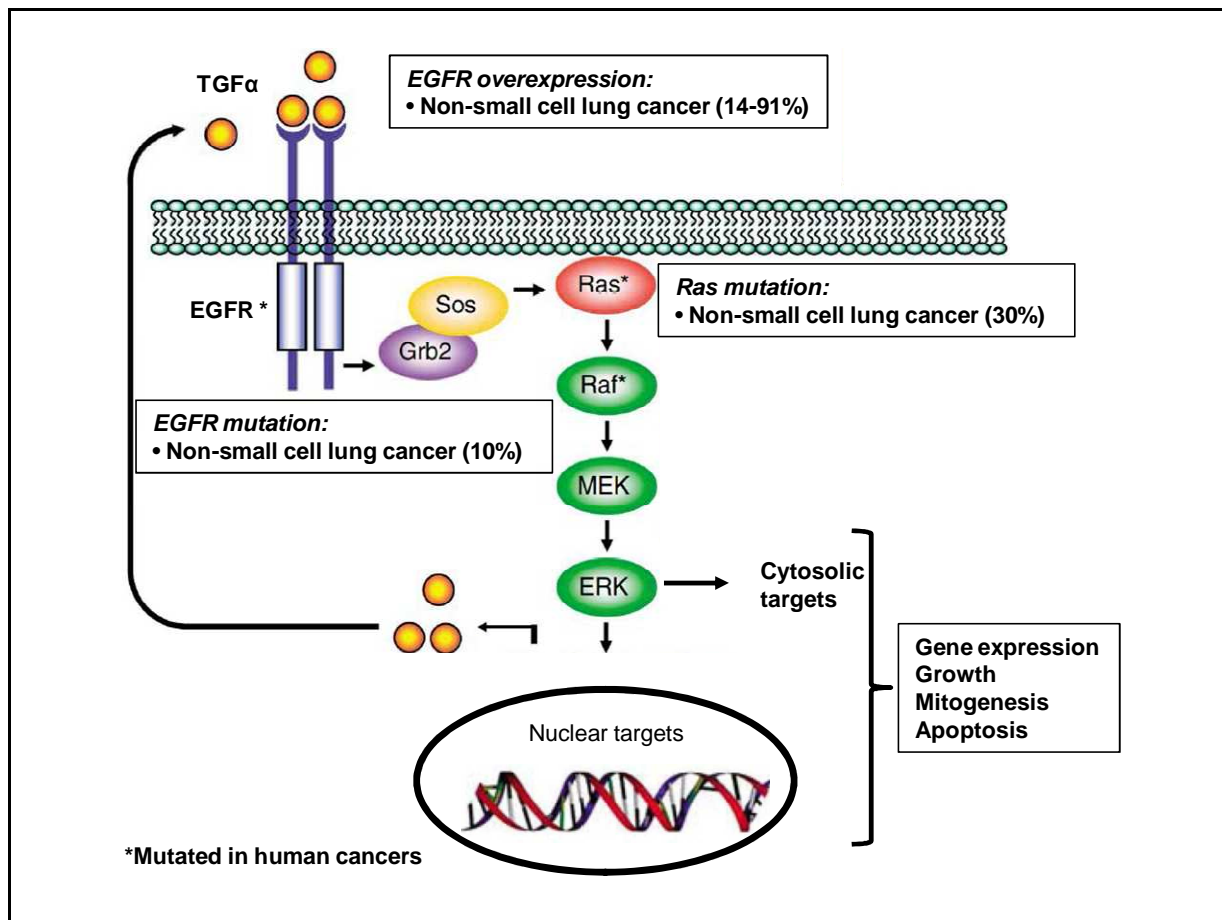
## 2.2. Cancer

Despite the enormous amount of research on cancer development and therapy, this disease continues to be a worldwide killer<sup>12</sup>. Cancer is defined as the abnormal growth of cells which tend to proliferate in an uncontrolled way<sup>13</sup> and is caused by both internal and environmental factors. Internal factors include inherited mutations, hormones or immune conditions and

environmental/acquired factors include tobacco, diet, radiation and infectious organisms<sup>12</sup>. The path to cancer is driven by accumulation of genetic and epigenetic alterations, involves deregulation of many signaling pathways and requires that somatic cells escape from various intrinsic tumor suppressor mechanisms leading to uncontrolled cell growth<sup>14</sup>. The identification of genes and pathways involved in cancer progression is necessary to enhance our understanding of the biology of this process, and to provide new targets for early diagnosis and facilitate targeted treatment<sup>15</sup>.

### **2.3. Lung cancer – NSCLC**

Lung cancer is the leading cause of cancer-related death worldwide due to its high metastasis rate, and thus a major health problem<sup>1</sup>. As the lung exposes an enormous area to the environment to efficiently load the blood with oxygen, the epithelial cells lining its surface are continuously exposed to air pollutants and are at high risk of oncogenic transformation<sup>16</sup>. Clinically, lung cancer can be divided into 2 groups: Small Cell Lung Cancer (SCLC) which begins in the nerve cells or hormone-producing cells of the lung and Non-Small-Cell Lung Cancer (NSCLC) which derives from epithelial cells. Approximately 75% of lung tumors are NSCLC, which includes squamous cell carcinoma, adenocarcinoma and large cell carcinoma<sup>1</sup>. The most frequent human NSCLC is adenocarcinoma. Molecular abnormalities in lung cancers are found in both growth-promoting oncogenes and growth-suppressing tumor suppressor genes<sup>1</sup>. A dozen regulators of growth factor signal transduction were identified to be altered in lung cancers, especially regulators of the EGFR-RAS-RAF-MEK-ERK signaling network resulting in alterations on regulation of cell cycle, gene expression and apoptosis (Fig. 2.3).

Modified from <sup>17</sup>

### Figure 2.3. Oncogene activation of the ERK-MAPK cascade.

Mutationally activated RAF, RAS and mutationally activated (by missense mutations in the cytoplasmic kinase domain in NSCLC) and/or overexpressed EGFR leads to persistent activation of the ERK-MAPK cascade in human cancers. Activated ERKs translocate to the nucleus, where they phosphorylate and regulate various transcription factors leading to changes in gene expression. In particular, ERK-mediated transcription can result in the upregulation of EGFR ligands, such as TGF $\alpha$ , thus creating an autocrine feedback loop that is critical for RAS-mediated transformation and RAF-mediated gene expression changes<sup>17</sup>.

The oncogene K-RAS is mutated in ~30% of the cases NSCLC, while EGFR is mutated in 10% of the cases<sup>17</sup>. *EGFR*, *C-RAF* and *MYC* are amplified in NSCLC<sup>1,18</sup>. C-RAF is a downstream effector of RAS signaling but although only the RAS GTPase is frequently mutated in lung cancer, C-RAF protein is found to be amplified in different lung cancers. Accumulated evidences



of deregulation in the EGFR-RAS-RAF-MEK-ERK pathway in lung cancer make this pathway an important subject of research and pharmaceutical scrutiny to identify novel target based approaches for cancer treatment<sup>17</sup>.

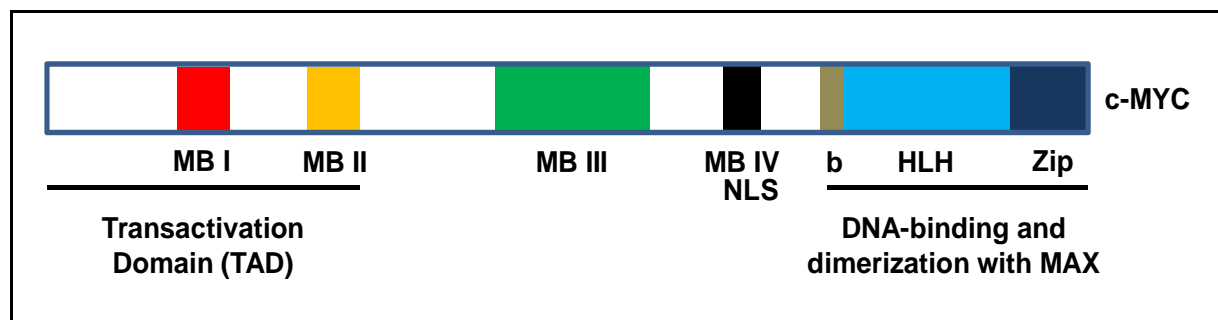
## **2.4. MYC**

### *2.4.1. MYC protein family*

MYC family of proto-oncogenes codes for basic helix–loop–helix leucine zipper (bHLHZip) transcription factors that regulate the expression of genes involved in DNA synthesis, RNA metabolism, and cell cycle regulation and are deregulated and overexpressed in most cancer cells<sup>19</sup>. Members of this family include the well-characterized *c-MYC*, *N-MYC* and *L-MYC* genes which have similar overall structures, consisting of three exons with extensive areas of homology<sup>20</sup>. The *c-MYC* gene is expressed during all stages of the cell cycle and is normally downregulated during differentiation. In contrast, N-MYC and L-MYC expression is limited to particular stages of embryonic development, and to immature cells of the hematopoietic and neuronal compartments in the adult<sup>21</sup>. Activation of *MYC* genes occurs by amplification or loss of transcriptional control, resulting in MYC protein overexpression. In SCLC *c-MYC*, *N-MYC* or *L-MYC* are often amplified and aberrantly expressed, whereas in NSCLC exclusively *c-MYC* is found affected and only in 5% – 10% of the cases<sup>22</sup>.

MYC-dependent transactivation requires heterodimerization with its bHLHZip partner protein MAX. Both the interaction with MAX and transactivation are essential for proliferative and oncogenic functions of *c-MYC*<sup>19</sup>. This dimerization enables specific binding of MYC:MAX complexes to 5'-CACGTG-3' and similar E-box DNA sequences in the promoters of target

genes<sup>21</sup>. The C-terminal 90 amino acids of the MYC protein are required for dimerization with MAX and sequence- specific DNA binding<sup>23</sup> (Fig. 2.4).



Modified from<sup>21</sup>

**Figure 2.4. Structure of the c-MYC protein.**

c-MYC contains at least six regions which are highly conserved between MYC paralogs and orthologs. The MYC N-terminal domain contains MYC Box I (MB I), MYC Box II (MB II) and MYC Box III (MB III). The MYC C-terminal domain contains the MYC Box IV, the primary nuclear localization signal (NLS) and the basic helix-loop-helix leucine zipper domains (bHLHZip).

The N-terminal part of MYC proteins contains four highly conserved elements, the MYC boxes I, II and III. MYC box I (MBI) is required for gene activation, although the deletion of this region only partially abolishes the transforming ability of MYC. MYC box II (MBII) is essential for the ability of MYC to transform, drive cell proliferation, inhibit differentiation, repress gene transcription, and activate certain target genes, while MYC Box III (MBIII), plays a role in transformation, lymphomagenesis and apoptosis<sup>24</sup>.

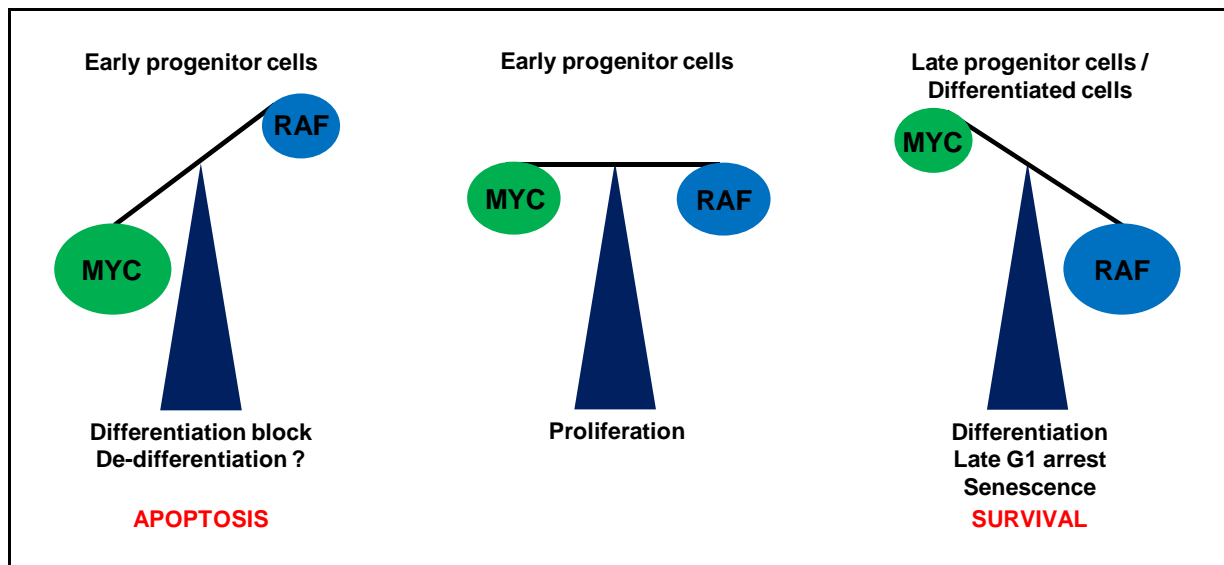
More recently a fourth box has been described to regulate DNA binding, transformation, and G2 arrest and apoptosis<sup>25</sup>. MYC exerts its main functions through gene regulation by recruiting transcriptional cofactors involved in modulation of RNA polymerase II function and of chromatin structure, including histone acetyl transferase (HAT) complexes. These are engaged

through interactions with the conserved MYC box II (MBII) in the transactivation domain (TAD) or with the bHLHZip domain<sup>21</sup> (Fig. 2.4). The binding sites of MYC-proteins are ~25,000 in the human genome, which by far exceeds the number of MYC molecules available in one cell, suggesting that a relatively brief binding of MYC leads to longer-lasting changes in the chromatin organization<sup>26</sup>.

Carcinogenic events which lead to MYC deregulation enforce cells to undergo a transition to a hyperproliferative state, increase cell migration and independent anchorage growth ability, decrease cell adhesion and lead to metastasis<sup>2</sup>. However, *MYC* activation also provokes intrinsic tumor suppressor mechanisms including apoptosis, cellular senescence and DNA damage responses that act as barriers for tumor development<sup>21</sup>. Distinct threshold levels of MYC discriminate between normal and oncogenic MYC activity: while low levels of deregulated MYC drive ectopic proliferation of somatic cells and oncogenesis, activation of apoptotic pathways requires MYC over-expression<sup>27</sup>.

#### 2.4.2. *Cooperation partners*

Although the c-MYC oncoprotein is required and sufficient for the induction of cellular proliferation, its role in the induction of apoptosis needs to be cancelled by the cooperation of another oncogenic partner to promote tumorigenesis progression. The cooperation of c-MYC with KRAS or LKB1 is sufficient to drive tumorigenesis<sup>2</sup>. Nevertheless, progression to metastasis is not achieved by the combination of these oncoproteins. In contrast, C-RAF cooperates with c-MYC in tumor progression and metastasis induction by suppressing apoptosis as described in the RAF-MYC balance model (Fig. 2.5)<sup>28,2</sup>.

Modified from<sup>29</sup>

**Figure 2.5. The balance model: Cooperation between RAF and MYC oncoproteins.**

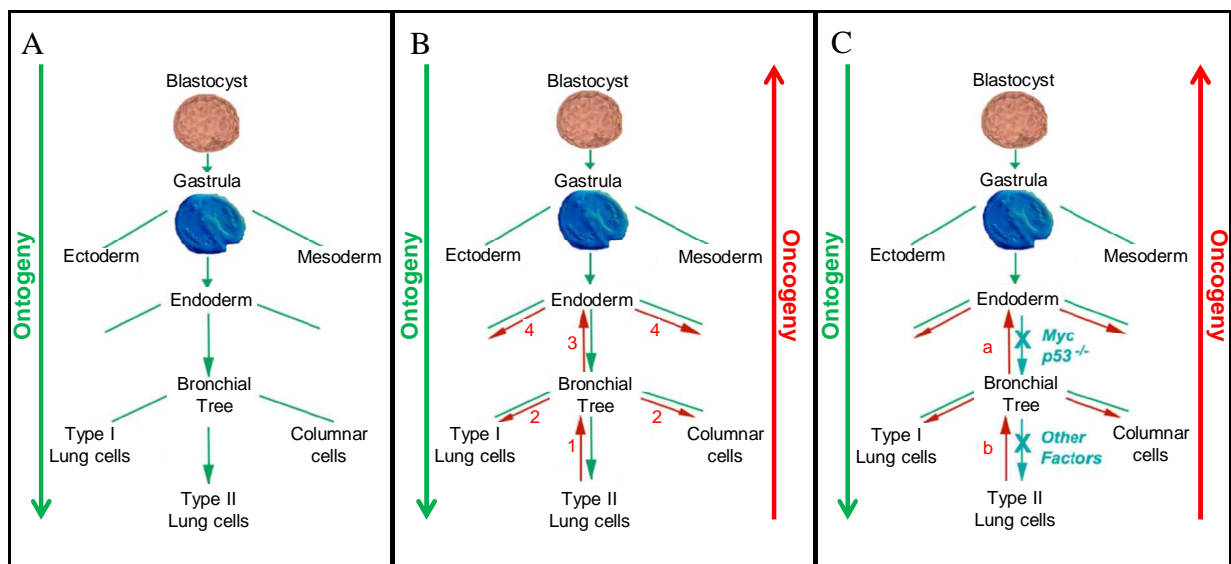
Different cellular responses regarding proliferation, differentiation, senescence, apoptosis and survival, depending on the relative expression/activity levels of RAF and MYC.

A hematopoietic lineage switch induced by a reprogramming of B lymphocytes to macrophages was previously observed as a result of RAF/MYC combination<sup>30</sup>. Moreover, the expression of c-MYC in addition to C-RAF in type II pneumocytes promotes rapidly NSCLC tumor growth and is sufficient to induce metastasis to liver and lymph nodes. This combination cause the appearance of a phenotypic switch from cuboidal to Alveolar Papillary Columnar Epithelial cells (APECs) that are the most rapidly growing tumor cells and also predominate in liver metastasis<sup>2</sup>.

### 2.5. Cancer stem cell hypothesis

The cancer stem cell hypothesis suggests that many if not all tumors arise from both genetic and epigenetic changes in fully differentiated cells that can lead to genetic and phenotypic instability. These alterations induce dedifferentiation resulting in the reactivation of a sub-set of genes

expressed in progenitor or organ-specific stem cell. The subpopulation of cells that dedifferentiate as a consequence of reprogramming events induced by oncogenes are called cancer stem cells or cancer initiating cells. These cells have the capacity to sustain tumor growth by self-renewal, differentiation into the cell types of the original cancer and potent tumor formation<sup>30</sup>. It has been shown for mixed leukemia lineage that myeloid progenitor cells acquire properties of leukemia stem cells without changing their overall identity. These cells do not become stem cells but rather develop stem cell like behavior by reactivating a subset of genes highly expressed in normal hematopoietic stem cells<sup>31</sup>. The plasticity of functionally mature cells is induced by oncogenes like *c-MYC* or *C-RAF*<sup>30</sup>. It has been postulated by Rapp et al. that oncogeny is a faulty reversal of ontogeny and that a prelude to metastasis is the acquisition of phenotypes that are more primitive than those characterizing organ specific stem cells (Fig. 2.6)<sup>29</sup>.

Modified from<sup>29</sup>

**Figure 2.6. Metastasis as a faulty reversal of ontogeny.**

(A) Endodermal origin of the lung. Following gastrulation the definitive endoderm gives rise to the primitive gut tube, followed by secondary bud formation and branching morphogenesis, resulting in the formation of the bronchial

tree. Upon terminal differentiation the most distal region of the lung is organized into alveoli, where two types of epithelial cells are found: type I cells and cuboidal type II cells<sup>29</sup>. (B) Induction of plasticity in type II lung cells, e.g. by a combination of oncogenic RAF and MYC, allows reversal of differentiation of the type II cells to earlier points in their ontogenic history<sup>2</sup>. This may lead to other lung cell types (1,2) or to cells mimicking the phenotype of cells from the primitive gut tube (3,4). Upon evasion from the primary tumor these cells home to tissues, which resemble their phenotype, e.g. liver. Dedifferentiation is accompanied by a gain of novel potential metastatic targets and increase in malignancy of the tumor<sup>29</sup>. (C) A differentiation block imposed by forced MYC expression or by p53 ablation (a) or by other factors (b) prevents redifferentiation and may further increase plasticity and heterogeneity of the transformed cell population<sup>29</sup>.

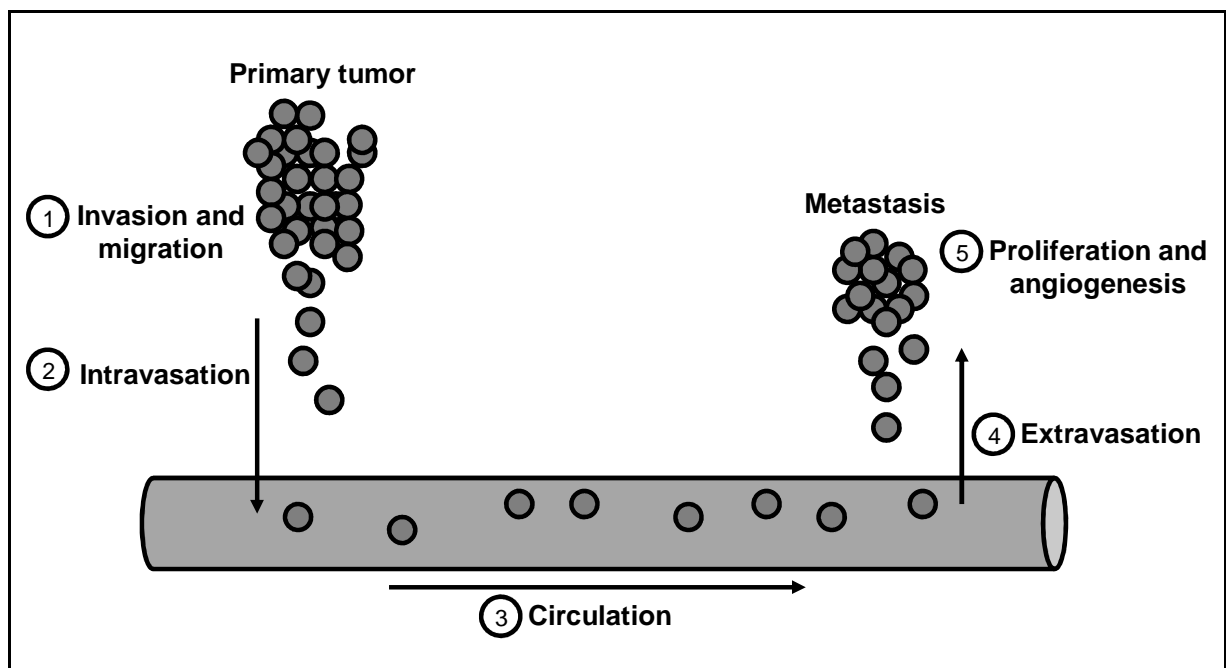
This dedifferentiation confers to the cancer cells the ability to populate organs different from its origin by loss of organ identity. The reprogramming events triggered by oncogenes might have important consequences for the prevention, the prognostic evaluation and the treatment of cancer<sup>30</sup>.

## **2.6. Metastasis**

The main reason for most of cancer related deaths is not the primary neoplasms, but secondary tumors, the metastasis<sup>32</sup>. The six hallmarks of cancer are distinctive and complementary capabilities that enable tumor growth and metastatic dissemination. They include sustaining proliferative signaling, evading growth suppressors, resisting cell death, enabling replicative immortality, inducing angiogenesis, and ultimately activating invasion and metastasis<sup>33</sup>. A tumor which has not yet reached an invasive phenotype is often referred as “carcinoma in situ”. The capability to leave a primary tumor, travel via the circulation to a distant tissue site and form a secondary tumor is referred as metastasis<sup>32</sup>.

Most cancer cells in a primary tumor have a ‘metastatic phenotype’, indicating that metastatic spread is an early event in tumorigenesis<sup>34</sup>. Metastasis is a complex multistep process which

includes local tumor cell invasion, entry into the vasculature followed by the exit of carcinoma cells from the circulation and colonization at the distal sites<sup>35</sup> (Fig. 2.7). The sequential nature of this metastatic cascade implies that failure to complete even one of these steps eliminates the possible development of secondary colonization<sup>36</sup>.



Modified from<sup>32</sup>

**Figure 2.7. Metastatic cascade.**

The biological process of metastasis is a complex cascade with multiple steps: invasion and migration, intravasation, circulation, extravasation and proliferation and angiogenesis.

In the first step of metastasis - *invasion and migration* -, individual cells detach from the primary tumor and invade adjacent tissue. The loss of E-cadherin by carcinoma cells, a key cell-to-cell adhesion molecule, is a well characterized alteration during this step<sup>33</sup>. Additionally, several lytic enzymes are secreted to degrade the ECM (extracellular matrix) and therefore facilitate

migration<sup>32</sup>. After invasion, tumor cells migrate as a response to chemokine and adhesive molecules gradients such as collagen and fibronectin<sup>37</sup>.

The intrusion of cancer cells into the blood and lymphatic vessels is referred to as *intravasation* and is followed by *circulation* of the tumor cells. To settle at distant sites, tumor cells have to travel through the blood stream and withstand the conditions present in the blood. These conditions include high concentrations of oxygen and cytotoxic lymphocytes which are toxic for the cancer cells<sup>32</sup>. Escape of cancer cells from the circulation (*extravasation*) is thought to be a major rate-limiting step in metastasis, with few cells being able to extravasate<sup>38</sup>. During *extravasation*, cells get stuck in the capillaries of a distant organ and leave the blood stream by penetrating the endothelium through proliferation and/or proteolytic enzymes<sup>32</sup>. The last step of the metastatic cascade includes colonization, proliferation and angiogenesis.

At this point, the neoplastic cell settles at distant organs and builds a secondary tumor. This second tumor proliferates and induces neo-angiogenesis, which greatly improves blood supply of oxygen and nutrients and a system for the removal of waste products, permitting rapid growth<sup>32,37</sup>. Angiogenesis is regulated by signaling proteins that bind to stimulatory or inhibitory cell surface receptors displayed by vascular endothelial cells. The well-known prototype of angiogenesis inducers and inhibitors is the Vascular Endothelial Growth Factor-A (VEGF-A) which is produced by hypoxic tumor cells and thrombospondin-1 (TSP-1), respectively<sup>37</sup>. Although metastasis is an inefficient process because few cells are able to overcome the adverse conditions between their entry into the circulation and settlement at a distant organ, the consequences of this process are often devastating due to high rate of treatment failure<sup>39</sup>.

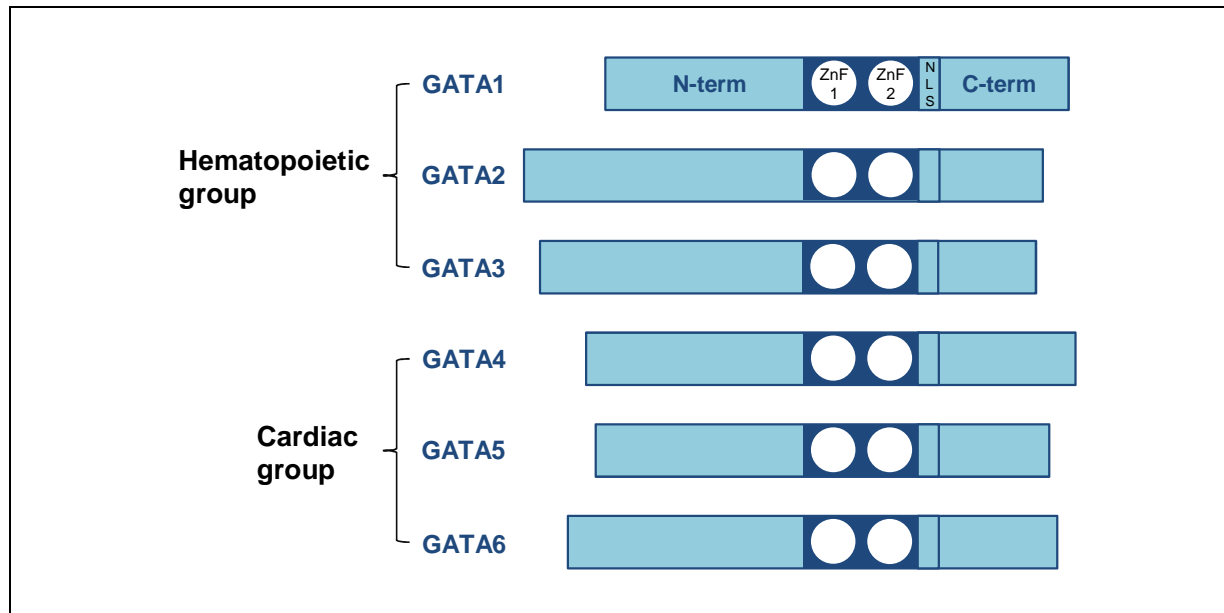


## 2.7. GATA family

GATA factors are a group of highly conserved transcriptional regulators that play crucial roles in the development, embryonic morphogenesis and differentiation of all eukaryotic organisms. Impaired function or reduced expression of these proteins contributes to malignant transformation due to failure of the affected cells to mature and exit the cell cycle. Therefore, a role of this family of genes in human cancers is not surprising<sup>40</sup>.

GATA factors bind to the common WGATAR motif found in the transcriptional regulatory regions of numerous genes. In vertebrates, this family comprises six members (GATA1-6) which share a conserved DNA-binding domain composed of two multifunctional zinc fingers involved in DNA-binding and protein-protein interaction with other transcriptional partners and/or cofactors (Fig. 2.8.)<sup>41</sup>. The members of the GATA family can be separated into two subgroups based on their temporal and spatial patterns. While GATA1/2/3 are expressed in hematopoietic cell lineages and are essential for erythroid and megakaryocyte differentiation, proliferation of hematopoietic stem cells, and development of T lymphocytes, GATA4/5/6 proteins are mainly found in tissues of mesodermal and endodermal origin such as the heart, gut, and gonads<sup>41</sup>. However, this characterization does not justice to the much broader tissue distribution of most GATA proteins<sup>40</sup>. Indeed, the abundant expression of GATA proteins in several cell types of various endocrine organs together with their ever expanding list of target genes strongly indicates that these factors are essential regulators of cell specific gene expression involved in development, differentiation, and function of endocrine cells<sup>41</sup>. GATA factors can function in undifferentiated progenitor cells interfering in their expansion, or direct the maturation and cell cycle withdrawal in terminally differentiating cells. Thus, it is to be expected that mutations, loss

or overexpression of GATA factors contribute to the development of cancer in humans, including leukemia, breast or gastrointestinal cancers<sup>40</sup>.



Modified from<sup>42</sup>

### Figure 2.8. Structure of the vertebrate family of GATA proteins.

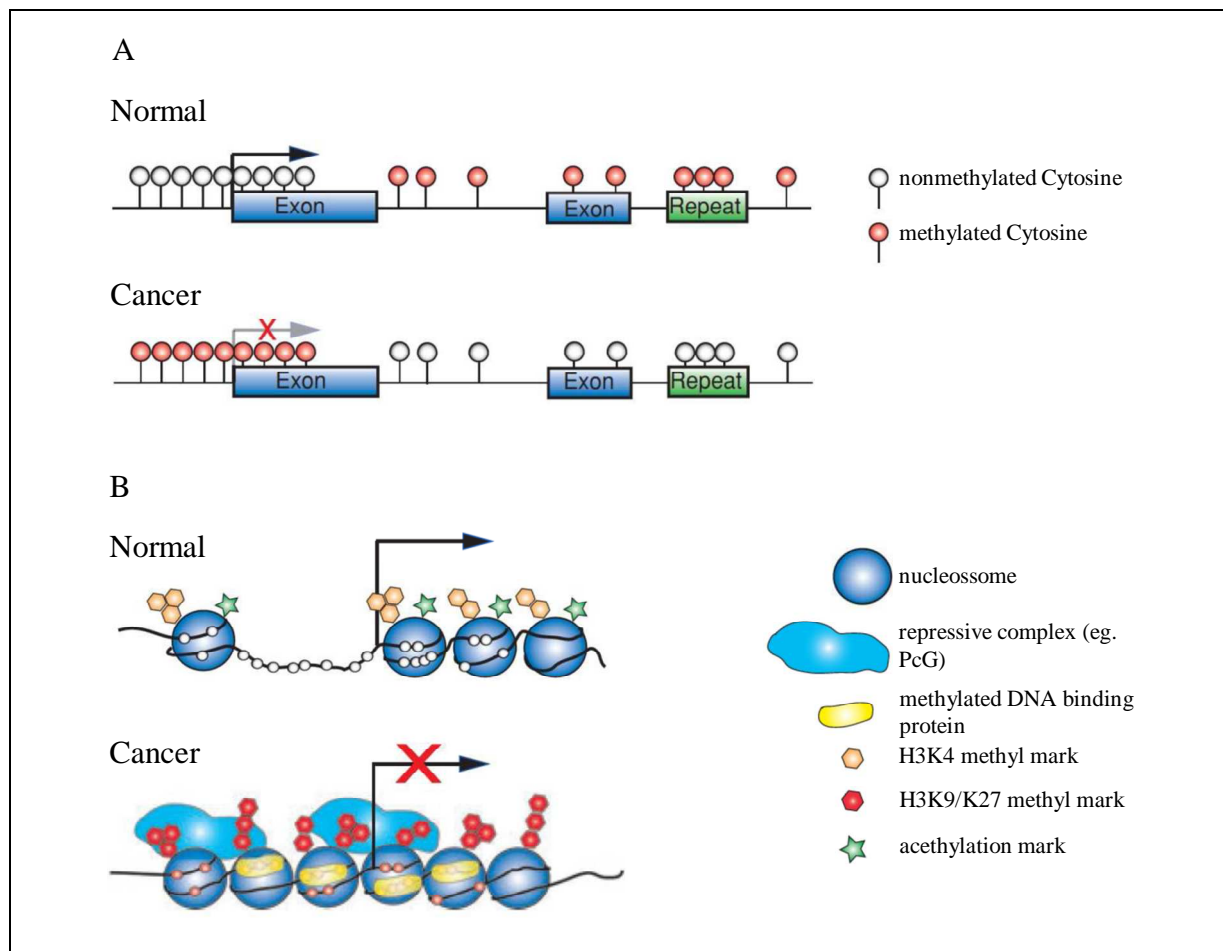
GATA factors share a conserved DNA-binding domain consisting of 2 zinc fingers (ZnF). The different GATA factors can be divided into 2 subgroups based temporal and spatial distribution: the hematopoietic subgroup (GATA1/2/3) and the cardiac subgroup (GATA4/5/6). Transactivation domains are found in both the N-terminal (N-term) and/or C-terminal (C-term) portions of the different GATA proteins. NLS, nuclear localization signal.

The member of this family, GATA4, plays a role in early endoderm development<sup>43</sup>, regulates genes involved in cardiac differentiation, is an important regulator of apoptosis and cell proliferation in humans and is essential for the maintenance of jejunal-ileal identities in adult mice<sup>44,45</sup>. In the intestine, GATA4 cooperates with TGF- $\beta$  to activate gut epithelial gene expression<sup>43</sup>. In addition, this transcription factor was recently shown to control the expression of

Bcl-2 antiapoptotic factor and the cell cycle regulator cyclin D2<sup>46</sup>. Its transcriptional activity was shown to be attenuated by direct methylation by the Polycomb-repressive complex 2 (PRC2)<sup>47</sup>.

### ***2.8. Epigenetic changes in cancer***

Epigenetics is defined as “heritable changes in gene expression that are not accompanied by changes in DNA sequence”<sup>48</sup>. Epigenetic mechanisms provide an "extra" layer of transcriptional control that regulates how genes are expressed. These mechanisms are critical for normal development and growth of cells<sup>49</sup>. In the cells, DNA is wrapped around clusters of globular histone proteins to form nucleosomes. These nucleosomes are organized into chromatin and changes in the structure of chromatin strongly influence gene expression. Genes are silenced if the chromatin is condensed and expressed if the chromatin is opened. These dynamic chromatin states are controlled by reversible epigenetic patterns of DNA methylation, histone modifications and nucleosome remodeling<sup>49</sup>. Like most biological processes, silencing can become deregulated resulting in the development of diseases like cancer<sup>48</sup>. The loss of normal DNA methylation patterns is the best understood epigenetic cause of disease<sup>49</sup>. DNA methylation is the addition of methyl groups to cytosines catalyzed by at least three DNA methyltransferases (DNMTs). The methylation takes place only at cytosine bases located 5' to a guanosine in a CpG dinucleotide. Most CpG islands are located in the proximal promoter regions in the mammalian genome, and are, generally, unmethylated in normal cells<sup>50</sup> (Fig. 2.9.A). DNMTs found at the replication fork, copy the methylation pattern of the parent strand onto the daughter strand during S-phase. This makes methylation patterns heritable over many generations of cell divisions. The silencing mediated by DNA methylation occurs in combination with histone modification and nucleosome remodeling, which together establish a repressive chromatin structure<sup>51</sup> (Fig. 2.9.B).

Modified from<sup>51</sup>

### Figure 2.9. Epigenetic patterns in normal and cancer cells.

(A) DNA methylation. In normal cells, nearly all of the CpG dinucleotides are methylated whereas CpG islands, mostly residing in 5' regulatory regions of genes, are unmethylated. In cancer cells, many CpG islands become hypermethylated, in conjunction with silencing of their cognate genes, while global hypomethylation, mostly at repetitive elements, occurs. (B) Chromatin and histone modification. Active genes are associated with acetylation of histone tails, methylation of lysine 4 on histone H3 (H3K4), and nucleosome depletion at their promoters. The promoters of silenced genes (drawn here in conjunction with DNA hypermethylation) become associated with nucleosomes, lose acetylation and H3K4 methylation marks, and gain repressive methylation marks such as lysine 9 or 27 on histone H3, which recruit repressive complexes<sup>51</sup>.

The building blocks of nucleosomes – the histones – undergo several post-translational modifications that regulate chromatin structure, gene expression and DNA repair. The key link

between DNA methylation and histone modification is the recruitment of histone deacetylases (HDACs) to methylated DNA during chromatin compaction and gene silencing<sup>51</sup>. The DNA in these transcriptionally silent regions is packed into compact nucleosomes containing deacetylated histones, in particular histone H3, and this state helps to maintain nucleosomes in a compacted and transcriptionally silent state<sup>50</sup>.

Together with acetylation, histone methylation is the most well studied histone modification. Histone methylation occurs mainly at histone lysine residues. In general, regions silenced by DNA methylation show hypermethylation and hypoacetylation of specific histone lysine residues, such as lysine 9 or 27 in histone H3, whereas hyperacetylation of histones H3 and H4, and methylation of lysine 4 of histone H3 characterize the transcriptionally active chromatin<sup>51</sup>. These epigenetic alterations lead to aberrant gene function and altered pattern of genes expression which are key features of cancer<sup>48</sup>. Loss of acetylation at lysine 16 and trimethylation at lysine 20 of histone H4 is a common hallmark of human cancer<sup>52</sup>, and global histone modifications patterns predict risk of prostate cancer<sup>53</sup>. Growing evidence suggests that these patterns may be generated by upstream-acting “programs” involving the Polycomb group complexes (PcGs) that went wrong. PcGs are proteins complexes responsible for the maintenance of long-term silencing of genes, mediated by the histone methyltransferase EZH2 of the Polycomb-repressive complex 2 (PCR2), which is known to be upregulated in tumors and is involved in tumor progression<sup>51</sup>. EZH2 methylates lysines 9 and 27 of histone H3, which are markers for silenced chromatin<sup>48</sup>. Also both hyper- and hypo methylation of individual CpG sites in the promoters are common in cancer either by loss of gene function like tumor suppressors or activation of genes that promote carcinogenesis<sup>50</sup>. Thus, it is today widely accepted that cancer is an epigenetic disease at the same level that it can be considered a genetic disease<sup>54</sup>.

### **2.9. Previous work and aim of the project**

It was previously shown by the group of Prof. Rapp that RAF/MYC combination leads to ectopic expression of intestinal selector genes, reminiscent of the ability of MYC to induce a myeloid lineage switch of RAF transformed B-cells<sup>29</sup>.

*Kerkhoff et al.* showed the induction of premalignant lesions at the age of two weeks in a mouse model for human NSCLC (Sp-C-C-RAF) where the *C-RAF* transgene is specifically expressed in lung alveolar type II epithelial cells<sup>18</sup>. In this model, no metastasis could be found in young or old animals. A compound mouse model that in addition to constitutive expression of C-RAF, expresses the transgene *c-MYC* in lung alveolar type II epithelial cells (Sp-C-C-RAF-BxB/Sp-C-c-MYC) have been shown to induce early macrometastasis to liver and lymph nodes indicating that c-MYC expression is a major determinant in this process. Moreover, the combination of c-MYC and C-RAF caused appearance of a phenotypic switch from cuboidal to Alveolar Papillary Columnar Epithelial cells (APECs) that are the most rapidly growing tumor cells and also predominated in liver metastasis. The transplantation of immunodeficient mice with a high c-MYC expressing A549 cell clone showed the development of metastasis in the liver and lymph nodes, establishing c-MYC as a strong metastasis inducing gene for NSCLC<sup>2</sup>.

The expression of the intestine maintenance transcription factor GATA4 has been observed in the lung tumors and liver metastasis of Sp-C-C-RAF-BxB/Sp-C-c-MYC compound and Sp-C-c-MYC single transgenic mice. In contrast, GATA4 was absent in the lung tumors of Sp-C-C-RAF-BxB animals, which expressed GATA6 instead - a transcription factor that is involved in airway regeneration. GATA6 is an upstream factor of TTF1, which in turn is necessary for the activity of the Sp-C promoter. The GATA4 ectopically expressed in lung cells was shown to be functional, as the expression of its target mucin2 was detected. The expression of Cdx2, another

selector gene that marks intestinal lineages was not detected in primary tumors or metastasis of any of the genotypes highlighting GATA4 as a novel MYC target<sup>2</sup>.

Although the data from the previous work directly apply to metastatic human lung cancer and identify a novel treatment target, the way in which these genes may contribute to metastatic process remained to be elucidated<sup>2</sup>.

Therefore, the aim of the present work was to investigate the role of GATA4 in MYC induced metastasis in more detail and to get insights into the molecular mechanisms and signaling pathways involved in metastasis of NSCLC.

### 3. Materials and methods

#### 3.1. Materials

##### 3.1.1. Instruments

| <b>Instrument</b>                     | <b>Model and Manufacturer</b>                                  |
|---------------------------------------|--|
| Array scanner                         | Illumina   |
| Cell counter chamber                  | Bürker   |
| CO <sub>2</sub> incubator             | Heracell 240i – Thermo Scientific                              |
| Electrophoresis power supply          | PowerPac 200 – Bio-Rad   |
| Electrophoresis unit for Agarose Gels | Sub-cell® GT - Bio-Rad   |
| Electroporator                        | MicroPulser™ - Bio-Rad   |
| Fluorescence microscope               | TCS SPE – Leica  |
| <i>In vivo</i> imaging system         | Maestro EX imaging system - CRi (Woburn, MA)                   |
| Low light imaging system              | Argus 100 - Hamamatsu, Bridgewater, NJ                         |
| Megacentrifuge                        | Megafuge 1.0 – Heraeus Instruments                             |
| Microcentrifuge                       | Centrifuge 5415D – Eppendorf                                   |
| Microplate reader                     | Infinite M200 – Tecan  |
| Microscope                            | DM IL – Leica  |
| Microtome                             | Leitz – Wetzlar  |
| Paraffin embedding machine            | EG1150 – Leica   |
| pH meter                              | pH 720 WTW series – inoLab                                     |
| Photometer                            | Biophotometer – Eppendorf                                      |
| Pipettes                              | P1000, P200, P100, P10 – Eppendorf                             |
| Real-Time PCR systems                 | Step One Plus – Applied Biosystems<br>LightCycler® 480 - Roche |
| Sequencer                             | Roche 454 FLX Standard   |
| Shaker                                | HT – Infors AG   |
| Spectrophotometer                     | NanoDrop® ND-1000 – peqlab                                     |
| Thermoblock                           | TDB-120 – Lab4you GmbH   |



| <b>Instrument</b> | <b>Model and Manufacturer</b>        |
|-------------------|--------------------------------------|
| Thermocycler      | T3 Thermocycler – Biometra           |
| Transilluminator  | Dark Hood DH 40/50 - Biostep         |
| Vortex            | Vortex Gene2 – Scientific Industries |
| Waterbath         | Amersham-Buchler                     |

### 3.1.2. Chemical reagents

| <b>Reagent</b>               | <b>Manufacturer</b> |
|------------------------------|---------------------|
| 1kb DNA ladder               | Fermentas           |
| Absolute QPCR SYBR Green Mix | Thermo Scientific   |
| Agarose, ultra pure          | Invitrogen          |
| Ampicillin                   | Sigma               |
| Bacto-Agar                   | Roth                |
| Bacto-Tryptone               | Roth                |
| $\beta$ -Mercaptoethanol     | Roth                |
| Bovine serum albumin (BSA)   | Sigma               |
| Chloroform                   | Roth                |
| DAPI                         | Sigma               |
| DEPC                         | Roth                |
| Diaminobenzidine (DAB)       | Sigma               |
| Dimethylsulfoxide (DMSO)     | Sigma               |
| Doxycycline                  | Sigma               |
| dNTPs                        | Fermentas           |
| EDTA                         | Sigma               |
| Entellan                     | Merck               |
| Eosin                        | Merck               |
| Ethanol                      | Roth                |
| Ethidiumbromide              | Invitrogen          |
| Fetal Calf Serum (FCS)       | Invitrogen          |

| <b>Reagent</b>                          | <b>Manufacturer</b> |
|---|---------------------|
| Formaldehyde                            | Roth                |
| Glacial acetic acid                     | Roth                |
| Glycerol                                | Sigma               |
| HCl                                     | Roth                |
| Hematoxylin                             | Merck               |
| HEPES                                   | Roth                |
| Hydrogenperoxide (30%)                  | Hartenstein         |
| Isopropanol                             | Roth                |
| Ketanest                                | Pfizer              |
| Lipofectamine™ 2000                     | Invitrogen          |
| Luciferin                               | Promega             |
| Methanol                                | Hartenstein         |
| Mowiol                                  | Calbiochem          |
| MTT dye                                 | Sigma               |
| NaCl                                    | Roth                |
| Paraformaldehyde (PFA)                  | Sigma               |
| Paraffin wax                            | Merck               |
| Phosphate-buffered saline (PBS)         | Gibco               |
| Polybrene                               | Sigma               |
| Puromycin                               | Sigma               |
| Rompum                                  | Bayer               |
| PerfeCTa® SYBR® Green FastMix®,<br>ROX™ | Quanta Biosciences  |
| Serum (rabbit, goat, donkey)            | Chemicon            |
| Sodiumdodecylsulfat (SDS)               | Roth                |
| Tamoxifen (OHT)                         | Sigma               |
| Tissue TEK (OCT)                        | Chemicon            |
| Trichostatin A (TSA)                    | Sigma               |
| Tris                                    | Roth                |
| Triton X-100                            | Sigma               |

| <b>Reagent</b> | <b>Manufacturer</b> |
|----------------|---------------------|
| Xylol          | Roth                |
| Yeast-extract  | Invitrogen          |
| Zeocin         | Sigma               |

### 3.1.3. Buffers and solutions

| <b>Solution</b>    | <b>Composition</b>  |
|--------------------|---|
| 6x DNA loading dye | 1,2 ml Glycerol<br>1,2 ml 0,5 mM Na <sub>2</sub> EDTA<br>300 µl 20% SDS<br>bromphenol blue<br>Water (up to 10 ml) |
| Lysis buffer       | 10 mM TrisHCl<br>1 mM EDTA<br>1% w/v of Tween 20<br>100 µg/ml of proteinase K                                     |
| Tail lysis buffer  | 50 mM EDTA<br>50 mM Tris-HCl (pH8.0)<br>0,5% SDS  |
| TE buffer          | 1 mM EDTA<br>10 mM Tris-HCl (pH8.0)   |

### 3.1.4. Enzymes

| <b>Enzyme</b>                              | <b>Manufacturer</b> |
|--|---------------------|
| Calf Intestine Alkaline Phosphatase (CIAP) | Fermentas           |
| DNaseI                                     | Fermentas           |
| Proteinase K                               | Roth                |
| Restrictionendonucleases                   | Fermentas           |
| RNaseA                                     | Fermentas           |

| <b>Enzyme</b>  | <b>Manufacturer</b> |
|----------------|---------------------|
| T4 Ligase      | Fermentas           |
| Taq Polymerase | Genecraft           |

3.1.5. Consumable material

| <b>Material</b>                           | <b>Manufacturer</b>          |
|---|------------------------------|
| 96-well plates                            | Nunclon A/S, Greiner bio-one |
| Cell culture flasks                       | Sarstedt                     |
| Cell culture plates                       | Sarstedt                     |
| Gene pulser cuvette, 0.1 cm electrode gap | Bio-Rad                      |
| Cryotubes                                 | Sarstedt                     |
| Falcon Tubes (15 and 50 ml)               | Sarstedt                     |
| Glass coverslips                          | Leica                        |
| Glass slides                              | Leica                        |
| Micro tube (1,5 and 2 ml)                 | Eppendorf                    |
| Pasteur Pipette                           | Hartenstein                  |
| Petri dish                                | Roth                         |
| Scalpel                                   | Hartenstein                  |
| Syringes                                  | Braun                        |

3.1.6. Antibodies

| <b>Antibodies (Immunochemistry)</b> | <b>Catalog Number – Manufacturer</b> |
|-------------------------------------|--------------------------------------|
| Anti-GATA4 (mouse)                  | sc-25310 AC – Santa Cruz             |
| Anti-Pro Sp-C (rabbit)              | gift from Jeffrey A. Whitsett        |

| <b>Antibodies (ChIP)</b> | <b>Catalog Number – Manufacturer</b> |
|--------------------------|--------------------------------------|
| Anti- chicken-MYC        | gift from Klaus Bister               |

| Antibodies (Immunochemistry) | Catalog Number – Manufacturer |
|------------------------------|-------------------------------|
| Anti- DNMT1                  | 39204 - Active motive         |
| Anti- DNMT3a                 | ab13888 - Abcam               |
| Anti-DNMT3b                  | 39207 - Activ motive          |
| Anti- EZH2                   | AC22 - Cell Signalling        |
| Anti-GATA4                   | sc-1237 - Santa Cruz          |
| Anti-GATA6                   | sc-9055 - Santa Cruz          |
| Anti-H3K4me2                 | 07-030 – Upstate              |
| Anti-H3K4me3                 | 07-473 – Upstate              |
| Anti-H3K9me2                 | ab1220 – Abcam                |
| Anti-H3K9me3                 | ab8898 – Abcam                |
| Anti-H3K27me3                | 07-449 – Upstate              |
| Anti-MAZ                     | ab85725 – Abcam               |
| Anti- POLII                  | 4H8 ab5408 –Abcam             |

| Secondary antibodies             | Manufacturer            |
|----------------------------------|-------------------------|
| Anti-mouse-biotinylated (rabbit) | Dako                    |
| Anti-rabbit-biotinylated (goat)  | Dako                    |
| Anti-goat-biotinylated (rabbit)  | Dako                    |
| Anti-mouse-Cy3 (goat)            | Jackson Immuno Research |
| Anti-goat-Cy5 (donkey)           | Jackson Immuno Research |
| Anti-rabbit-Cy3 (donkey)         | Jackson Immuno Research |

### 3.1.7. *Plasmids*

| Name                          | Source                      | Resistance                           |
|-------------------------------|-----------------------------|--------------------------------------|
| pLKO.1-puro-shGATA4-24        | Sigma Mission® shRNA        | Amp <sup>R</sup> , Puro <sup>R</sup> |
| pBpuro c-MYC-ER <sup>TM</sup> | T. Littlewood <sup>55</sup> | Amp <sup>R</sup> , Puro <sup>R</sup> |
| pEGZ                          | F. Ceteci                   | Amp <sup>R</sup> , Zeo <sup>R</sup>  |

| Name                     | Source               | Resistance                           |
|--------------------------|----------------------|--------------------------------------|
| pEGZ-GATA4 -11           | This work            | Amp <sup>R</sup> , Zeo <sup>R</sup>  |
| pGL3 Luciferase Reporter | Promega              | Amp <sup>R</sup>                     |
| pGL3_GATA4_Prom_455      | This work            | Amp <sup>R</sup>                     |
| pLKO.1-puro-shGATA4-26   | Sigma Mission® shRNA | Amp <sup>R</sup> , Puro <sup>R</sup> |
| pLKO.1-puro-shMAZ-345    | Sigma Mission® shRNA | Amp <sup>R</sup> , Puro <sup>R</sup> |

### 3.1.8. *Oligonucleotides for genotyping*

| Mouse Line      | Name      | Sequence (5'→3')            |
|-----------------|-----------|-----------------------------|
| Sp-C-c-MYC      | SpC_S1    | GAGGAGAGGAGAGCATAGCACC      |
|                 | SpC-cMyc  | AAGGACTTGGCTGGCAGACAGG      |
| Sp-C-c-RAF-BxB  | CRaf_s    | GCTGGTGTTCATGCACTGCAG       |
|                 | CRaf_as   | AAAGACTCAATGCATGCCACG       |
| Sp-C-rtTA       | rtta_s    | TCCTGGCTGTAGAGTCCCTG        |
|                 | rtta_as   | CTCCAGGAACCCACTCTCTG        |
| Tet-o-C-RAF BxB | Tet-o_new | TAGAAGACACCGGGACCGATCCAG    |
|                 | CRaf_as   | AAAGACTCAATGCATGCCACG       |
| Tet-o-c-MYC     | Tet-o_new | TAGAAGACACCGGGACCGATCCAG    |
|                 | Teto-myc  | CTGGTTCACCATGTCTCCTCCTCCCAG |

### 3.1.9. *Oligonucleotides for cloning*

| Name            | Sequence (5'→3')                   |
|-----------------|------------------------------------|
| GATA4_fwd       | AAAAAAGAATTCATGTATCAGAGCTTGGCCATGG |
| GATA4_P_455_fwd | AAAAAACTCGAGGGAAGTAGCATCCAGCC      |
| GATA4_P_rev     | AAAAAAAAGCTTGCTGCAGCGGCGACGAA      |
| GATA4_rev       | AAAAAAGAATTCTTACGCAGTGATTATGTCCCC  |

3.1.10. Oligonucleotides for Real-Time PCR

| Name         | Sequence (5'→3')  |
|--------------|---|
| β-actin (HS) | sense: ACGCAGTCAATAAGTGATACCA<br>anti-sense: GGATGTTTCCTGGTCAGCCT       |
| ANG1 (HS)    | sense: AAACAGCTGGAACCCATCTCCCGT<br>anti-sense: CCGGCCCTGTGGTTTGGCATC    |
| BMP4 (HS)    | sense: GTGCCATCCCGAGCAACGCACT<br>anti-sense: GCGTGGCCCTGAATCTCGGCG      |
| CD30 (HS)    | sense: CCGTGTCTGCGAATGTGACCCG<br>anti-sense: GGGAAGCCGGCTCACAGACCGT     |
| GATA4 (HS)   | sense: CTACATGGCCGACGTGGGAG<br>anti-sense: CTCGCCTCCAGAGTGGGGTG         |
| GFP          | sense: GCAAGCTGACCCTGAAGTTCATC<br>anti-sense: TCACCTTGATGCCGTTCTTCTG    |
| HIF1A (HS)   | sense: TTAAC TTTGCTGGCCCCAGCCGC<br>anti-sense: TGGCGTTTCAGCGGTGGGTAATGG |
| HKDC1 (HS)   | sense: CCACGGGCTGGCCACGGTC<br>anti-sense: ACATTCGCACTGACCTCCGTCCA       |
| HNF4A (HS)   | sense: AGCTGGCGGAGATGAGCCGGG<br>anti-sense: ACCTGGGAACGCAGCCGCTTG       |
| KCNAB2 (HS)  | sense: TGGGCAAGTCTGGCCTGCGG<br>anti-sense: GCCGGCTGCGTAGACTTCTGCTG      |
| LAMC2 (HS)   | sense: AGGGACCGCTGTTTGCCCTGC<br>anti-sense: GCACCCCGCATCCGTGAGCA        |
| MYC (GG)     | sense: CGGCCTCTACCTGCACGACC<br>anti-sense: GACCAGCGGACTGTGGTGGG         |
| MYC (HS)     | sense: GCCCACCACCAGCAGCGACTCT<br>anti-sense: CGCCTCCCTCCACTCGGAAGGAC    |
| mucin2 (HS)  | sense: CGACTAACAACTTCGCCTCCG<br>anti-sense: CGCGGGAGTAGACTTTGGTG        |

| Name         | Sequence (5'→3')   |
|--------------|--|
| NFKB1 (HS)   | sense: AGCCCAGCGAGGCCACCGTT<br>anti-sense: GCAGTGAGATGGCGCTGGACGG        |
| SLC6A15 (HS) | sense: TGGCTGCCTGGGTCATGGTTTGC<br>anti-sense: GGGGTAAACATGTGGCGAATGCCATC |
| TGF-β1 (HS)  | sense: CCTGGCGATACCTCAGCAACCGGC<br>anti-sense: TGCTGTCACAGGAGCAGTGGGCG   |
| VEGFA (HS)   | sense: CCAGGCTGCACCCATGGCAGA<br>anti-sense: AGCAGCCCCCGCATCGCATC         |
| CHIPGATA4_up | sense: CGGAGACCCCAGAGCCTG<br>anti-sense: CTCTCTACCTCCAGACAAGC            |

### 3.1.11. *Oligonucleotides for bisulfite sequencing*

| Name                | Sequence (5'→3')                                      |
|---------------------|---|
| COGATA4-prom_up     | TAATAAAGTTGATTTTGGGTATTATAG                           |
| COGATA4-prom_lo     | CCCTACCTACTAAACCTAAAATTC                              |
| 454-COGATA4-prom_up | GCCTCCCTCGCGCCATCAGXXXTAATAAAGTTGATTTTGG<br>GTATTATAG |
| 454-COGATA4-1_lo    | GCCTTGCCAGCCCGCTCAGXXXCCCTACCTACTAAACCT<br>A AAAATTC  |

### 3.1.12. *Kits*

| Kit                              | Manufacturer |
|----------------------------------|--------------|
| DNeasy Blood & Tissue Kit        | QIAGEN       |
| EpiTect Bisulfite Kit            | QIAGEN       |
| First Strand cDNA Synthesis Kit  | Fermentas    |
| ONE-Glo™ Luciferase Assay System | Promega      |
| peqGold TriFast™                 | Peqlab       |



| <b>Kit</b>                    | <b>Manufacturer</b> |
|-------------------------------|---------------------|
| QIAquick Gel Extraction Kit   | QIAGEN              |
| QIAquick PCR Purification Kit | QIAGEN              |
| QIAprep Spin Maxiprep Kit     | QIAGEN              |
| QIAprep Spin Miniprep Kit     | QIAGEN              |
| TOPO TA Cloning kit           | Invitrogen          |

### 3.1.13. Bacterial strains

| <b>Strain</b>        | <b>Source</b>                                      |
|----------------------|--|
| <i>E. coli</i> DH10b | Department of Microbiology, University of Würzburg |

### 3.1.14. Cell lines

| <b>Line</b>   | <b>Source</b>   |
|---------------|---|
| A549          | Human alveolar basal epithelial adenocarcinoma<br>Department of Microbiology, University of Würzburg              |
| A549 GATA4-11 | Human alveolar basal epithelial adenocarcinoma<br>This work   |
| A549/GFP      | Human alveolar basal epithelial adenocarcinoma<br>Michael Heß, Department of Biochemistry, University of Würzburg |
| A549 J5-1     | Human alveolar basal epithelial adenocarcinoma<br>Professor U. R. Rapp <sup>2</sup>                               |
| A549 MYC-ER   | Human alveolar basal epithelial adenocarcinoma<br>This work   |
| Caco-2        | Human epithelial colorectal adenocarcinoma<br>Department of Microbiology, University of Würzburg                  |
| HeLa          | Human cervical cancer<br>Department of Microbiology, University of Würzburg                                       |

| <b>Line</b>   | <b>Source</b>                                      |
|---------------|--|
| Phoenix ampho | Department of Microbiology, University of Würzburg |

3.1.15. *Mouse lines*

| <b>Line</b>            | <b>Source</b>          |
|------------------------|------------------------|
| Athymic Nude - Foxn1nu | Harlan Winkelmann GmbH |
| Sp-C-c-MYC             | Gift from R. Halter    |
| Sp-C-C-RAF-BxB         | Professor U. R. Rapp   |
| Sp-C rtTA              | Gift from J. Whitsett  |
| Tet-o-c-MYC            | Gift from T. Wirth     |
| Tet-o-C-RAF-BxB        | Professor U. R. Rapp   |

3.1.16. *Media and additives***Bacterial culture**

| <b>Luria-Bertani (LB) Medium</b> | <b>g for 1 Liter of Water</b> |
|----------------------------------|-------------------------------|
| Bacto-tryptone                   | 10                            |
| NaCl                             | 10                            |
| Yeast extract                    | 5                             |

After the substances were dissolved in water, the pH was adjusted to 7.5 using NaOH. For production of plates, 15 g of bacto-agar were added. All media were autoclaved for 20 min at 120°C. Antibiotics for the production of selective plates were added after cooling of the autoclaved liquids to about 45°C. The plates were stored at 4°C.

| <b>Antibiotic</b> | <b>Stock solution</b>         | <b>Final concentration</b> |
|-------------------|-------------------------------|----------------------------|
| Ampicillin        | 100 mg/ml in H <sub>2</sub> O | 100 µg/ml                  |

3.1.17. Eukaryotic cell culture

| Medium | Manufacturer |
|--------|--------------|
| DMEM   | Invitrogen   |

| Antibiotic              | Stock solution | Final concentration |
|-------------------------|----------------|---------------------|
| Fetal Calf Serum (FCS)  | Invitrogen     | 10x stock           |
| Penicillin/Streptomycin | Invitrogen     | 10x stock           |
| Trypsin-EDTA            | Invitrogen     |                     |

3.2. **Methods**3.2.1. Bacterial manipulation**Preparation of electrocompetent cells**

For preparation of electrocompetent cells, 30 ml LB medium were inoculated with *E. coli* DH10b and incubated over night at 37°C. 1 ml of the overnight culture was diluted with 100 ml LB medium. When the culture reached the OD<sub>600</sub>, it was equally transferred into two 50 ml tubes and incubated on ice for 15-30 min. After incubation, the cultures were centrifuged for 10 min at 6000 rpm at 4°C and supernatants were discarded. The pellets were re-suspended in 1 ml of 10% glycerol and the tubes were filled up to 50 ml with 10% glycerol. Following centrifugation at 6000 rpm for 10 min at 4°C, the supernatants were discarded and the pellets were re-suspended in 1 ml of 10% glycerol. 10% glycerol was added to the suspension up to 25 ml. The suspensions were centrifuged again and the pellets re-suspended and filled up to 10 ml with 10% glycerol. After a last centrifugation step, the pellets were re-suspended with 500 µl of 10% glycerol and stored at -80°C.

### **Transformation of electrocompetent cells**

Electroporation was used to transform *E. coli*. Frozen electrocompetent cells prepared as described above were used. 1 to 5 µg of DNA were added to 50 – 70 µl of competent cells on ice. After 1 min of incubation on ice the mixture was gently transferred to a pre-chilled 0.1 cm electroporation cuvette and electroporated (Gene Pulser at 1.8 kV, 25 µF and 200 Ohm, program: bacteria). After electroporation the cells were immediately resuspended in LB medium and then gently transferred into a sterile 1.5 ml tube. After transformation the bacteria were plated on LB-agar plates containing a selective antibiotic. After incubation at 37°C overnight, a single colony could be picked and expanded in LB medium containing the selection antibiotic and used for DNA preparation.

### **Purification of Plasmid-DNA**

To amplify plasmid DNA, a colony of *E. coli* previously transformed with the according plasmid was grown in 50 ml of LB medium overnight. From the pellet of this culture, the plasmid-DNA was isolated using the QIAprep Spin Miniprep or Maxiprep Kit as described in the manual.

#### *3.2.2. Analysis of DNA-molecules*

### **Electrophoresis of DNA in agarose gels**

For separation of DNA fragments on agarose gel, a suspension of agarose (0.8-2%) in 1xTAE-buffer was cooked until the agarose was completely dissolved. After cooling to about 50°C, 0.5g/ml of ethidium bromide was added to the solution, and after it was poured into the gel apparatus. After gel solidification, it was loaded with the DNA mixed with loading dye and electrophoresis was performed in 1xTAE buffer at 120V for 30min. The DNA bands were visualized under UV-light.

### **Extraction of DNA fragments from agarose gel**

The DNA fragments separated by agarose-gel electrophoresis visualized by UV-light could be excised with a sterile scalpel from the gel. Afterwards this DNA was isolated from the gel using the QIAGEN Gel Extraction kit according to the manual.

### **3.2.3. Polymerase Chain Reaction (PCR)**

The Polymerase Chain Reaction (PCR) was used for amplification of specific regions of a DNA target. PCR was performed in an 30 µl reaction mix containing 3 µl of 10x Taq-Polymerase buffer, 1 µl of 2mM dNTP-mix, 0.5 µl of 20 pM forward and reverse primer and 0.3 µl of Taq-polymerase, filled up with water. The PCR reaction typically consisted of 20-40 cycles. An initialization step for 10 min at 95°C was followed by a cycling of the denaturation step (for 30 sec at 95°C), the annealing step (temperature depending on the primers used) and the elongation step (30 sec-1 min at 72°C). Finally, before cooling down the reaction mix, an additional elongation step was carried out at 72°C for 10 min. PCR reactions were performed as described unless other conditions are mentioned.

### **3.2.4. Enzymatic manipulation of DNA**

#### **Restriction digestion of DNA using restrictionendonucleases**

Restrictionendonucleases specifically bind to doublestranded DNA and cut in or next to their 4-8 base pairs target sequence. For digestion of 0.5 µg of DNA, it was incubated for 2 h at 37°C with 0.5-1 µl of each restrictionendonuclease used, 2 µl of the appropriate buffer and water up to a final volume of 20 µl. After digestion, the enzymes were inactivated for 20 min at their specific

inactivation temperature. The exact composition of the according buffers and the reaction conditions are described in the catalogue of the enzyme supplier.

### **Dephosphorylation of digested plasmid- DNA**

To prevent re-ligation of linearized plasmid- DNA the 5'-phosphate-groups were removed from the DNA- ends. This was achieved by incubating 0.9  $\mu$ l of Calf Intestine Alkaline Phosphatase (CIAP) and 2.1  $\mu$ l of CIAP buffer together with 20  $\mu$ l of digested DNA for 2 h at 37°C. To remove the phosphatase and buffer from the reaction mix, PCR purification was performed using QIAquick PCR Purification Kit (according to the included manual).

### **Purification of PCR products**

To remove the nucleotides and the Taq-polymerase buffer from the PCR product, the PCR reaction solution was purified using the QIAquick PCR Purification Kit according to the included manual.

### **Ligation of DNA fragments**

Ligation of DNA fragments was catalyzed by DNA Ligase. For this reaction, the concentration of the insert was about three times higher than the vector concentration. 1.5  $\mu$ l of 10x ligation buffer and 1-2 units of T4-Ligase were added to the vector and insert and water was filled up to 15  $\mu$ l. The reaction was performed for 2 h at 22°C or overnight at 14°C.

#### **3.2.5. Isolation of RNA**

##### **RNA isolation from eukaryotic cells**

To isolate RNA, the cells were centrifuged for 5 min at room temperature (500 rpm) and the pellet was then resuspended in 1 ml peqGold TriFast for cell lysis. After 5 min of incubation at

room temperature, 200 µl of chloroform p.A. were added. The mixture was incubated for 3-10 min at room temperature. After incubation, centrifugation for 5 min at 12000 rpm separated the mixture in three phases. The upper colorless phase containing RNA was transferred into a fresh 1.5 ml cap and 500 µl of isopropanol were added. After incubation on ice for 5-15 min, the solution was centrifuged for 10 min at 4°C (12000 rpm). The supernatant was discarded and 1 ml of 75% ethanol was added. After vortexing, new centrifugation was performed for 10 min at 4°C (12000 rpm). The supernatant was discarded and the pellet was washed again with ethanol as described before. The pellet was then air dried and resuspended in 40 µl of RNase free DEPC treated dH<sub>2</sub>O.

### **Quantification of RNA**

Quantification of extracted RNA from each sample was done using a spectrophotometer. RNA in the solution was quantified by the absorbance of light (260 nm) in spectrophotometer.

#### **3.2.6. Real-Time PCR**

##### **cDNA synthesis**

cDNA was synthesized from RNA isolated from eukaryotic cells. For cDNA synthesis, the First Strand cDNA Synthesis Kit was used according to the included manual. DNA concentration was determined using a spectrophotometer. DNA in the solution was quantified by the absorbance of light (260 nm) in spectrophotometer.

##### **Real-Time PCR**

Depending on the cDNA-quality, 0.5-2 µl of cDNA was used as template for Real-Time PCR analysis. 10 µl of the PerfeCTa<sup>®</sup> SYBR<sup>®</sup> Green FastMix<sup>®</sup>, ROX<sup>™</sup> Master mix (if not specified

otherwise), the template cDNA, 0.5  $\mu$ M of the specific forward and reverse primers for the gene of interest or for the housekeeping gene, respectively, were used in a 20  $\mu$ l reaction. If not specified otherwise, the conditions used were: 1 cycle: 95°C x 15 minutes; 42 cycles: 95°C x 15 seconds / annealing temperature x 40 seconds, read; melting curve 65°C - 95°C, read every 1°C. To calculate the relative amount of the transcript of the gene of interest, the amplification efficiency was raised to the power of the threshold cycle (Ct-value). This gives the number of cycles necessary for the product to be detectable. The resulting value was normalized against the level of the housekeeping gene for all samples in the same experiment. Assays were performed in triplicates following the manufacturer's instructions in the Step One Plus detection system (if not specified otherwise).

### 3.2.7. Bisulfite sequencing

#### **DNA isolation from paraffin sections for bisulfite sequencing**

After GATA4-staining sections were air dried and GATA4-positive and -negative tumor regions were scratched from the slide using a scalpel. Material was collected in 30  $\mu$ l of lysis buffer and incubated overnight at 37°C. For inactivation of proteinase K samples were heated at 95°C for 20 min. DNA was then precipitated and used for 454- and bisulfite sequencing.

#### **Conventional- and next generation- bisulfite sequencing**

For conventional bisulfite sequencing DNA from cultured cells was prepared using the DNeasy Blood & Tissue Kit according to the specifications of the manufacturer. Ca. 250 ng up to 1  $\mu$ g of DNA was bisulfite treated with the EpiTect Bisulfite Kit according to the manufacturer's instructions. Deaminated DNA was amplified by PCR using the following primers COGATA4-prom\_up and COGATA4-prom\_lo (annealing temperature 55°C) listed on the Material section.



PCR conditions were as follows: 95°C for 3 min followed by 40 cycles at 95°C for 30 sec, annealing temperature for 40 sec and 72°C for 45 sec. At last, the reaction was incubated at 72°C for 3 min. PCR products were gel extracted using the QIAquick Gel Extraction Kit and cloned using the TOPO TA cloning Kit for sequencing, according to the manufacturer's instructions. DNA from picked clones was prepared using the QIAprep Spin Miniprep Kit and sent for sequencing (GATC Konstanz, Germany).

For next generation bisulfite sequencing DNA from cultured cells or paraffin section was prepared as described above. Ca. 250 ng up to 1 µg of DNA was bisulfite treated with the EpiTect Bisulfite Kit according to the manufacturer's instructions. Deaminated DNA was amplified by PCR using the primer mentioned above, but with the 454-adaptor sequence added and an identifier 4-base code for each tissue sample: 454-COGATA4-prom\_up and 454-COGATA4-1\_lo listed in the Material section. PCR conditions were as follows: 95°C for 3 min followed by 40 cycles at 95°C for 30 sec, annealing temperature for 40 sec and 72°C for 45 sec, followed by a 3 min incubation at 72°C. PCR products were subsequently purified using the QIAquick gel extraction Kit. For sequencing, equimolar amounts of all amplicons were combined in a single tube. Roche 454 FLX Standard sequencing was provided by the Core Genomics and Proteomics Core Facility of the DKFZ and performed by Achim Breiling.

### 3.2.8. Array-based DNA methylation profiling (Infinium-chip)

Analysis of the whole genome methylation status in A549 and A549 J5-1 cells was performed by Achim Breiling at the Division of Epigenetics from The German Cancer Research Center (DKFZ) in Heidelberg, using Infinium HumanMethylation27 bead chip technology (Illumina) according to the manufacturer's instructions.

### 3.2.9. Chromatin immunoprecipitation

Chromatin immunoprecipitation experiments were carried out by Achim Breiling. Crosslinked chromatin from A549 control cells or A549 J5-1 cells was prepared and immunoprecipitated as described previously<sup>56</sup>. ChIP-grade antibodies are listed in the Material section. Immunoprecipitates were dissolved in 30 µl of TE buffer. 1 µl was analysed by Real-Time PCR using a primer pair specific for the *GATA4* promoter region (CHIPGATA4\_up and CHIPGATA4\_lo) in 10 µl PCR reactions, using the Absolute QPCR SYBR Green Mix and a Roche LightCycler 480. PCR conditions: 1 cycle: 95°C x 15 min; 42 cycles: 95°C x 15 sec / 60°C x 40 sec, read; melting curve 65°C - 95°C, read every 1°C. Cycle threshold numbers for each amplification were measured with the LightCycler 480 software and enrichments were calculated as percentage of the input.

### 3.2.10. Freezing cell lines

Trypsinized cells were spun down in a centrifuge for 5 min at room temperature (1000rpm) and the pellet was washed with PBS, counted using a Neubauer chamber and diluted in ice-cold medium containing 20% FCS and 10% DMSO to obtain at least  $1-2 \times 10^6$  cells per ml. 1 ml of this cell suspension was then transferred into a cryotube and stored at -80°C for at least 24 h. For prolonged storage the cryotubes were then transferred to liquid nitrogen. For reculturing of the frozen cells, the cell suspension was defrosted at 37°C and immediately put into prewarmed medium. To remove the toxic DMSO, the cells were spun down for 5 min at 37°C (1000rpm) and the pellet was resuspended in warm medium and cultured at 37°C.

*3.2.11. Transfection of eukaryotic cells using lipofectamine*

Introduction of plasmid DNA into eukaryotic cells was carried out with a cationic lipid (Lipofectamine TM 2000) enabling the DNA to pass the cell membrane. The procedure was performed according to the manual. For stable transfection, appropriate antibiotics for selection were added 48 hrs after transfection.

*3.2.12. Viral infection of cell lines*

For viral transfection, the viral plasmid (pBpuro c-MYC-ER<sup>TM</sup> 55, pLKO.1-puro-shGATA4, pLKO.1-puro-shMAZ or pEGZ GATA4) was transfected into the amphotrophic retrovirus producer cell line Phoenix using lipofectamine, as described above. The transfected cells were incubated at 37°C for 48 hours, and supernatant was then collected and centrifuged at 500 rpm at 4°C and used for infection of the eukaryotic cells in the presence of 8 µg/ml of polybrene. 24 h after infection, appropriate antibiotics were added to the medium for selection.

*3.2.13. Soft agar assay*

For the soft agar assay, the bottom agar was prepared using an autoclaved stock of 5% sea plaque agarose, which was microwaved and mixed with DMEM medium to a final concentration of 0.5% agarose. 5ml of 0.5% agarose were poured in a 60 mm dish. For the top agar the 5% stock was diluted to 0.6% agarose with DMEM medium and stored in a waterbath at 40°C. Dilutions of the cells were prepared in 1 ml of medium (10000 cells per 60mm dish) and then mixed 1:1 with the 0.6% agarose. The mixture was poured on top of the solidified bottom agar. After solidification of the top agar, the dishes were incubated in a wet chamber at 37°C for 21-28 days, when the colonies number was counted.

#### 3.2.14. Immunocytochemistry

Immunocytochemistry was performed on cells grown on coverslips. After fixation using 4% PFA-PBS for 15 min at room temperature, cells were washed with PBS. To prevent unspecific antibody binding, cells were blocked with 4% goat serum, 0,3% Triton X-100 in PBS for 1 h at room temperature. The primary antibody (GATA4, sc-25310) was diluted 1:200 in 4% goat serum in PBS and applied over night at 4°C. After washing with PBS the cells were incubated with the secondary antibody (Anti-mouse-Cy3 – from Goat) diluted 1:100 in 4% goat serum in PBS for 2 h at room temperature. Before mounting with mowiol, cells were counterstained using DAPI (1:200) for 20 min at room temperature. Cells were observed under fluorescence microscopy.

#### 3.2.15. Luciferase reporter assay

A 455 bp fragment upstream of the transcription start site of *GATA4* was amplified from genomic DNA from HeLa cells using the primers GATA4\_P\_455\_fwd and GATA4\_P\_rev listed in the Material section. The fragment was subcloned into XhoI and HindIII sites of the pGL3 Luciferase Reporter- Basic Vector by enzymatic reaction. A549 and A549 J5-1 cells were transfected independently with the pGL3 vector containing the *GATA4* promoter and with the pGL3 control vector containing luciferase under control of a SV40 promoter. Caco-2 cells were transfected with the same vectors and used as a positive control, as they normally express *GATA4*<sup>57</sup>. To measure luciferase activity, ONE-Glo Luciferase Assay System was used and performed in 96 well plates according to the recommendations in the manual. The microplate reader was pre-heated to 37°C and the luminescence was measured with an integration time of 100 ms.

*3.2.16. Proliferation assessment of adherent cells*

To assess the proliferation of A549 and A549 GATA4-11 cells a MTT assay was used. Cell suspensions were plated into 96-well plates at  $1.3 \times 10^4$  cells/per well. Twelve parallel wells were designated for each experimental group. Cells were grown for 48 hours. At this time point, 50  $\mu$ l of MTT (5 mg/ml) were added to the wells and incubated at 37°C for 30 min in the dark before the culture medium was discarded, and the reaction terminated by adding 150  $\mu$ l of undiluted DMSO. The optical density (OD) at a wavelength of 540 nm was read on a microplate reader to determine cell numbers.

*3.2.17. Wound healing assay*

To assess the migration ability of cancer cells, a wound healing test was used. The cells were seeded in a 6-well plate (3 wells with A549 and 3 wells with A549 GATA4-11 cells) and when they reached confluence after 72 h, a straight scratch was made in the monolayer using a pipette tip (100  $\mu$ l), simulating a wound. The images were captured at the beginning and at regular intervals during cell migration until close the wound.

*3.2.18. Animal experiments*

All animal experiments were performed according the German law for animal protection. Animals used in transplantation experiments were sacrificed by hypoxia in a carbon dioxide chamber. All the other animals were sacrificed under general anesthesia by heart perfusion with 4% PFA-PBS and the lungs, livers and lymph nodes were collected for histology.

### 3.2.19. Preparation of tissue-sections

The fresh tissue collected from mouse was washed with PBS and fixed in 4% PFA in PBS at 4°C overnight. After washing with PBS, the tissue was stored in 70% ethanol at 4°C until the embedding procedure. For paraffinization, tissues were sequentially embedded in the following solutions at room temperature: 50% ethanol (40 min), 70% ethanol (40 min), 80% ethanol (40 min), 90% ethanol (40 min), 95% ethanol (40 min), 3 x 100% ethanol (40 min), 2 x chloroform:ethanol (1:1) (30 min) and chloroform (30 min). After paraffinization the tissues were transferred into melted paraffin and incubated for 1 h at 65°C and then in fresh paraffin 2 h or overnight at 65°C. Finally, the tissue was casted into paraffin blocks. Paraffin blocks were sectioned into 6-10 µm microsections and used for the further histological analysis.

### 3.2.20. Hematoxylin and eosin (HE) staining

For histological analysis of paraffin sections, the tissues were stained with hematoxylin and eosin (HE). First, paraffin had to be removed from the sections, and then the tissues were stained with HE, dehydrated and mounted with entellan. For the staining, the sections were embedded in the following solutions: 2 x xylol (10 min), 3 x 100% ethanol (5 min), 70% ethanol (10 min), millipore water (5 min), hematoxilyn (30 sec), tap water (5 min), Millipore water (5 min), eosin (20 sec), millipore water (5 min), 70% ethanol (10 min), 3 x 100% ethanol (5 min) and 2 x xylol (10 min).

### 3.2.21. Immunohistochemistry

Immunohistochemistry was performed on paraffin sections. After deparaffinization and rehydration, sections were boiled in 10 mM citrate buffer for 10-20 min for antigen retrieval. To

quench the endogenous peroxidase activity sections were incubated with methanol or PBS containing 1-3% H<sub>2</sub>O<sub>2</sub>. Non-specific antibody binding was prevented by incubation with 5% of serum with 0.2% Triton X-100 in PBS for 1 hour at room temperature. After blocking, sections were incubated with the primary antibody (GATA4, sc-1237, Santa Cruz (1:200); Pro Sp-C, gift from Jeffrey A. Whitsett (1:5000)) over night at 4°C. After washing, sections were incubated with the corresponding biotinylated secondary antibodies (Dako) at 1:200-600 for 1 hour at room temperature. For staining ABC reagent was applied (Vectastain Elite ABX Kit, Vector Labs) and color was developed with diaminobenzidine (DAB). For counterstaining haematoxylin was used. After dehydration the stainings were mounted with entellan. For immunofluorescence staining, the following secondary antibodies were used: donkey anti-goat Cy5 and donkey anti-rabbit Cy3 at 1:200 dilutions.

#### 3.2.22. Genotyping of transgenic mice

DNA for genotyping was obtained from the mouse tails cut in the age of 3-4 weeks. The tails were lysed in 190 µl of tail lysis buffer and 12 µl of 0.4 mg/ml of proteinase K and incubated overnight at 54°C. The resulting lysate was centrifuged at 10000 rpm for 5 min and the supernatant was diluted 1:10 with water and used as a PCR template. PCR reaction was carried out as described above with primers for genotyping listed in the material part.

#### 3.2.23. Transplantation experiments

For transplantation experiments, A549/GFP and A549 GATA4-11 cells were injected subcutaneously in Athymic Nude - Foxn1nu mice. Before injection, the cells were washed two times with sterile PBS and counted.  $2.5 \times 10^6$  cells were resuspended in 100 µl of PBS and

injected subcutaneously into the Athymic Nude - Foxn1nu mice. The tumor size was measured two times per week and the animals were sacrificed when the tumors were necrotic or close to 2 cm of diameter.

#### 3.2.24. *In vivo bioluminescence imaging*

##### **Imaging of luciferase expression**

Bioluminescence imaging of luciferase expression in compound mice (Sp-C-C-RAF BxB/Sp-C-rtTA/tet-O-c-MYC) was performed as described<sup>58</sup>. Briefly, mice were anesthetized with ketamine/rompun and subsequently received an i.p. injection of an aqueous solution of the substrate D-luciferin (125 mg/kg). The animals were then placed in a light-tight chamber and imaged with a CCD camera. Images were acquired 20 min after luciferin administration. Signal intensity was quantified as the sum of all detected photon counts within the region of interest after subtraction of background luminescence, using the Argus100 Low Light Imaging System.

##### **Imaging of GFP expression**

Bioluminescence imaging of GFP expression in live animals was performed weekly. For imaging and quantification of GFP intensity a Maestro EX imaging system built equipped with a GFP-Filter Set (445 - 490 nm excitation filter and 515 nm longpass emission filter) was used. Quantitative measurements were performed using the Maestro Software 2.10.0.

### 3.3. *Statistical Analysis*

Statistical analyses of data sets were performed using the Graphpad Prism version 4.0 software. For all tests, statistical significance was considered to be at  $P < 0.005$ .



The correlation between methylation and expression profiles of A549 and A549 J5-1 cells was calculated by Tobias Müller at the Department of Bioinformatics of the University of Würzburg using bioinformatic tools.

## 4. Results

### *4.1. MYC expression in NSCLC tumor cells induces cell type change and metastasis formation*

It was previously reported that the combination of *c-MYC* and *C-RAF* transgenes in type II cells is sufficient to rapidly induce metastasis to liver and lymph nodes. The combination of these two transgenes also causes appearance of a phenotypic switch from cuboidal to Alveolar Papillary Columnar Epithelial cells (APECs) in NSCLC tumors. Furthermore, cells with this phenotype have shown that they develop tumors which grow more rapidly, and are also predominate in liver metastasis<sup>2</sup>.

In this work, a triple transgenic mouse model was used to test the appearance and reversibility of this switch. The transgenic mice (Sp-C-C-RAF BxB/Sp-C-rtTA/tetO-c-MYC) express constitutively C-RAF BxB and conditionally c-MYC, under the control of an inducible promoter. The promoter used in this system contains a tetracycline-responsive element (Tet-O), which can be bound by the reverse tetracycline-controlled transcription activator protein (rtTA) in the presence of doxycycline, inducing the transcription of c-MYC<sup>59</sup>. This mouse model expresses rtTA under the control of a tissue-specific promoter, Sp-C. Therefore, these mice express the oncogenic c-MYC tissue-specifically by doxycycline feeding. The DOX treatment of the triple transgenic mice rapidly induced appearance of columnar cells in their lung tumors (Fig. 4.1.A). As these animals express luciferase under the control of the Tet-O promoter, the animals fed with DOX food were imaged after 1 week of treatment, showing that MYC expression was induced (Fig. 4.1.B). Following this period, DOX food was withdrawn for 4 weeks, and the animals were imaged again at this time point.

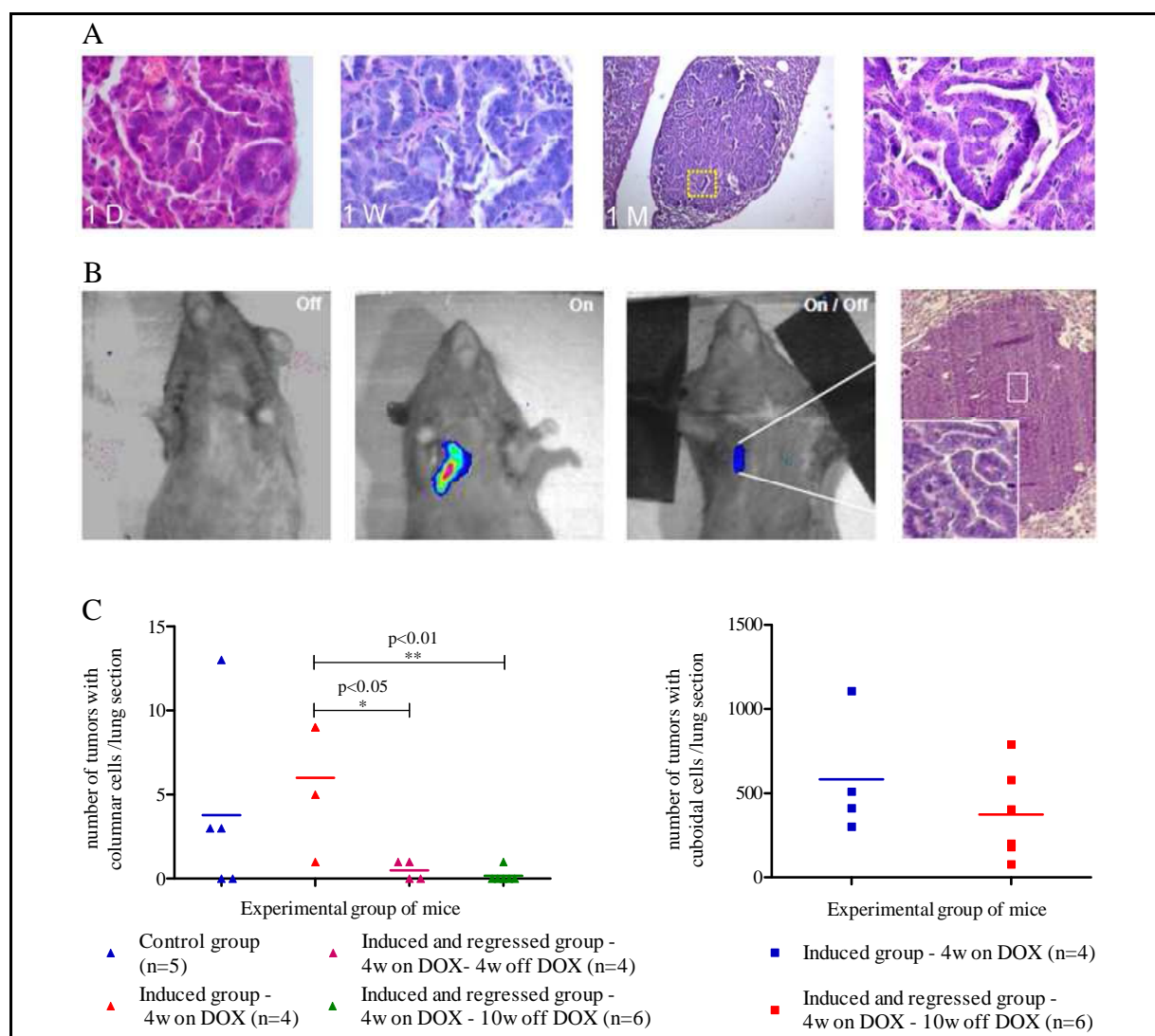


#### Figure 4.1. Conditional MYC expression in type II pneumocytes expressing C-RAF BxB.

(A) HE staining of lung tumor sections from inducible (Sp-C-C-RAF BxB/Sp-C-rtTA/tetO-c-MYC) compound mice shows the kinetics of columnar cell appearance<sup>2</sup>. D: day, W: week, M: month. Right hand panel is a magnification of the yellow box. Scale bar 100  $\mu$ m. (B) Luciferase imaging of inducible mice – Sp-C-C-RAF BxB/Sp-C-rtTA/tetO-c-MYC. Six weeks old compound mice were imaged for *in vivo* luciferase expression following one week On DOX/4 weeks Off DOX schedule demonstrating inducibility. HE staining of a lung tumor section of the On/Off DOX mouse. Inset highlights persistent papillary tumor area<sup>2</sup>. (C) Regression experiment in triple transgenic animals (Tet-o-c-MYC/Sp-C-rtTA/Sp-C-C-RAF BxB). A group of 4 animals fed with doxycycline for 4 weeks showed an increase of tumors with columnar cells, when compared with the control. On the other hand, when the doxycycline feeding was removed for 4 weeks after 4 weeks of induction, a highly significant decrease in the number of tumors with columnar cells was observed. The number of columnar tumors in the lung of the animals where the doxycycline

was withdrawn for 10 weeks also decreased drastically. These data shows that the withdrawal of MYC is reverting the switch from cuboidal to columnar tumor cells; w - weeks.

This result shows the reversibility of *c-MYC* transgene expression. Histological analysis of the imaged lung tumor showed persistence of columnar cells in the center of one remaining tumor that otherwise displays a cuboidal phenotype (Fig. 4.1.B)<sup>2</sup>. Extension of the observation period after DOX removal to 10 weeks demonstrated elimination of columnar cells in tumors of all mice analyzed (Fig. 4.1.C). These data suggest a “shock from oncogene withdrawal” –effect<sup>60</sup>.

The addition of *c-MYC* to oncogenic C-RAF in these animals showed the development of liver macrometastasis after 7 months of MYC induction (Fig. 4.2.), in contrast to single transgenic animals Sp-C-C-RAF BxB, which although were uniformly tumor positive at 2 weeks of age<sup>2</sup>, were not able to develop metastasis.

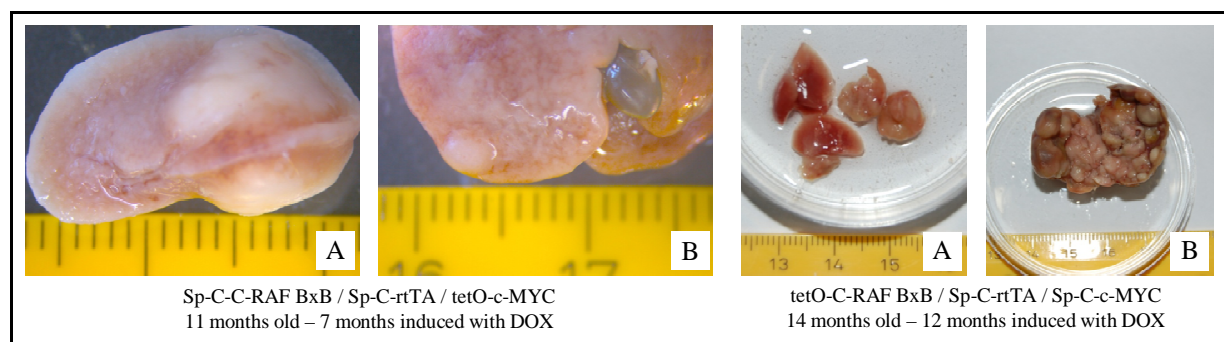


**Figure 4.2. Macroscopic inspection of organs from Sp-C-C-RAF BxB/Sp-C-rtTA/tetO-c-MYC animals after DOX induction.**

(A) Primary tumor in lung. (B) Metastatic tumors in liver.

Another mouse model which constitutively expresses *c-MYC* under the control of Sp-C promoter, and conditionally expresses C-RAF BxB under the control of the TetO promoter,

---

following the same principle of the model described above, was inspected for the development of metastasis in the liver. After 12 months of C-RAF BxB induction combined with constitutive c-MYC expression showed the development of highly pronounced macrometastasis (Fig. 4.2)

#### **4.2. MYC induces GATA4 expression in NSCLC**

GATA6-WNT pathway is required for epithelial stem cell development and airway regeneration<sup>61</sup>. In turn, GATA4 is involved in maintenance of adult intestine<sup>45</sup>. It was shown by our group a GATA6 to GATA4 switch in Sp-C-c-MYC and Sp-C-C-RAF-BxB/Sp-C-c-MYC lung tumors and liver metastases. In the present work it is shown that the expression of the transgene promoter, Sp-C, is collocated in a fraction of cells with GATA4-expression (Fig. 4.3.A). Interestingly, a high percentage of GATA4 positive cells lost promoter activity of the Sp-C promoter and therefore the expression of c-MYC. This suggests that MYC induces GATA4 expression, but this expression is maintained even after the loss of c-MYC, by an epigenetic, self-perpetuating mechanism. The ability of MYC to induce GATA4 was tested *in vitro* using the cell line A549 J5-1, which highly expresses chicken v-MYC<sup>2</sup>. Real-Time PCR was performed for analysis of mRNA levels from the parental cell line, A549 and the MYC expressing cells, A549 J5-1 (Fig. 4.3.B). The levels of GATA4 mRNA and its target mucin2<sup>62</sup> were measured, and it was possible to confirm that MYC is inducing expression of functional GATA4 *in vitro* (Figs. 4.3.C and 4.3.D).

A fusion of MYC with an estrogen receptor (ER), which depends on the presence of tamoxifen (OHT) to go into the nucleus, was introduced in A549 cells (Fig. 4.4.A) and the transfected cells were selected with puromycin.

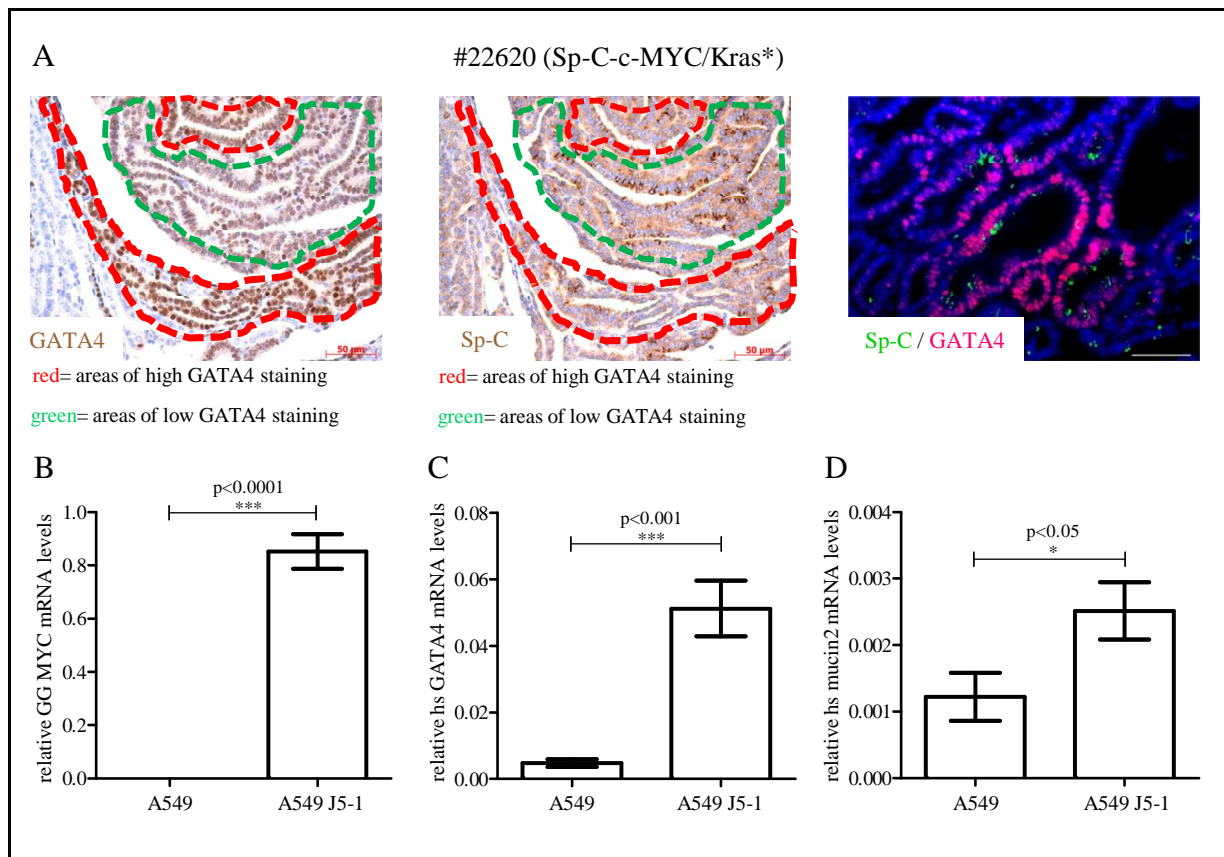


**Figure 4.3. MYC induces GATA4 expression and its target mucin2.**

(A) Staining of mouse lung tumor sections for Sp-C and GATA4 shows mutually exclusive expression patterns between them. Lung tumor serial sections were stained for Sp-C and GATA4 (left and middle panel). GATA4 high/Sp-C negative- and GATA4 low/Sp-C positive tumor regions were encircled with red and green dashed lines, respectively. The most right panel shows double immunofluorescence staining of a mouse lung tumor section for Sp-C and GATA4. Note that the majority of GATA4 positive tumor cells (red) are negative for Sp-C (green). Dapi (blue) shows nuclei. Scale bar = 50  $\mu$ m. (Collaboration with Fatih Ceteci and Simone Hausmann). (B) Chicken v-MYC mRNA levels were measured in the cell line A549 J5-1. Results show the absence of chicken v-MYC in the parental cell line A549 in contrast to the high expression observed in A549 J5-1 cells. (C) MYC shows ability to induce GATA4 expression *in vitro*. (D) The target of GATA4 in the intestine, mucin2, is upregulated in MYC expressing A549 cells, demonstrating the functionality of GATA4. All the values represent SD of the mean. Statistical differences between groups as indicated.

The newly prepared cells were seeded in soft agar to perform anchorage independent assay. MYC expression was induced with 100 nMolar of OHT for 4 weeks and at this time point the

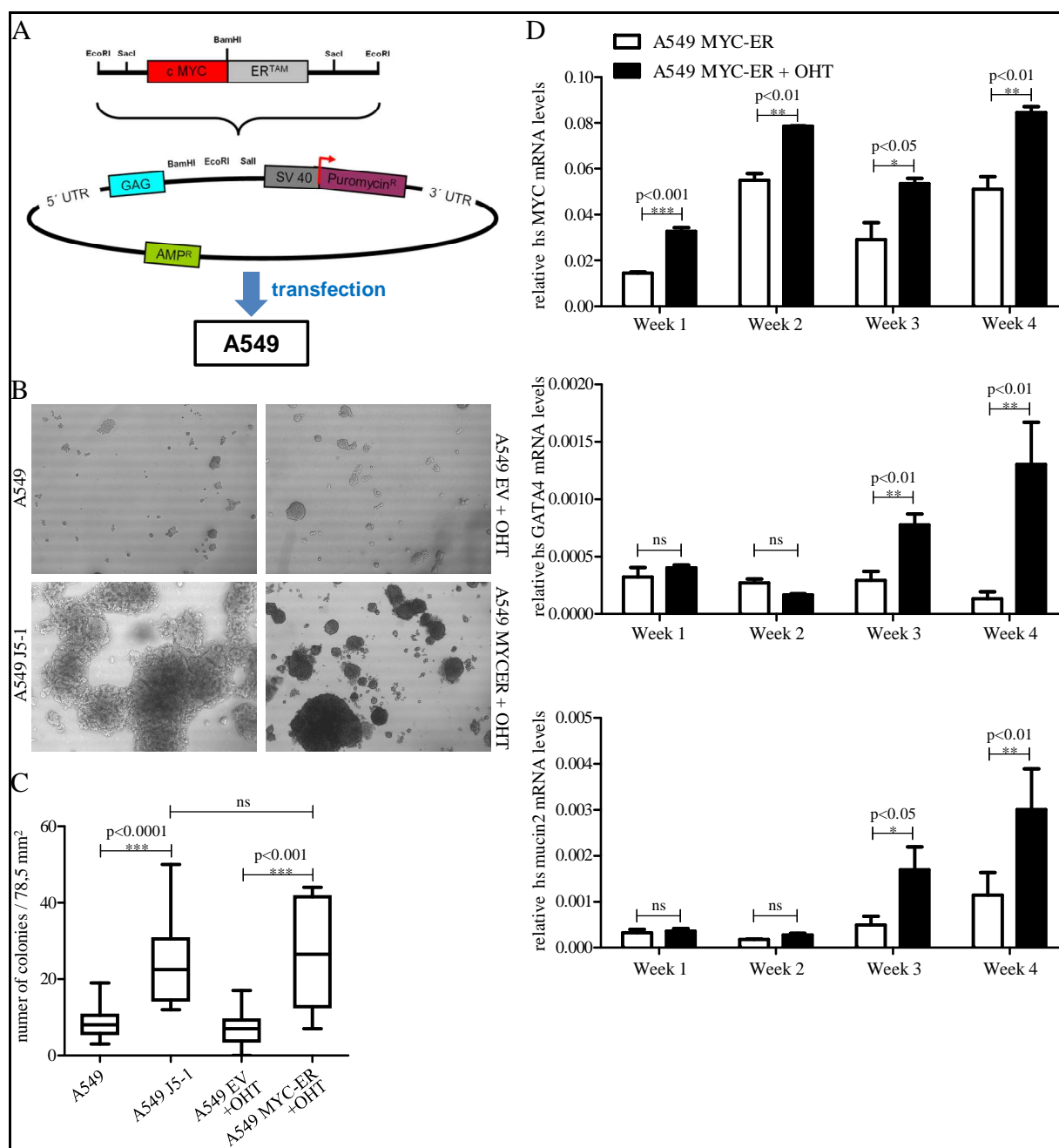


**Figure 4.4. Inducible expression of human c-MYC in A549 cells.**

(A) Establishment of a MYC-inducible NSCL cell line. A MYC-ER fusion was inserted in the puromycin-resistant plasmid pBabe, in the ECORI site<sup>55</sup>. A549 cells were transfected with the resulting plasmid. Cells carrying the plasmid were selected with puromycin. (B) Pictures from the colonies formed by A549 and A549 EV (Empty Vector) in the presence of OHT (controls), and A549 J5-1 and A549 MYC-ER in the presence of OHT, after 3 weeks in soft agar. Magnification 20x. (C) Quantification of the colonies formed by the different cells lines

---

(conditions as indicated). A549 MYC-ER cells show, in the presence of OHT, comparable ability to form colonies to the A549 J-51 cells, indicating the induction of anchorage independent growth ability by MYC. All the values represent SD of the mean. Statistical differences between groups as indicated. (D) mRNA levels of human MYC, GATA4 and mucin2 in induced and not induced A549 MYC-ER cells over time. GATA4 and its target mucin2 are upregulated after 3 weeks of MYC induction in A549 MYC-ER cells, although MYC upregulation is detected as early as 1 week after induction. All the values represent SD of the mean. Statistical differences between groups as indicated; ns – non significant.

number of colonies formed was counted. A549 and not induced A549 MYC-ER cells were used as control. A549 MYC-ER showed a significant higher number of colonies formed when compared with the controls. Moreover, the new cell line after OHT-induction, showed the same ability to form colonies anchorage independently as the cell line A549 J5-1 (Figs. 4.4.B-C).

The expression of MYC induced by tamoxifen was measured by Real-Time PCR (Fig. 4.4.D). These cells showed a significant overexpression of MYC after 1 week of induction with 100 nMolar of OHT. Moreover, we could show GATA4 and mucin2 mRNA upregulation after 3 weeks of MYC induction, although MYC induction occurs as early as 1 week after tamoxifen addition (Fig. 4.4.D). This suggests that the epigenetic changes at *GATA4* promoter level take effect at this time point.

### ***4.3. GATA4 knock-down in MYC expressing NSCLC cells inhibits the metastatic potential induced by MYC***

A549 J5-1 cells show the ability to develop metastasis when transplanted in Rag<sup>-/-</sup> mice<sup>2</sup>. To test the role of GATA4 in this gained feature, a shRNA-mediated knockdown of GATA4 was performed in A549 J5-1 cells. The cells were infected with a shRNA-producing virus (sh26) and Real-Time PCR analysis for the expression of the GATA4 and its-target gene *mucin2* was



performed (Fig. 4.5.A) in parallel with an anchorage independent growth assay in soft agar (Fig. 4.5.B). The mRNA levels of GATA4 and mucin2 were significantly increased in A549 J5-1 cells, when compared with the parental cell line A549. After sh-RNA mediated knockdown, GATA4 and its target mucin2 mRNA levels decreased significantly in A549 J5-1 cells. These cells were seeded in soft agar and the number of colonies was counted after 3 weeks (Fig. 4.5.C).

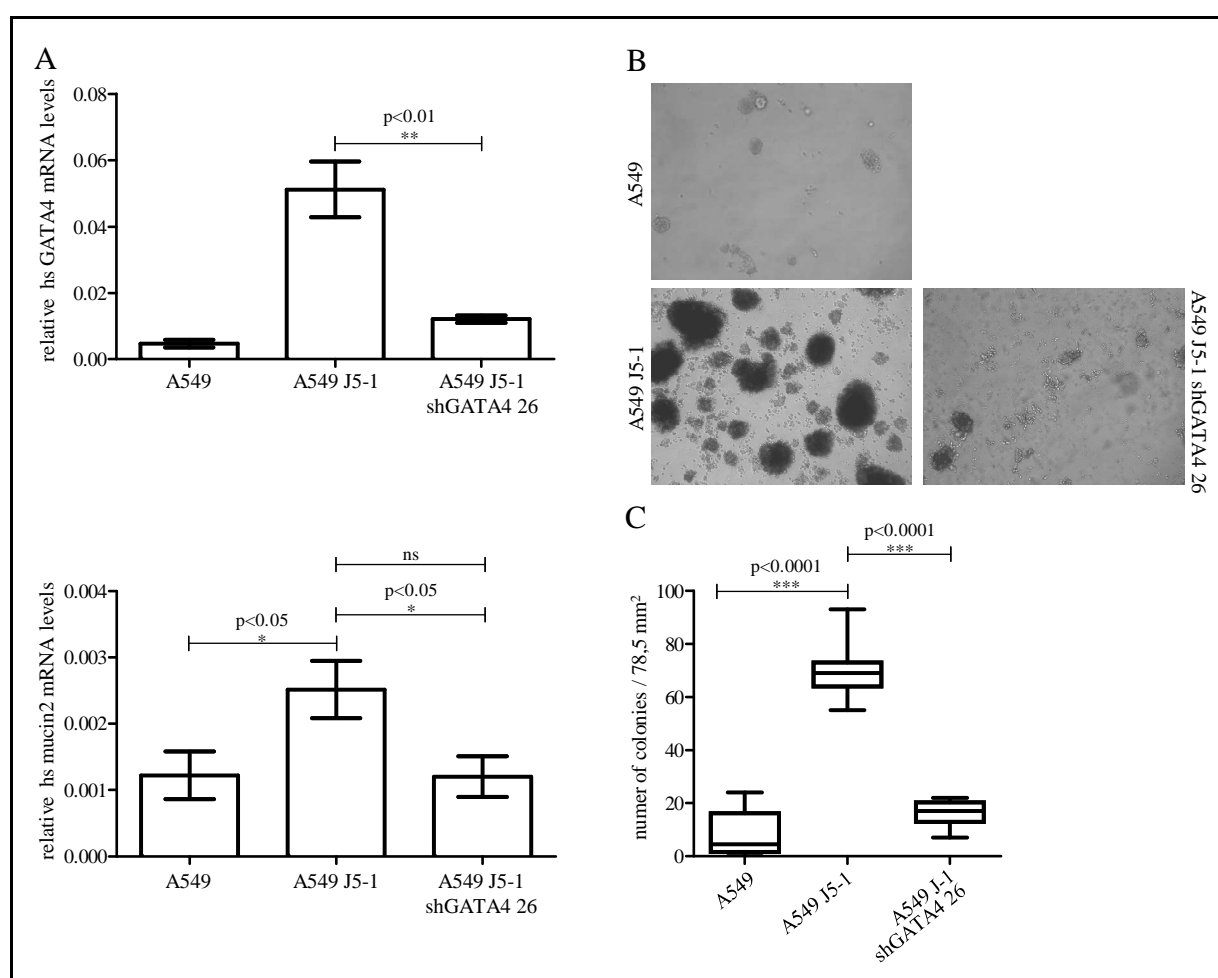


**Figure 4.5. GATA4 knockdown in A549 J5-1 cells.**

(A) Real-Time PCR analysis of A549 J5-1 cells for GATA4 and its target gene *mucin2* after GATA4 knock-down. Results show a significant upregulation of GATA4 and mucin2 in A549 J5-1 cells. shRNA 26 efficiently reduced the expression of the GATA4 and its target gene *mucin2* in A549 J5-1 cells. All the values represent SD of the

---

mean. Statistical differences between groups as indicated. (B) Pictures from the colonies formed by A549, A549 J5-1 and A549 J-51 shGATA4 26 cells after 3 weeks in soft agar. Magnification 20x. (C) Quantification of the colonies formed in soft agar by A549 J5-1 cells after GATA4 knockdown. A549 J5-1 cells show a highly significant reduction in the number of colonies formed after infection with the shRNA26-expressing virus. All the values represent SD of the mean. Statistical differences between groups as indicated; ns – non significant.

This assay showed that the knockdown of GATA4 in A549 J5-1 cells revert their ability to grow anchorage independently, an ability which has been induced by MYC. These data suggest that the expression of GATA4 is necessary for the induction of anchorage independent growth by c-MYC.

#### ***4.4. MYC induces changes in GATA4 promoter activity***

To gain more insight regarding the expression of GATA4 induced by MYC in NSCLC, a vector containing the firefly luciferase gene under the control of *GATA4* promoter was transfected into NSCLC cells, A549 and A549 J5-1. The expression of luciferase enabled the measurement of the activity of the *GATA4* promoter by luminescence assessments. Using the genomic DNA from HeLa cells as a template, a PCR reaction was performed using specific primers (*GATA4\_P\_455\_fwd* and *GATA4\_P\_rev*, listed in the Material section). A 455 bp fragment upstream of the transcription start site of *GATA4* was amplified (Fig. 4.6.A) and cloned into the pGL3 vector, which already contains firefly luciferase (Fig. 4.6.B). Therefore, A549 (control) and A549 J5-1 cells were transfected with this vector carrying the gene of luciferase under the control of *GATA4* promoter 455. Caco-2 cells were transfected with the same vectors and used as a positive control, as they normally express GATA4<sup>57</sup>. After incubation allowing the expression of the luciferase controlled by the *GATA4* promoter, a luciferase assay was performed by Sebastian Kress, and luminescence was measured. Thereby the promoter activity was recorded in A549, A549 J5-1

and Caco-2 cells for different time points making up a kinetic assay. The measured luminescence was normalized against the respective cell number and the control. As control, each cell line was transfected with the pGL3 control vector containing luciferase under control of a SV40 promoter.

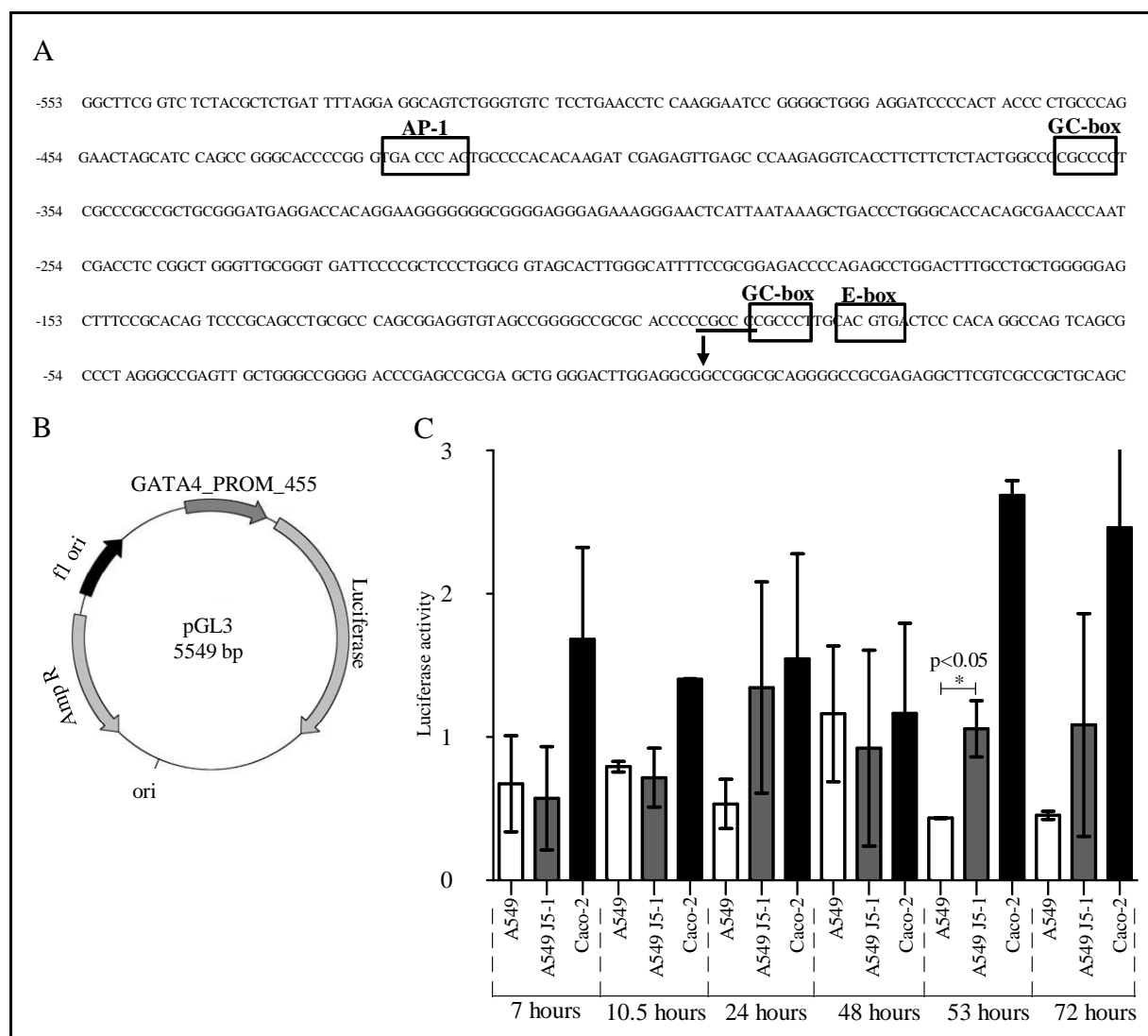


**Figure 4.6. *GATA4* promoter activity.**

(A) Nucleotide sequence of the 5'-upstream region of the human *GATA4* gene (modified from<sup>63</sup>). Nucleotides are numbered from the transcriptional start site (vertical arrow). The potential binding sites for transcription factors are boxed according to the consensus sequence: AP-1: TGACT(C/A)A, E-box: CANNTG and GC-box: GGGCGG or CCGCCC. Overlapping GC-box is underlined. (B) Modified PGL3 luciferase reporter vector: luciferase gene under

---

the control of *GATA4* promoter. This plasmid holds a promoter sequence with 455 bp upstream of the transcription start of *GATA4*. Additional description: Luciferase, cDNA encoding the modified firefly luciferase; Amp<sup>R</sup>, gene conferring ampicillin resistance in *E. coli*; f1 ori, origin of replication derived from filamentous phage; ori, origin of replication in *E. coli*. Arrows within Luciferase and the Amp<sup>R</sup> gene indicate the direction of transcription; the arrow in the f1 ori indicates the direction of ssDNA strand synthesis. (C) *GATA4* promoter activity in MYC expressing cells. In a kinetic assay the activity of the *GATA4* promoter controlling firefly luciferase was measured at different time points in A549, A549 J5-1 and Caco-2 cells. Activity of *GATA4* promoter 455 was higher in A549 J5-1 cells, when compared to A549 cells. This difference was observed from 24 h on, but significantly, it was observed just at 56 hours. All the values represent SD of the mean. Statistical differences between groups as indicated.

The activity of the *GATA4* promoter 455 was higher in A549 J5-1 cells than in the control cells A549 (Fig. 4.6.C). Measurements of luminescence in the first 10.5 h after transfection showed low luciferase expression in both cell lines, and consequently, no difference in *GATA4* promoter 455 activities. However, 24 h post- transfection the expression of luciferase increased, showing at this time point a major difference between activities of the promoter in the two cell lines, although still not significant. At the time point 53 hours, the activity of *GATA4* promoter was significantly higher in A549 J5-1 cells, when compared with the control cell line. Therefore, these data suggests *GATA4* upregulation by direct transcriptional interaction with MYC.

#### ***4.5. MYC induces GATA4 promoter demethylation in c-MYC/KRas-mutant typeII-pneumocytes***

As the *GATA4* promoter resides in a large CpG island, the hypothesis, that DNA methylation plays a role in *GATA4* regulation was tested. Thus, Achim Breiling performed 454-bisulfite-sequencing of a 389 bp long CpG-rich region, which contains the promoter region of the *GATA4* gene (Fig. 4.7), on *GATA4*-positive and –negative regions of a Sp-C-c-MYC/KRas-mutant lung tumor and on a *GATA4*-positive liver metastasis (Fig. 4.8.A).

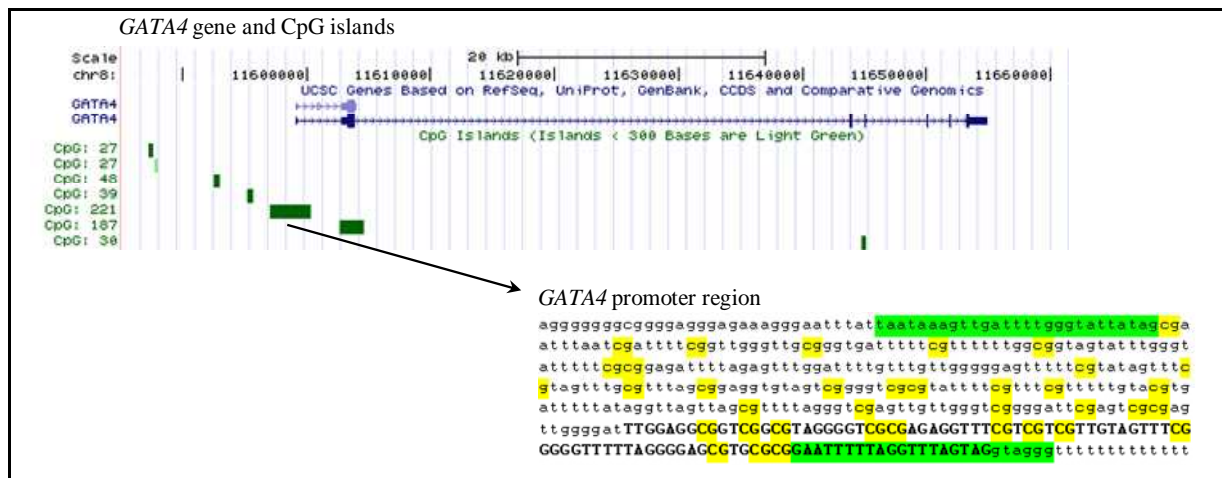


**Figure 4.7. CpG Islands present at the GATA4 promoter.**

CpG-islands in the the *GATA4* gene were identified by the UCSC Genome browser<sup>64</sup>. Below, a fragment of the promoter region containing the transcription start site is shown in the deaminated status (all Cs not in a CG context are transformed to T). CpG-sites in the CpG-island are indicated in yellow. The primer sequences used for bisulfite sequencing are highlighted in green.

The overall methylation of the examined region did not change, but looking closer, a significant lower methylation could be seen for the CpG-sites 13-18 and most significantly 19-22 in the *GATA4*-positive tumor and metastasis material (Fig. 4.8.B and Table 4.1), indicating a significant hypomethylation of these regions in *GATA4*-expressing tissue.

#### **4.6. MYC induces GATA4 promoter demethylation in human NSCLC cells**

To test whether ectopic MYC expression is sufficient to induce demethylation of the *GATA4* promoter in a human NSCLC cell line, Achim Breiling performed bisulfate sequencing of the same region analyzed above, but in A549 and A549 J5-1 cells. Also in A459 cells the *GATA4* promoter region was strongly methylated, which does not change significantly upon MYC expression (83% and 85%, respectively).

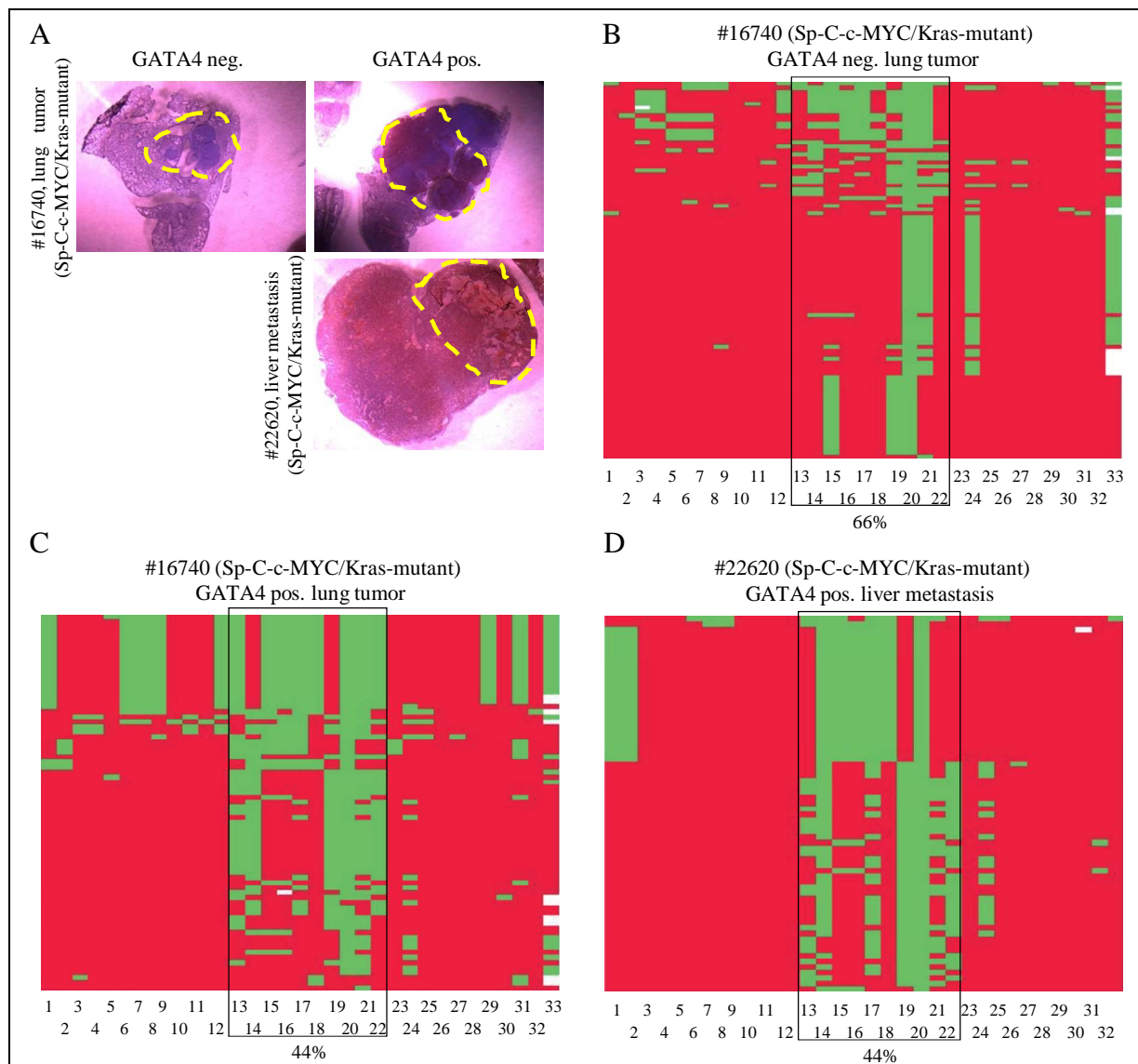


**Figure 4.8. Methylation pattern of *GATA4* promoter in a *GATA4* negative and positive region and corresponding liver metastasis.**

(A) *In vivo* material used for 454-sequencing. Lung and liver paraffin sections of Sp-C-c-MYC/KRas-mutant animals were stained for *GATA4*. The DNA from *GATA4*-positive and –negative regions (indicated with the yellow circles) was isolated. (B-D) 454-sequencing of the CpG-rich region near the *GATA4* promoter (for exact primer location see Fig. 4.7). DNA was isolated from lung tumor regions stained negatively and positively for *GATA4* and from *GATA4*-positive liver metastasis, respectively. Sequencing results are shown as heatmaps in which each row represents one sequence read. Individual red boxes indicate methylated and green boxes indicate unmethylated CpG dinucleotides. Sequencing gaps are shown in white. CpGs showing the highest degree of change between DNA from *GATA4*-positive and –negative tumor tissue are boxed. The overall methylation of the region is 76% for both

GATA4-positive and –negative lung tumors and 73% for the liver metastasis. A significant decrease in methylation of the CpGs 13-22 (boxed) was observed in GATA4 positive tissue. For statistical tests see Table 4.1. The DNA used for the 454-sequencing was isolated from GATA4-stained paraffin-sections as illustrated in A.

| CpG | GATA4 neg.<br>lung tumor | GATA4 pos.<br>lung tumor | GATA4 pos.<br>liver metastasis | p-values            |
|-----|--------------------------|--------------------------|--------------------------------|---------------------|
| 13  | 91%                      | 35%                      | 69%                            | 0.00000 / 0.00006 * |
| 14  | 77%                      | 49%                      | 12%                            | 0.00002 / 0.00000 * |
| 15  | 63%                      | 56%                      | 57%                            | 0.38834 / 0.47138   |
| 16  | 79%                      | 55%                      | 58%                            | 0.00017 / 0.00073 * |
| 17  | 79%                      | 51%                      | 27%                            | 0.00002 / 0.00000 * |
| 18  | 90%                      | 68%                      | 61%                            | 0.00008 / 0.00000 * |
| 19  | 56%                      | 52%                      | 40%                            | 0.58037 / 0.02354   |
| 20  | 3%                       | 5%                       | 0%                             | 0.23474 / 0.11188   |
| 21  | 31%                      | 21%                      | 67%                            | 0.03541 / 0.00000 * |
| 22  | 90%                      | 36%                      | 51%                            | 0.00000 / 0.00000 * |

\* p<0.05 for both GATA4 positive samples, DMC

**Table 4.1 – Statistical significance of methylation percentage differences at *GATA4* promoter of *GATA4* positive and negative lung tumors and *GATA4* positive liver metastasis tissues.**

The table shows the percentage of methylation (percentage of remaining cytosines after bisulfite conversion) for the CpG dinucleotides 13 to 22 shown in Fig. 4.8 in the three tumor types. The last column shows the p-values as determined using Fisher's exact test comparing each of the *GATA4* positive sample set (second and third column) with the *GATA4* negative set (first column). Rows with p-values below 0.05, indicating a statistical significant difference between *GATA4* negative and *GATA4* positive sample sets and therefore differently methylated CpGs (DMCs), are marked by an asterisk.

Nevertheless, also in these cell lines, a significant change in methylation was observed at CpG-sites 19-22 from 60% in the A549 cells to 23% in the A549 J5-1 cells (Fig. 4.9.A).

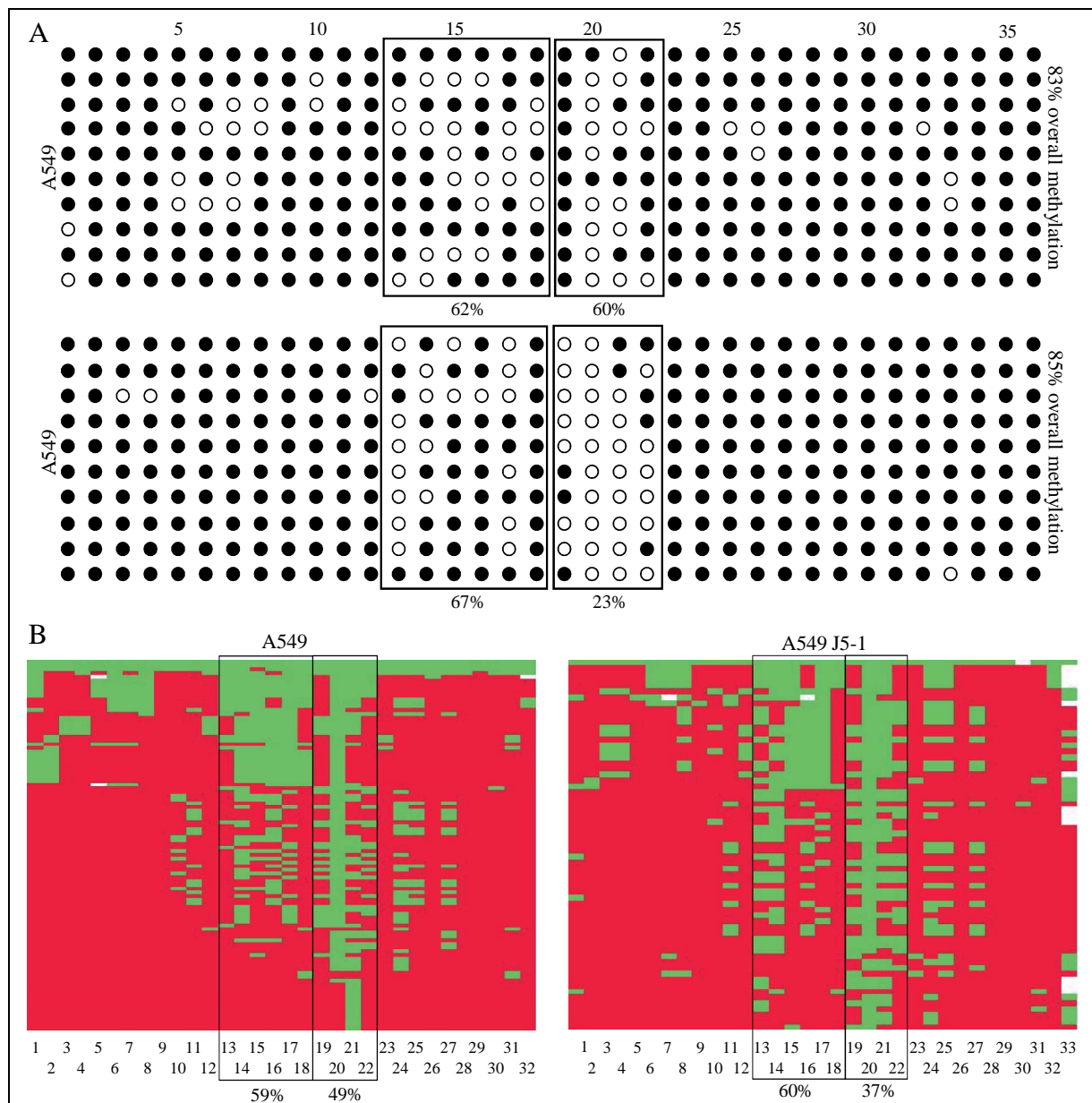


**Figure 4.9. Site-specific demethylation of CpG dinucleotides in the promoter region of *GATA4* upon MYC expression in A549 cells.**

(A) Bisulfite sequencing of the *GATA4* promoter in A549 and A549 J5-1 cells (for exact primer location see Fig. 4.7 and Fig. 4.10.A). Open circles = unmethylated CpGs; filled circles = methylated CpGs. Each row represents a single clone. No significant change in the overall methylation status of the CpG-rich region near the *GATA4* promoter was observed, but the CpGs 19-22 were differentially methylated. (B) 454-sequencing of the same region as in “A” (for exact primer location see Fig. 4.7). Sequencing results are shown as heatmaps in which each row represents one sequence read. Individual red boxes indicate methylated and green boxes indicate unmethylated CpG dinucleotides.



Sequencing gaps are shown in white. There is no significant change in the overall methylation-status of the region, but significant demethylation of the CpGs 19-22 (left box) was observed. Note that the most pronounced change in the degree of methylation is seen in CpG 22. For statistical analysis see Table 4.2.

This was basically confirmed using 454-bisulfite-sequencing, which was also performed by Achim Breiling. As shown in Fig. 4.9.B, the overall methylation was 72% and 71%, in A549 and A549 J5-1 cells, respectively, whereas the methylation of the CpG-sites 19-22 significantly changed from 49% in the A549 cells to 37% in the A549 J5-1 cells (Figs. 4.9.B, Table 4.2).

| CpG | A549 | A549 J5-1 | p-values  | CpG |
|-----|------|-----------|-----------|-----|
| 19  | 72%  | 51%       | 0.00111 * | 19  |
| 20  | 16%  | 5%        | 0.00733 * | 20  |
| 21  | 39%  | 32%       | 0.30010   | 21  |
| 22  | 70%  | 59%       | 0.03170 * | 22  |

\* p<0.05, DMC

**Table 4.2 – Statistical significance of methylation percentage changes at *GATA4* promoter upon MYC expression in A549 cells.**

The table shows the percentage of methylation (percentage of remaining cytosines after bisulfite conversion) for the CpG dinucleotides 19 to 22 shown in Fig. 4.9 in A549 and A549 J5-1 cells. The last column shows the p-values as determined using Fisher's exact test comparing both samples.

#### ***4.7. Epigenetic landscape of the *GATA4* promoter changes upon MYC expression***

To complement the analysis of epigenetic modifications in the *GATA4* promoter, histone modifications in the same region were mapped by chromatin immunoprecipitation (ChIP) with the collaboration of Achim Breiling. Locations of ChIP primer pairs are shown in Fig. 4.10.A. Chromatin was prepared from A549 control and MYC expressing A549 J5-1 cells and

precipitated with antibodies against histone H3 dimethylated at lysine 9 (H3K9me2), histone H3 trimethylated at lysine 9 (H3K9me3), histone H3 dimethylated at lysine 4 (H3K4me2), histone H3 trimethylated at lysine 4 (H3K4me3) and histone H3 trimethylated at lysine 27 (H3K27me3).

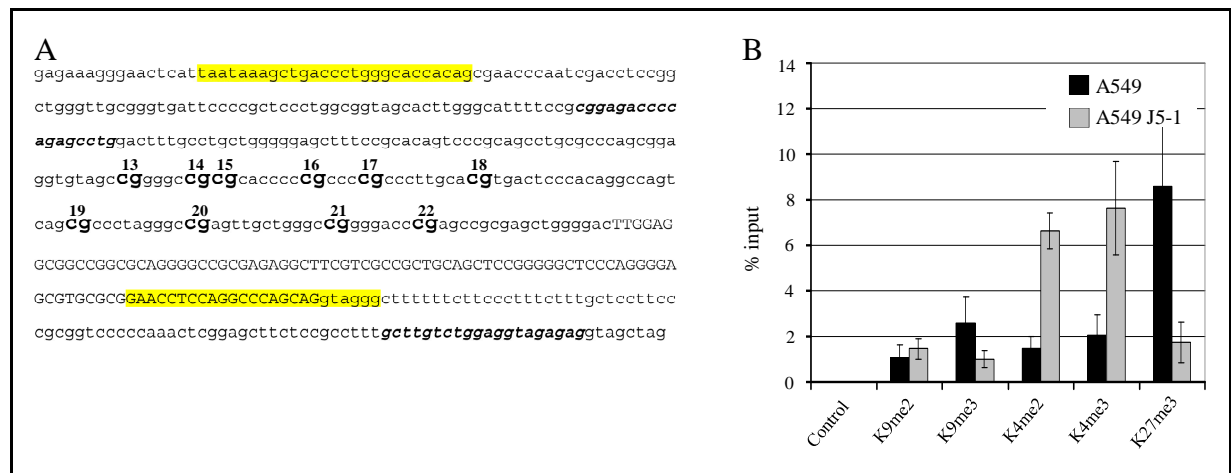


**Figure 4.10. Chromatin immunoprecipitation (IP) analysis of the *GATA4* promoter region in control (A549) and MYC expressing cells (J5-1).**

(A) Genomic promoter region of *GATA4*. The first exon is indicated with capital letters. Sequences corresponding to the primer pair used for bisulfite sequencing are highlighted in yellow. CpG dinucleotides 13-22 are shown in bold. The primer sequences used for ChIP analysis are shown in bold and italics. (B) IP was repeated at least three times with chromatin from biological replicates using antisera specific for H3K9me2, H3K9me3, H3K4me2, H3K4me3 and H3K27me3. Immunoprecipitated DNA was analyzed by Real-Time PCR and a primer specific for the *GATA4* promoter region was used (shown in A). Enrichments are shown as percentage of the total input.

As shown in Fig. 4.10.B, corresponding to the strong methylation on the DNA level in A459 control cells, were found mainly repressive histone marks in the *GATA4* promoter region (H3K9me3 and H3K27me3), most prominently trimethylation of lysine 27 of histone H3, which would indicate repression by Polycomb Group (GcP) proteins. In contrast, in the MYC expressing line J5-1 the levels of repressive marks are low, whereas both active marks on H3K4 are enriched, indicating ongoing transcription at the *GATA4* promoter. These results suggest a

---

significant change in the epigenetic landscape of the *GATA4* promoter upon MYC expression: DNA-hypomethylation of a region encompassing CpGs 13-22 (Figs. 4.8.B-D and 4.9.B), which is accompanied by an epigenetic switch from repressive to active histone marks (Fig. 4.10.B).

#### **4.8. MYC leads to changes in protein occupancy at the *GATA4* promoter region**

In order to find out which proteins might interact with the *GATA4* promoter in A549 control and MYC expressing A549 J5-1 cells, in particular if there are specific binding sites in the region covered by CpGs 13-22, a fragment of the *GATA4* promoter region corresponding to the segment amplified by the bisulfite primers was analyzed with the MatInspector software<sup>65</sup>. This revealed the presence of consensus binding sites for the MYC associated zinc finger protein - MAZ, which usually are shared by the SP1 transcription factor, a MYC-related E-box, a Y-box and consensus sequences for the general transcription factor TFIID between CpGs 15 and 22 (Fig. 4.11.A).

To validate these potential binding sites and to get an insight into the protein presence at the *GATA4* promoter in control and MYC expressing cells, Achim Breiling performed ChIP using antibodies against chicken v-MYC (chk-MYC), GATA4, GATA6, MAZ, the three major DNA methyltransferases (DNMT1, DNMT3a and DNMT3b), Enhancer of Zeste 2 (EZH2) and the large subunit of the RNA-polymerase II (POL II) and chromatin prepared from A549 control cells and the J5-1 cell line. In the repressed case (A549 control), strong binding of MAZ and EZH2 to the *GATA4* promoter was found, which was paralleled by the presence of DNMT1 (Fig. 4.11.B).

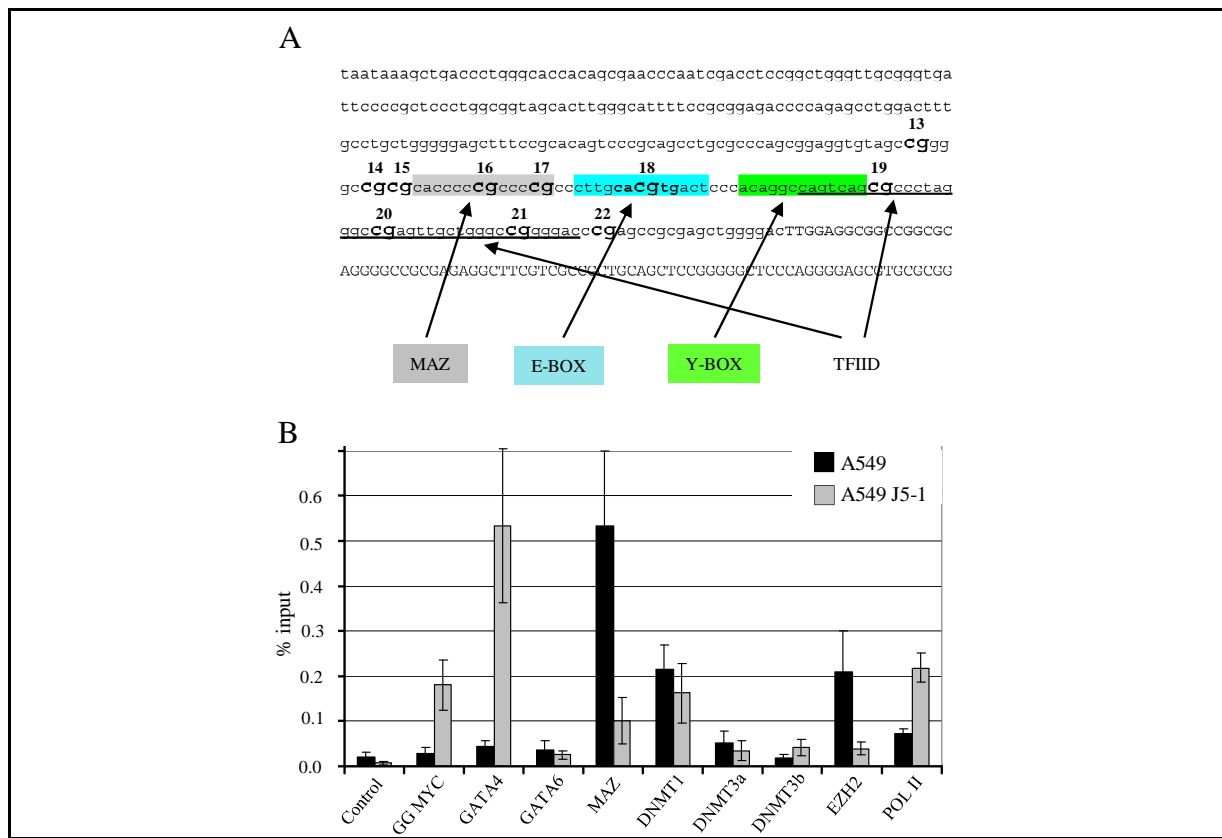


**Figure 4.11. Protein presence in the *GATA4* promoter.**

(A) Consensus binding sites in the region covered by CpGs 13-22 of *GATA4* promoter. The region directly upstream of the GATA transcription start site was analyzed for transcription factor binding sites using the MatInspector software<sup>65</sup>. The first exon is indicated with capital letters. Potential binding sites for MAZ and TFIID, an E-box, a Y-box and CpGs 13-22 are indicated. (B) CHIP assay monitoring occupancy of the *GATA4* promoter by candidate proteins chicken v-MYC (chk-MYC), GATA4, GATA6, MAZ, the three major DNA methyltransferases (DNMT1, DNMT3a and DNMT3b), Enhancer of Zeste 2 (EZH2) and the large subunit of the RNA-polymerase II (POL II). Binding of chicken v-MYC and GATA4 to the *GATA4* promoter was significantly higher in the MYC expressing A549 J5-1 cells than in the parental A549 cells. In contrast, binding of MAZ to the *GATA4* promoter was significantly higher in the parental A549 cells when compared to the A549 J5-1. Enrichments are shown as percentage of the total input.

In A549 J5-1, MAZ and EZH2 binding is greatly reduced, whereas chk-MYC (the protein expressed in this cell line) and GATA4 itself are found enriched on the *GATA4* promoter. DNMT1 levels do not change, which goes in line with the observation that the overall

---

methylation of the region does not change in MYC expressing cells. GATA6, as GATA4 antagonist, could not be found interacting neither in control nor in J5-1 cells. In line with the observed activation of the *GATA4* promoter in J5-1 cells, an increased interaction of POL II with the promoter was observed (Fig. 4.11.B).

#### ***4.9. MAZ displacement in A549 cells leads to GATA4 expression***

MAZ has been described as a recruiter of DNMTs<sup>66</sup>. As it was observed in the CHIP assay that MAZ is displaced from the *GATA4* promoter after MYC expression in A549 cells, the hypothesis that the displacement of MAZ can prevent *de novo* methylation of *GATA4* promoter in a new cell cycle, and therefore permit GATA4 expression was postulated. Thus, a shRNA-mediated knockdown of MAZ in the A549 cells was performed.

For this, the cells were infected with a shRNA-producing virus, containing the puromycin resistance gene. The infection was considered successful since the infected cells showed resistance to puromycin. The newly prepared cells were seeded in soft agar to test if the lack of MAZ in A549 is able to induce anchorage independent growth. After 3 weeks the number of colonies was counted (Figs. 4.12.A and 4.12.B). The knockdown of GATA4 mediated by the shRNA 345 producing virus was able to induce anchorage independent growth ability in A549 cells in a significant manner. This result suggests that the knockdown of MAZ might be sufficient to transform A549 cells from a non-metastatic to metastatic phenotype. Moreover, and as postulated above, A549 cells where MAZ has been knockdown showed an upregulation of GATA4 and its target mucin2 (Figs. 4.12.C and 4.12.D). Altogether, these data suggest that MAZ might be involved in the regulation of GATA4 expression by an epigenetic mechanism, which is started by MYC.

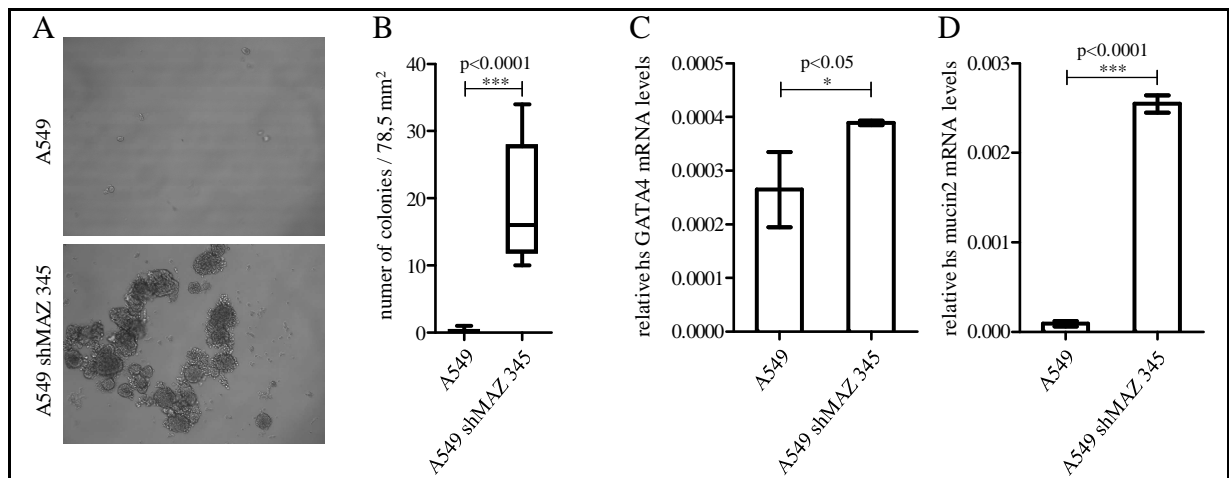


**Figure 4.12. MAZ knockdown in A549 cells leads to GATA4 upregulation and increases the ability of the cells to grow anchorage independently.**

(A) Anchorage independent growth ability of A549 cells after knockdown of MAZ. Pictures from the colonies formed by A549 and A549 shMAZ 345 cells after 3 weeks in soft agar. Magnification 20x. (B) Quantification of the colonies formed by the A549 cells after infection with shRNA-producing virus MAZ 345. The soft agar assay plate with the A549 shMAZ 345 cells shows a highly significant increase in the number of colonies formed, when compared with the parental cell line, A549. All the values represent SD of the mean. Statistical differences between groups as indicated. (C)(D) GATA4 and mucin2 mRNA levels were measured by Real-Time PCR in A549 and A549 shMAZ 345 cells. The results show a significant increase in both GATA4 and mucin2 mRNA levels in MAZ knocked-down cells, compared with the parental cell line, A549. All the values represent SD of the mean. Statistical differences between groups as indicated.

#### ***4.10. Histone deacetylase inhibition in MYC expressing cells does not lead to an increase of GATA4 activity***

Beside its role recruiting DNMTs, MAZ has also been described to recruit HDACs<sup>66</sup>. If repression of GATA4 via MAZ recruited HDACs is important, histone deacetylase inhibition can lead to GATA4 activation, simulating the displacement of MAZ from the *GATA4* promoter. To answer this question, A549 cells were treated with 50 ng of trichostatin A (TSA), which inhibits HDACs activity, from 24 hours to 4 weeks and mRNA levels of mucin2 were measured for each sample (Fig. 4.13). Against the expectations, expression of the GATA4 target, mucin2

was reduced upon TSA treatment. As TSA treatment affects many other genes, there might be many explanations for this result, like for example, the activation of some MYC or GATA4 repressor. Nevertheless, this data suggests that HDACs are not involved in the epigenetic changes induced by MAZ displacement from *GATA4* promoter.

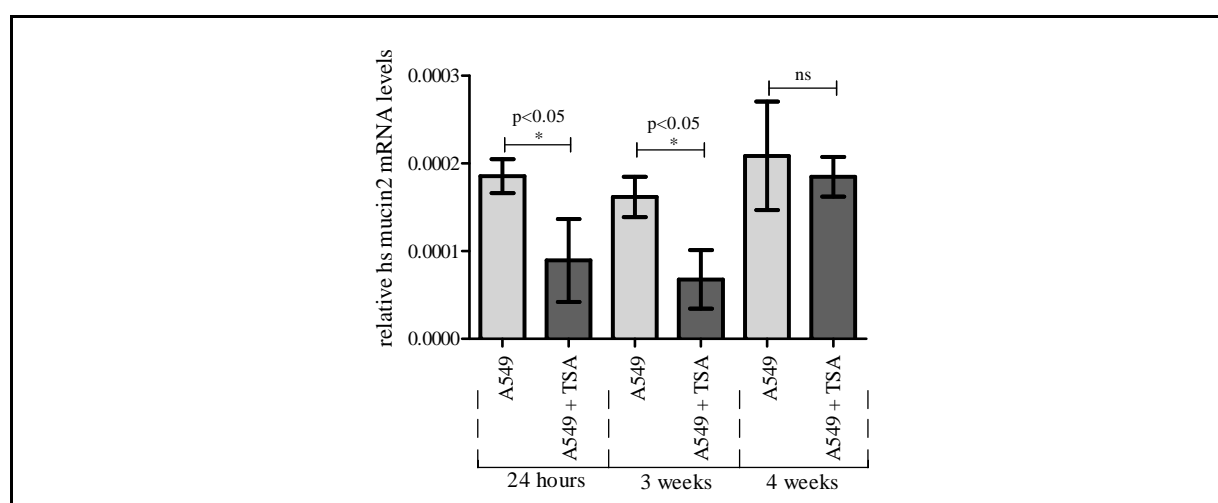


**Figure 4.13. Inhibition of HDACs activity does not lead to GATA4 activation.**

Mucin2 mRNA levels were measured in A549 cells by Real-Time PCR, before and after treatment with TSA. The results show mucin2 mRNA levels from 24 hours up to 4 weeks of TSA treatment. The GATA4 target gene, *mucin2* is downregulated as early as 24 hours after TSA treatment, and this behavior is maintained over time. All the values represent SD of the mean. Statistical differences between groups as indicated; ns – non-significant.

#### **4.11. Methylation profile of A549 cells changes upon MYC expression**

The hints given from the experiments above about epigenetic changes occurring at *GATA4* promoter after MYC induction arouse the interest about the whole genome methylation changes. Therefore, analysis of the whole genome methylation status upon MYC expression in A549 cells was performed by Achim Breiling using Infinium HumanMethylation27 bead chip technology (Illumina). Data from this experiment displayed in a scatter plot (Fig. 4.14.A), shows a wide

distribution of the points representing CpG islands, which means that many genes changed their methylation status in A549 J5-1 cells, when compared with the control cell line A549. For this purpose, interesting are the points which scatter away from the midline. Those genes show the strongest changes in their methylation status after MYC induction. This shows that the methylation profile of A549 cells changes upon MYC expression, supporting the hypothesis of an epigenetic mechanism induced by MYC.

#### ***4.12. Epigenetic changes induced by MYC in A549 cells alter the expression profile***

Microarray analyses of A549 and A549 J5-1 cells have been performed by Ellen Leich. The experiment was carried out using RNA isolated from A549 and A549 J5-1 cells. The correlation of the expression and methylation profile before and after MYC expression in A549 cells was analyzed by Tobias Müller from the Department of Bioinformatics using statistic tools (Figs. 4.14.B and 4.14.C). The correlation analysis pretends to disclose the effect of methylation changes in the expression status of the whole genome. A correlation could be found, although there are more genes downregulated and stronger methylated upon MYC introduction in A549 cells, than genes that were demethylated and upregulated in the same cells. From these mathematical analyses, a set of few genes in which demethylation was correlated with protein upregulation, were picked for further analyses (Table 4.3). The upregulation of this set of genes in MYC expressing A549 cells was confirmed individually, by measurement of their mRNA levels (Fig. 4.15). All the genes tested in this experiment showed to be upregulated in A549 J5-1 cells when compared to the parental cell line A549. These genes are therefore interesting candidates to be involved in the induction of metastatic potential of A549 J5-1 cells, induced by MYC.



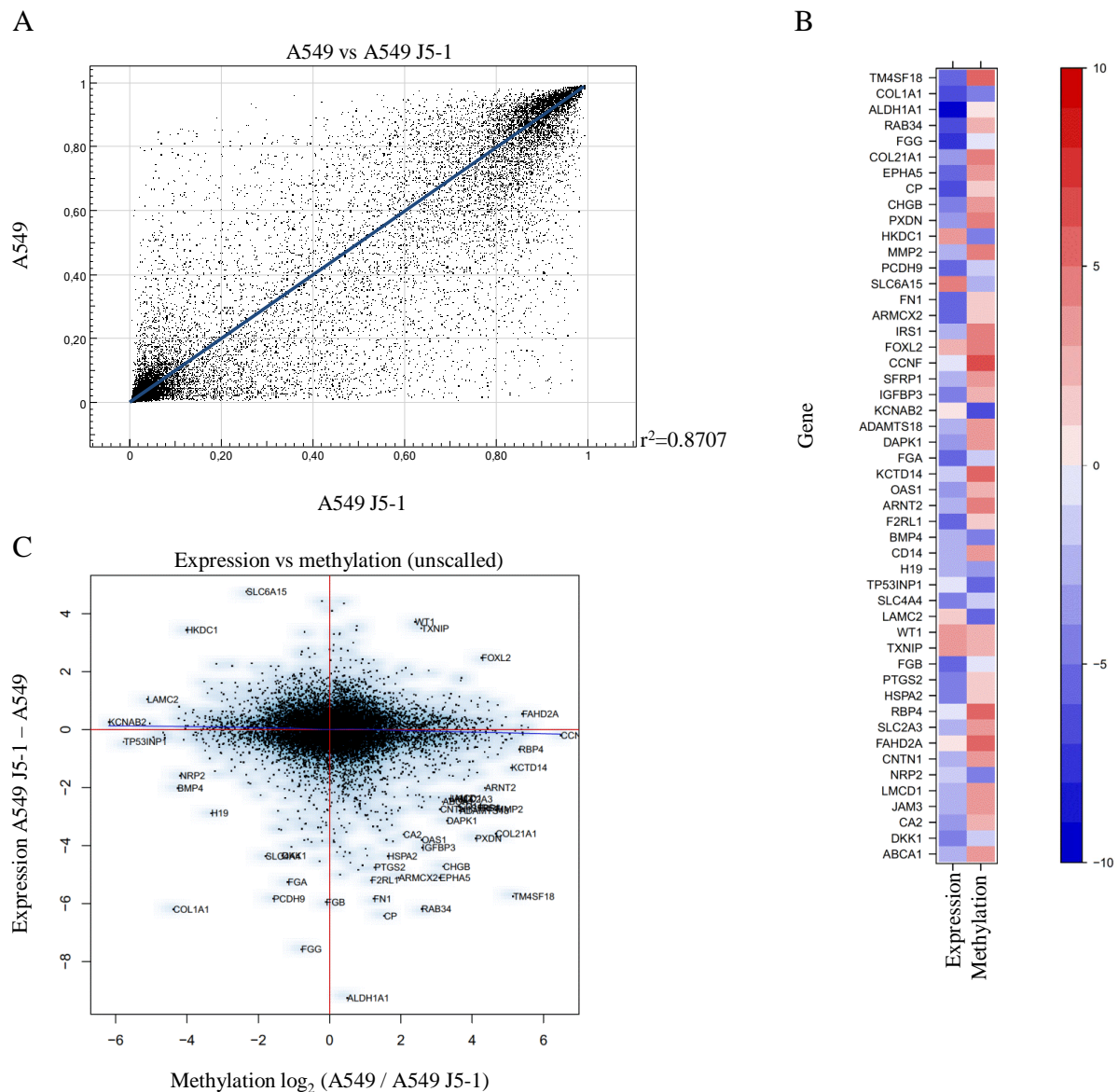


**Figure 4.14. MYC induces alteration in the overall methylation and expression profiles.**

(A) Correlation between methylation levels in A549 and A549 J5-1 DNA. Each spot represents a single CpG. The blue line crosses all the spots in the graph where the ratio of methylation did not change upon MYC expression. (B-C) Correlation between overall methylation and expression changes upon MYC expression in A549 cells. The overall analysis shows that there are many genes downregulated and stronger methylated upon MYC introduction in A549 cells, while there are only a few genes that are demethylated and upregulated.

| Gene     | Expression A549 | Expression A549 J5-1 | Difference (Exp A549 – Exp A549 J5-1) | % Met A549 | % Met A549 J5-1 | Difference (% Met A549 – % Met A549 J5-1) |
|----------|-----------------|----------------------|---------------------------------------|------------|-----------------|---|
| LAMC2    | -2.05           | -1.72                | 0.33                                  | 79.72      | 2.28            | 77.43                                     |
| HKDC1    | -2.76           | -1.13                | -1.63                                 | 38.86      | 2.44            | 36.42                                     |
| KCNAB2_1 | -3.15           | -2.56                | 0.59                                  | 58.56      | 0.82            | 57.74                                     |
| SLC6A15  | -0.87           | 2.09                 | -2.96                                 | 14.13      | 2.77            | 11.36                                     |

**Table 4.3. Values of methylation and expression for selected genes.**

The table shows the absolute values of expression in A549 and A549 J5-1 cells of the genes listed. Absolute differences of expression (A549 - A549 J5-1) are shown in the 4th column. The values of methylation of both cell lines are showed in the 5th and 6th column, as a percentage; in the last column, the absolute difference between methylation percentages is displayed (A549 – A54 J5-1). Met (methylation), Exp (expression).

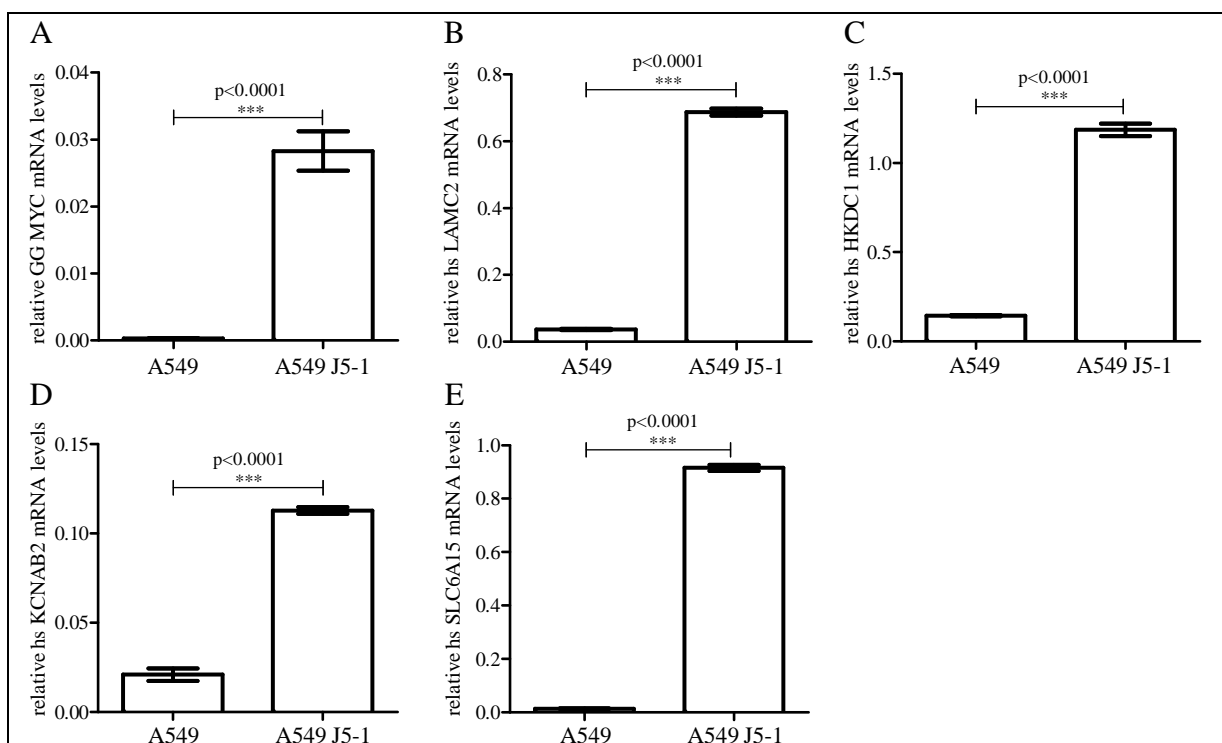


**Figure 4.15. A549 J5-1 cells show upregulation of the indicated genes.**

(A-E) The upregulation of a set of genes in which demethylation is correlated with protein upregulation in A549 J5-1 cells was confirmed by Real-Time PCR analyses. All the values represent SD of the mean. Statistical differences between groups as indicated.

---

#### ***4.13. Overexpression of GATA4 in A549 cells changes their anchorage independent growth ability***

To further test the functional role of GATA4 in NSLC, a new cell line overexpressing GATA4 was prepared. For this, the coding sequence of human *GATA4* was subcloned into the EcoRI site of the retroviral vector pEGZ by using the oligonucleotides GATA4\_FWD and GATA4\_REV listed in the Materials section. This vector incorporates in addition the EGFP and zeocin-resistance gene. After infection of A549 cells with the construct pEGZ/GATA4, positively infected cells were selected with zeocin. Following selection, pools of 10 infected cells were seeded in 96 well-plates, and tested for GATA4 and EGFP expression. The infected cells pool showing higher levels of GATA4 mRNA was the number 11, and was consequently expanded to use in further experiments (Figs. 4.16.A and 4.16.B). This new cell line (from now called A549 GATA4-11) was afterwards tested by immunocytochemistry using an antibody specific for human GATA4. As shown in Fig. 4.16.C, A549 GATA4-11 cells show GATA4 and GFP expression. Moreover, GATA4 showed to be localized in the nucleus.

As shown in Fig. 4.16.D, A549 GATA4-11 cells have a different morphology compared to the parental cell line A549, when grown in adherent culture and show a tendency to detach from the surface. The cell proliferation rate of A549 GATA4-11 and A549 cells in adherent culture was measured by MTT assay (Fig. 4.17.A). This assay showed that GATA4 is not altering the proliferation rate of A549 cells, when grown in adherent culture. The ability to grow anchorage independently of GATA4 expressing and non-expressing A549 cells was compared in a soft agar assay. Although there is no difference between proliferation rate of the two cell lines in adherent culture, when grown in soft agar, the size and number of colonies formed by A549 GATA4-11 cells was significantly higher when compared to the A549 cells (Figs. 4.17.B-C). These results

show that the expression of GATA4 in the human NSCLC cell line A549 highly significantly increases the ability for anchorage independent growth.

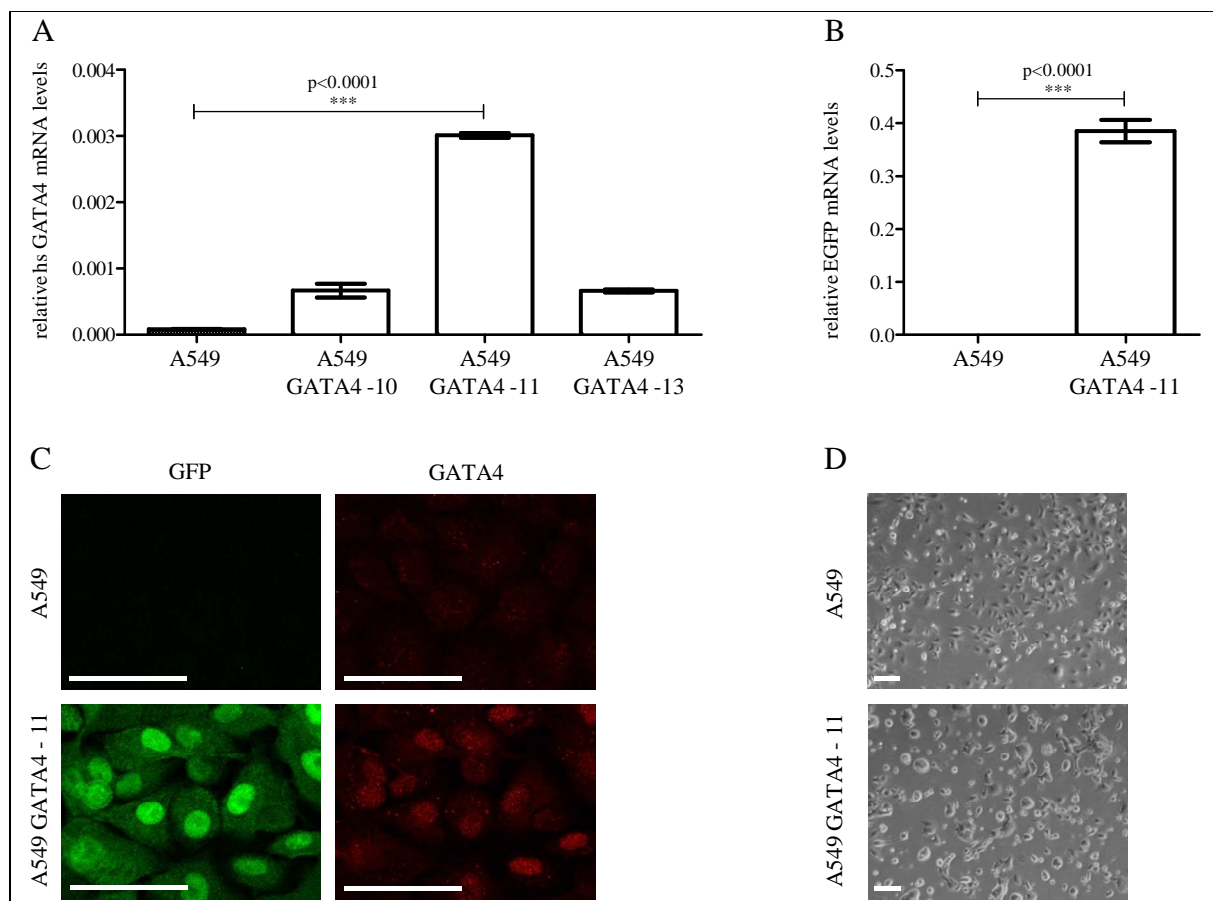


**Figure 4.16. A549 cells infected with pEGZ/GATA4 vector show GATA4 and EGFP expression.**

(A-B) Relative mRNA levels of GATA4 and EGFP in A549 cells infected with the plasmid pEGZ/GATA4 measured by Real-Time PCR. Numbers 10/11/12 refer to different pools of 10 cells seeded in a 96 wells plate after infection and selection with appropriate antibiotic. The best candidate pool was number 11, showing the highest level of GATA4 mRNA levels. This pool also showed high EGFP expression. (C) Immunocytochemistry for human GATA4 in A549 and A549 GATA4–11 cells. GATA4 expression was detected in the nucleus of the latest cells. GFP expression was also detected in these cells by fluorescence microscopy. Red (Cy5) colored cells are GATA4 positive; Green cells are GFP positive; Scale bars = 50  $\mu$ m. (D) Phase microscopic observation of GATA4 expressing A549 cells. After introduction of human GATA4 in A549 cells, the cells change their morphology and tend to detach. Scale bar = 100 $\mu$ m.

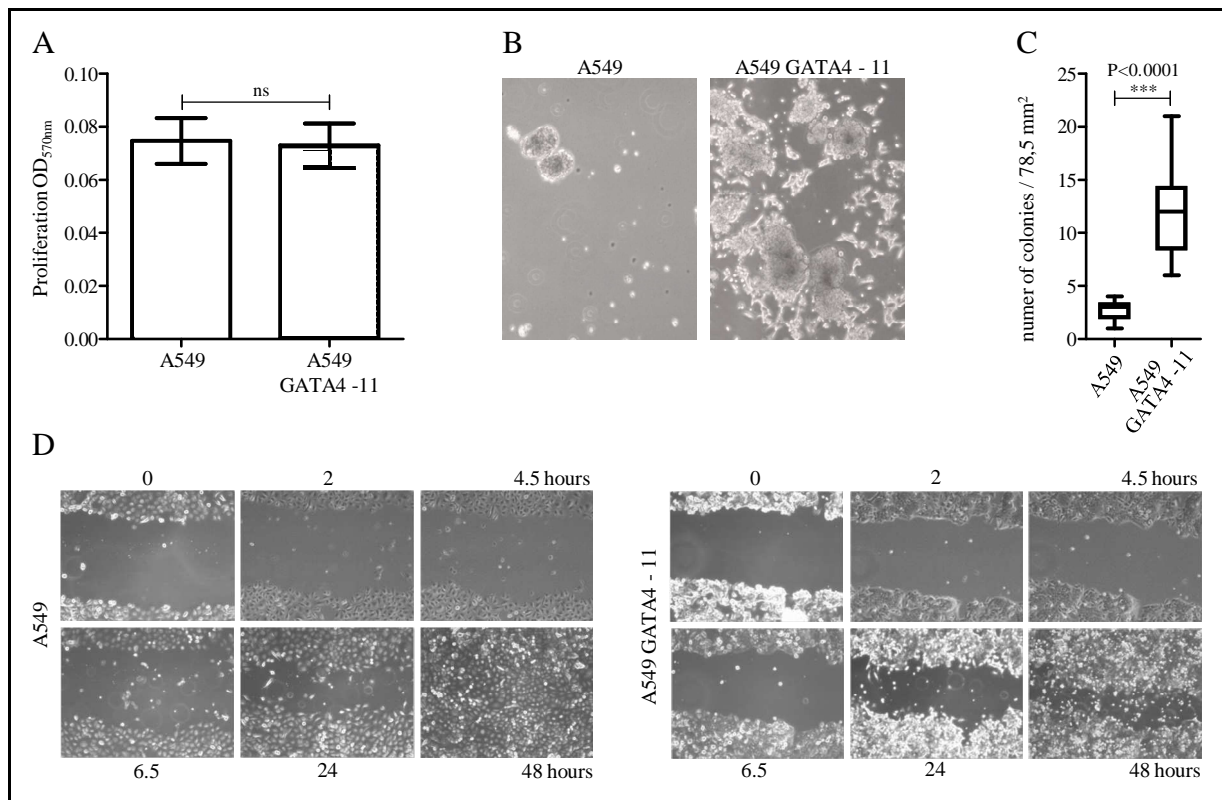


**Figure 4.17. Characterization of A549 GATA4-11 cells.**

(A) Proliferation rate of A549 cells does not change upon GATA4 expression in adherent culture. Proliferation was assessed by MTT assay. All the values represent SD of the mean. Statistical differences between groups as indicated. ns: Not significant. (B) Growing in soft agar resulted in an increase of number and size of colonies in the case of A549 GATA4-11 cells. Magnification 20x. (C) The number of colonies formed in soft agar by the cell line A549 GATA4-11 was significantly higher when compared to the parental cell line A549. All the values represent SD of the mean. Statistical differences between groups as indicated. (D) Images from a time-lapse sequence of A549 and A549 GATA4-11 cells migrating to heal a wound. A549 cells show the healing of the wound at 48 hours, while A549 GATA4-11 were not able to heal the same sized wound in that time frame. The latest cells show a decrease in their migration potential, when compared with the parental cell line; ns – non-significant.

#### **4.14. GATA4 expressing A549 cells show a decrease in their migration ability**

Because active migration of tumor cells is a prerequisite for tumor-cell invasion and metastasis<sup>67</sup>, a wound healing assay was performed to access the migration potential of GATA4 expressing A549 cells. The migration behavior of these cells and of the control A549 was monitored during

---

48 hours (Fig. 4.17.D). Unexpectedly, this experiment showed healing of the wound at 48 hours in the case of A549 cells, while the GATA4 expressing A549 cells did not heal the wound in this time frame, suggesting a reduced migration potential of A549 GATA4 – 11 cells.

#### ***4.15. GATA4 expression in A549 cells leads to accelerated tumor growth in vivo***

If the expression of GATA4 induced by MYC is sufficient to induce metastasis, the transplantation of a GATA4 expressing NSCLC cell line - A549 - in immunodeficient mice should lead to metastasis. To test this possibility,  $2.5 \times 10^6$  A549/GFP and A549 GATA4-11 cells were subcutaneously implanted in nude mice, respectively. Accelerated tumor growth was observed in the A549 GATA4-11 transplanted animals when compared to the animals injected with the control cells (Fig. 4.18.A). Taking advantage of GFP expression in the transplanted cells, tumor growth could also be monitored by GFP fluorescence measurements, which showed much higher GFP fluorescence in tumors from A549 GATA4-11 cells indicating again accelerated tumor growth induced by GATA4 (Figs. 4.18.B and 4.18.C). Among the differences between the two groups, it was still noticeable that tumors from GATA4 group presented in general a reddish color as blood vessels could be seen with naked eye, which was not observed in the control group (Fig. 4.19.A). Moreover, 12 out of 15 tumors from the GATA4 group started to bleed very early (27 days after transplantation), which suggests increased tumor vascularization. Due to fast tumor growth (reaching the allowed 2 cm tumor size very quickly) and premature tumor bleeding, the animals transplanted with A549 GATA4-11 cells had to be sacrificed 27 to 38 days after transplantation (Fig. 4.19.B). Whole body imaging of cells expressing GFP was done weekly (Fig. 4.18.C).

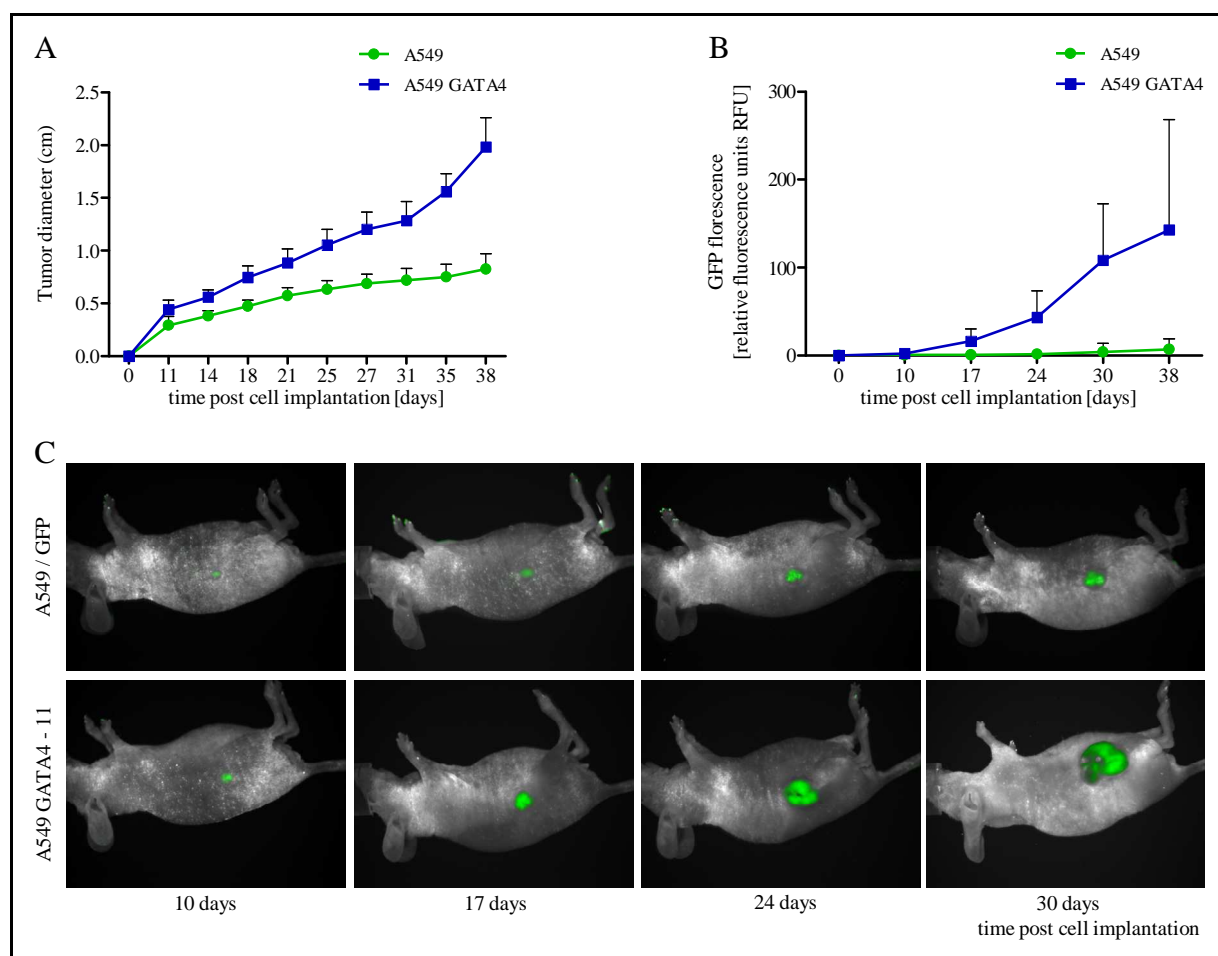


**Figure 4.18. Xenograft assay of tumor (NSCLC tumors A549 cell derived) growth after GATA4 addition.**

The tumor cells were injected subcutaneously in nude mice. (A) Tumor diameters were measured twice per weeks and are indicated as the mean  $\pm$  SD. (B) Tumor GFP fluorescence was measured once per week using the Maestro Software 2.10.0. (C) Whole body imaging of NSCLC cells expressing GFP (upper panels) and GFP in addition to GATA4 (lower panels) growing in nude mice over time.

No GFP expression was observed in organs or lymph nodes adjacent to the primary tumors, neither in the GATA4 or control group, indicating no development of metastasis. After sacrifice, the organs extracted were imaged in a petri dish and no GFP expression could be observed except in the primary tumors (Fig. 4.19.C).

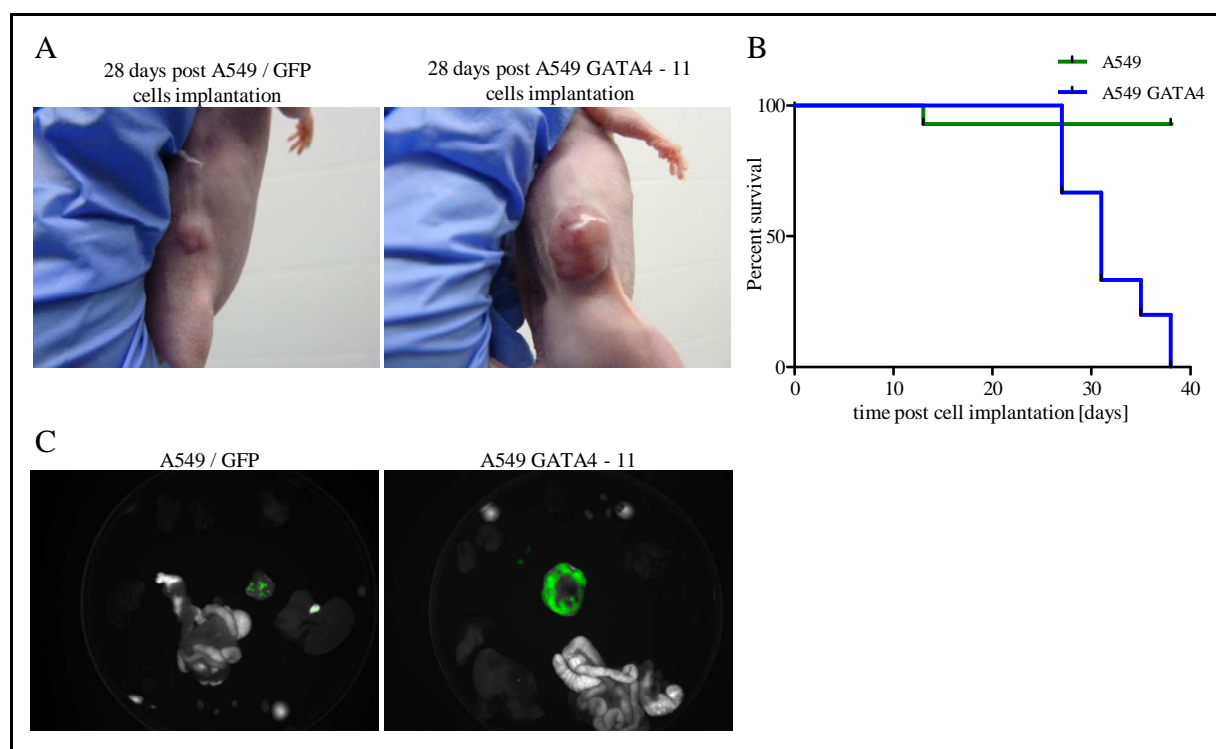


**Figure 4.19. GATA4 induces fast NSCLC tumor growth in nude mice.**

(A) Differences in tumor size and vascularization between mice injected with A549/GFP and A549 GATA4-11 cells, 28 days after implantation. (B) Kaplan-Meier survival curves for nude mice implanted with A549/GFP and A549 GATA4-11 cells. Data plotted as percent of animals surviving in each group. (C) Organs imaging of NSCLC cells expressing GFP (left panel) and GFP in addition to GATA4 (right panel). Primary tumors in green.

#### **4.16. A549 cells show downregulation of angiogenic factors upon GATA4 expression**

Angiogenesis is a process necessary for a tumor to become metastatic<sup>68</sup>. Therefore, the expression of a set of genes known as angiogenic factors was evaluated in the GATA4 expressing A549 cells, and corresponding parental cell line (Fig. 4.20).

None of these genes, usually upregulated during metastasis development, showed upregulation in the A549 GATA4-11 cell line in comparison with A549 cells. Differently, all the tested genes



showed downregulation in GATA4 expressing cells (Fig. 4.20), which goes in line with the results from the wound healing assay.

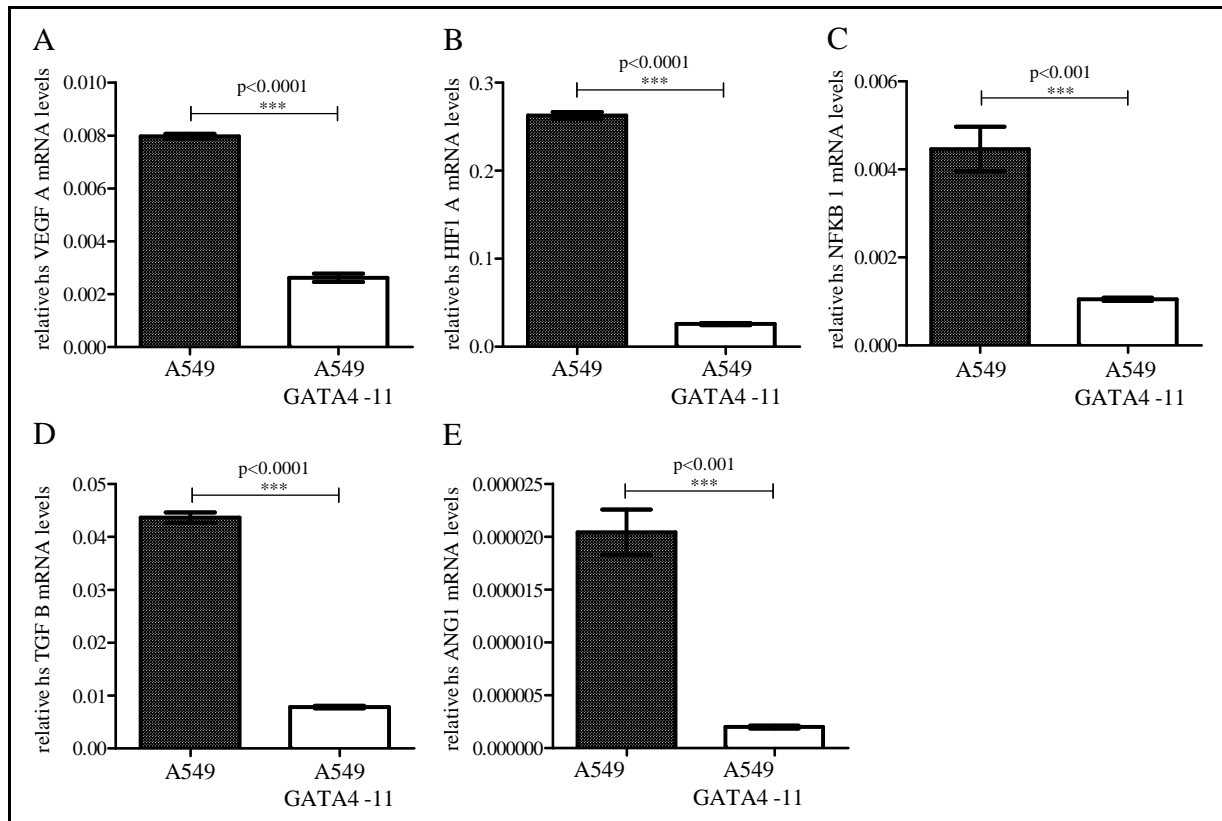


**Figure 4.20. A549 cells show downregulation of angiogenic factors upon GATA4 expression**

(A-E) Relative mRNA levels of angiogenic factors: VEGF A, HIF1 A, NFKB1, TGF beta and ANG1 in A549 and A549 GATA4-11 cells measured by Real-Time PCR. All the genes show downregulation upon GATA4 expression. All the values represent SD of the mean. Statistical differences between groups as indicated.

#### **4.17. A549 cells show downregulation of pluripotent stem cells markers, but not of CD30**

Based on the theory that tumor cells progressively acquire stem cell properties as a consequence of oncogene-induced plasticity<sup>30</sup>, and that MYC is involved in the induction of pluripotent stem

cells<sup>69</sup>, the question whether GATA4 has the same effect in NSCLC cells was addressed. Therefore, mRNA levels of commonly used pluripotent stem cell markers (BMP4, HNF4A and CD30)<sup>70,71,72</sup> were measured in GATA4 expressing A549 cells (Fig. 4.21). The pluripotent stem cell markers BMP4 and HNF4A showed downregulation upon GATA4 expression in A549 cells, in contrast to the marker CD30, which showed upregulation in the same cells, comparing with the control A549. Thus, these data do not exclude that GATA4 can induce dedifferentiation in A549 cells.

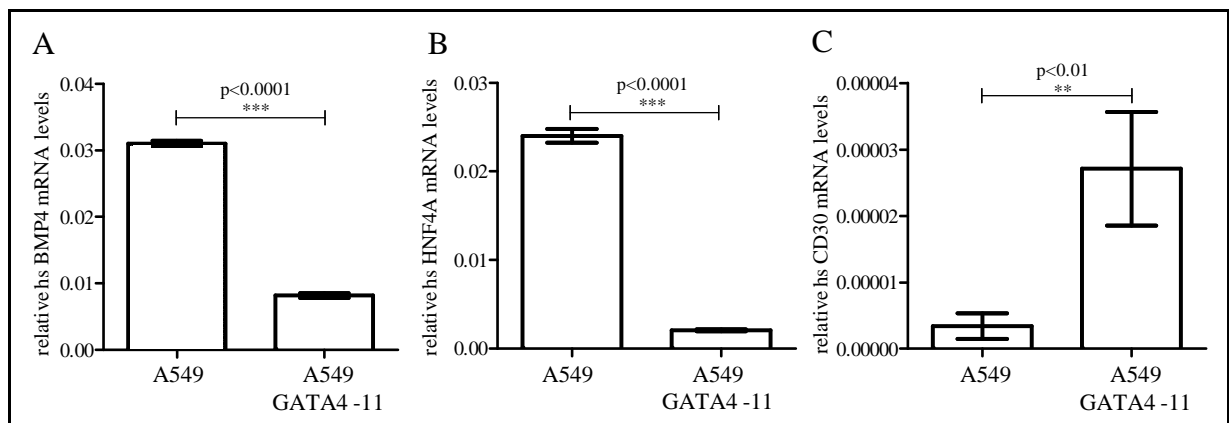


**Figure 4.21. A549 cells show downregulation of pluripotent stem cell markers upon GATA4 expression, but not of CD30.**

Relative mRNA levels of pluripotent stem cell markers: BMP4, HNF4A and CD30 in A549 and A549 GATA4-11 cells measured by Real-Time PCR. (A-B) BMP4 and HNF4A show downregulation upon GATA4 expression. (C) In contrast, CD30 is upregulated in GATA4 expressing cells, when compared to the parental cell line, A549. All the values represent SD of the mean. Statistical differences between groups as indicated.

## 5. Discussion

### 5.1. *MYC induces a phenotypic and lineage switch in NSCLC*

In this work, an epigenetic switch induced by MYC in NSCLC is reported. The results demonstrate that MYC induces epigenetic alterations at the *GATA4* promoter level leading to its upregulation. Such alterations include site-specific demethylation and acquisition of active histone modification marks in *GATA4* promoter. Importantly, a novel epigenetic mechanism by which MYC activates *GATA4* leading to a metastatic phenotype in NSCLC is proposed and novel potential targets for the development of anti-metastatic therapy are suggested.

It was previously reported that constitutive expression of C-RAF under the control of the Sp-C promoter, or C-RAF BxB - an N-terminal deleted form of C-RAF that lacks RAS-binding domain -, gives rise to thousands of well differentiated adenomas, poorly vascularized, that do not progress to metastasis in mice<sup>18</sup>. In contrast, inducible or constitutive expression of nuclear c-MYC was shown to be sufficient to induce early macrometastasis in RAF-driven-NSCLC mice, by suppressing apoptosis. Moreover, c-MYC is able to convert a non-metastatic NSCLC cell line A549, into metastasizing cells<sup>2</sup>. A second reported consequence of cooperation between C-RAF and c-MYC is the rapid induction of a new Alveolar Papillary Epithelial Cell type, APEC, which affects a large fraction of cells. The original phenotype of these cells is a cuboidal type. A higher proliferation index in primary lung tumors was shown for the APEC cells and they are the predominant cell type found in the corresponding solid metastasis<sup>2</sup>. In the present work, this phenotypic switch was shown and could be reverted after c-MYC withdrawal *in vivo*, by the disappearance of APECs, which suggest a “shock from oncogene withdrawal” – effect<sup>60</sup> (Fig. 4.1). In spite of the cuboidal to columnar phenotypic switch has been observed in all mice

overexpressing the two oncogenes in type II cells, only a fraction of them proceeds to develop metastasis<sup>2</sup>. Therefore the requirement of additional events for the metastasis switch has to be considered. A comparable phenotypic switch from cuboidal to columnar cells has been observed by Rapp et al. upon deletion of p53 in Sp-C-C-RAF BxB transgenic mice<sup>16</sup>. c-MYC upregulation can be the reason for the switch previously reported, since p53 transcriptionally represses c-MYC<sup>73</sup>.

In addition to the phenotypic switch, a lineage switch was previously observed in the tumors from animals expressing c-MYC in type II cells. GATA4, which is exclusively expressed in the lung during its development or in the intestine of adult mice<sup>74,45</sup>, was found in the tumors of single Sp-C-c-MYC or compound mice, but not in single Sp-C-C-RAF animals. In contrast, GATA6, a transcription factor involved in airway regeneration and normally expressed in the lung<sup>61</sup>, was found in single Sp-C-C-RAF transgenic animals and in the case of tumor tissues from c-MYC single and compound transgenic mice, it gave place to GATA4 expression. This mutually exclusive expression of GATA6/GATA4 is expected for a lineage switch process. The same lineage switch was reported in tumor tissue of metastasis with origin in lung tumors from animals expressing c-MYC in type II cells<sup>2</sup>, suggesting that the switch occurred in the primary tumor is important for the development of metastasis induced by c-MYC.

In the present work, it was observed the loss of the transgenic promoter Sp-C in a high percentage of GATA4 positive cells of the primary tumors from Sp-C-c-MYC, showing that GATA4 expression is kept after loss of c-MYC, through the loss of its promoter (Fig. 4.3.A). These observations show that MYC induces a lineage switch, where GATA4 expression is induced and that GATA4 expression is afterwards independent of MYC expression, suggesting a self-sustaining mechanism for this GATA transcription factor. Moreover, this switch may drive

NSCLC progression to metastasis<sup>29</sup>. GATA4 transcription factor is activated by phosphorylation by ERK and protein kinase A in gonadal cells<sup>75</sup>. After a first activation by MYC, a similar mechanism might be involved in the subsequent GATA4 activation in NSCLC reported in this work.

### ***5.2. MYC drives GATA4 expression in human NSCLC cells***

As observed in murine lung tumors, here is shown that MYC also induces the expression of the transcription factor GATA4 in the metastatic cell line A549 J5-1<sup>2</sup> and in the MYC inducible cell line A549 MYC-ER *in vitro* (Figs. 4.3.C and 4.4.D). In addition to GATA4 upregulation, the inducible cell line shows increased ability to grow anchorage independent in soft agar after MYC expression, mimicking metastatic behavior of A549 J5-1 cells (Figs. 4.4.B-C). GATA4 is normally expressed in the intestine, and has mucin2 as its functional target<sup>45,62</sup>. The upregulation of mucin2 in MYC expressing cells proved the functionality of GATA4 induced by MYC in NSCLC (Figs. 4.3.D and 4.4.D). In fact, *GATA4* is a lineage selector gene, and its upregulation might suggest a dedifferentiation of the cells and loss of organ identity which goes in line with the theory that the metastatic process is a recapitulation of ontogeny<sup>29</sup>. Moreover, a controlled addition of MYC to A549 cells showed that the upregulation of GATA4 induced by MYC starts 3 weeks after ectopic MYC expression although MYC upregulation is detected as early as 1 week after induction. This suggests that a multi-step mechanism might be involved in the changes induced by this oncogene (Fig. 4.4.D).

Here, the involvement of GATA4 in the metastatic behavior induced by MYC could be shown, since A549 J5-1 cells lacking GATA4 expression showed a decreased ability to form colonies in soft agar comparing with the GATA4 expressing A549 J5-1 cells (Fig. 4.5). The ability of A549

J5-1 cells to grow in the absence of anchorage is a required step for the cells to metastasize<sup>76</sup>, and the lack of GATA4 seems to revert, at least partially, this metastatic behavior which has been induced by MYC. It was earlier reported that GATA4 promotes the expression of the anti-apoptotic factor Bcl2 and cyclin D2<sup>46</sup>. In fact, altered expression of GATA4 has been correlated with a broad range of tumors emerging from gastrointestinal tract, lungs, ovaries and brain. The forced expression of GATA4 in colorectal cancer cell lines was previously reported to increase their proliferation and migration capacities<sup>40</sup>. Another study showed that elevated GATA4 levels are associated with poor prognosis in ovarian granulose cell tumors<sup>77</sup>.

### **5.3. MYC induces GATA4 promoter demethylation**

The *GATA4* promoter activity of a 455 bp fragment 5'-upstream the transcription start of the human *GATA4* gene was assessed, and results showed that MYC expressing A549 cells have a higher activity of *GATA4* promoter, when compared with MYC non-expressing cells, A549 wild-type (Fig. 4.6). This data suggests that MYC is enough to alter *GATA4* promoter activity, and is in line with the evidence that MYC activates GATA4, also showed in this work. Indeed, it was interesting to see what is happening at the *GATA4* promoter level, taking advantage of the recent explosion of knowledge of how epigenetic events modulate gene transcription<sup>50</sup>.

Growing evidence now suggests that epigenetic alterations are at least as common as mutational events in the development of cancer<sup>50,30</sup>. Tumor-specific promoter hypermethylation is well documented<sup>50</sup>. Epigenetic silencing is also known as a frequent event in NSCLC, i.e. of p16, H-cadherin, death-associated-protein (DAP), kinase1 (DAPK1), 14-3-3 sigma and the candidate tumor suppressor gene RASSF1A<sup>1</sup>. However, comparatively little is known about the role of

promoter hypomethylation in gene activation in cancer, especially in NSCLC. In the present work, it was shown that GATA4 upregulation in NSCLC is accompanied by demethylation of its promoter upon MYC expression *in vitro* and *in vivo* (Figs. 4.8 and 4.9). Interestingly, MYC did not alter the overall methylation level of *GATA4* promoter, but it induced site-specific demethylation. Hypomethylation was observed in the CpG islands 13-18 of the *GATA4* promoter from lung tumors and respective liver metastasis extracted from mice expressing ectopic MYC. The same effect was observed in the CpG islands 19-22, also in the promoter of MYC-expressing A549 cells. Interestingly, the region of the *GATA4* promoter between CpG islands 13 and 22 comprises the binding site for MYC – an E-BOX sequence<sup>78,79</sup> – which was previously shown to activate GATA4. E-BOX motif of the proximal *GATA4* promoter has been reported to be a key regulatory element of GATA4 transcript expression *in vitro*<sup>80</sup> and *in vivo*<sup>81</sup>. Therefore, hypomethylation of this specific region might be of great importance for the metastasis-inducing mechanism by MYC, especially because this effect was observed in metastatic tissue, as well as in the primary tumor (Fig. 4.8). Y-BOX sequence is also present in the referred region of *GATA4* promoter. Y-BOX binding protein 1 regulates expression of many important genes<sup>82</sup> and has been reported to be involved in the development of metastasis in patients with gastric and breast cancer<sup>83</sup>. This protein might bind to the hypomethylated region of the *GATA4* promoter regulating its expression, or even acting as a partner in metastasis development.

The occurrence of hypo or hypermethylation in cancer cells has been controversially discussed. One of the first studies screening methylation levels in human cancers reported substantial hypomethylation in genes of cancer cells compared with their normal counterparts and progressive hypomethylation in metastasis<sup>84</sup>. On the other hand, several studies report aberrant hypermethylation in various types of cancer, especially silencing wild-type tumor

suppressors<sup>85,50,1,86</sup>. Hypermethylation of *GATA4* in lung cancer have also been reported<sup>40,86</sup>. In fact, the data from the present work may seem inconsistent with these reports, but here, it was observed hypomethylation of *GATA4* in metastatic cells and tissues, while in the revised literature, methylation studies were mainly made in primary tumors or non-metastatic cell lines. Therefore, as this study lacks the comparison of methylation levels of the primary tumors with analogous normal tissue, no statement can be made to corroborate previous findings about hypermethylation in primary tumors.

Actually, a study about methylation of *GATA* genes in lung cancer using several lung cancer cell lines revealed *GATA4* silencing by hypermethylation in most of the tested cells, including A549<sup>86</sup>. Curiously, the only cells extracted from metastasis tissue, H157 were unmethylated in the *GATA4* promoter region analyzed<sup>86</sup>.

In another report, analysis of *GATA4* promoter methylation in ovarian cancer tissues collected from patients, showed that a rapidly invasive ovarian cancer (High-Grade Serous Ovarian Cancer) kept *GATA4* promoter unmethylated in all cases, while tumors from patients with other type of ovarian cancers which are less invasive and develop slower, showed hypermethylation of *GATA4* promoter<sup>87</sup>.

Indeed, it is not surprising that in the present work it has been shown an involvement of *GATA4* upregulation by hypomethylation of its own promoter in the development of metastasis. The role of *MYC* in the induction of such epigenetic changes is likely, not only based on the data here presented, but also because of the well known preference of *MYC* to bind to promoter and CpG-rich regions<sup>79</sup>.



---

#### ***5.4. MYC induces the enrichment of active histone marks and changes protein occupancy at the GATA4 promoter***

DNA methylation acts in cooperation with histone tail modifications and has the ability to alter the chromatin condensation status. Patterns of both events were shown to be altered in cancer<sup>88</sup>. Histones are no longer considered to be simple ‘DNA-packaging’ proteins; they are recognized as dynamic regulators of gene activity that undergo many post-translational chemical modifications, such as acetylation, methylation, phosphorylation, ubiquitination and sumoylation<sup>89</sup>. Acetylation and methylation of specific lysine residues in the tails of nucleosomal core histones, in particular Histone 3, are known to have an important role in regulating chromatin structure and therefore gene expression<sup>89</sup>. In general, histone hypoacetylation and hypermethylation are characteristic of DNA sequences that are methylated and repressed in normal cells<sup>88</sup>. Alterations in DNA methylation and in histone modification patterns potentially affect the structure and integrity of the genome and change normal patterns of gene expression, which might be causal factors in cancer<sup>53</sup>. A signal that separates regions of transcriptionally active chromatin from regions of transcriptionally inactive chromatin seems to be given by the specific methylation markers in histone H3<sup>50</sup>. Transcriptionally repressive chromatin has been related with methylation of lysine 27 (lys27)<sup>90</sup> and of lysine 9 (Lys9) in the histone 3 tail<sup>50</sup>, in opposition to methylation of lysine 4 (Lys4) on histone 3 tail, which characterizes the transcriptionally active chromatin<sup>50</sup>. It was previously shown that several lysine residues, including lysines 4, 9, 27, and 36 of Histone 3, are preferred sites of methylation and that lysine methylation can occur on the  $\epsilon$ -nitrogen atom as mono-, di-, or trimethylated forms<sup>91</sup>.

In the present work, corresponding to the strong methylation on the *GATA4* promoter of A459 control, non-metastatic cells, were found mainly repressive histone marks H3K9me3, and most

---

prominently trimethylation of lysine 27 of histone H3 (Fig. 4.10). The enrichment of H3K27me3 at *GATA4* promoter of the non-metastatic cells A549 can indicate repression by polycomb group proteins (PcG)<sup>47</sup>. Indeed, polycomb-repressive complex 2 (PRC2) is known to repress gene expression by trimethylating of Lys27 on histone H3, establishing repressive epigenetic marks<sup>92</sup>. PRC2 methylates H3K27 via its catalytic subunit – Enhancer of Zeste 2 (EZH2) - which transfers a methyl group from S-adenosyl methionine (SAM) to Lysin 27 residue at H3<sup>92,93</sup>. In fact, in this work EZH2 was found to be enriched at *GATA4* promoter of A549 wild-type cells, in contrast to the low binding of the Enhancer detected at *GATA4* promoter of MYC-expressing A549 cells (Fig. 4.11). *GATA4* binds and recruits the transcriptional co-activator p300 to specific chromatin loci, which acetylates *GATA4* augmenting its transcriptional activity<sup>94</sup>. It was recently shown that *GATA4* methylation by PRC2 impairs its acetylation by p300 and reduces its recruitment of p300 to chromatin, resulting in reduced *GATA4* transcriptional potency<sup>47</sup>. These facts support our findings that *GATA4* expression is repressed in A549 cells, and that this event is accompanied by an enrichment of the PRC2 methylation target - H3K27 (Figs. 4.10 and 4.11).

In contrast to the enrichment of repressive histone marks at the *GATA4* promoter of wild-type A549 cells, in the MYC expressing line J5-1 the levels of repressive marks are low, whereas both active marks on H3K4 are enriched, indicating ongoing transcription at the *GATA4* promoter (Fig. 4.10). It is widely assumed that the key rate-limiting step in gene activation is the recruitment of RNA polymerase II (Pol II) to the core promoter<sup>95</sup>. The recruitment of Pol II was previously reported to co-occur with the enrichment of the active histone marks H3K4 di- and trimethylated<sup>96</sup>. This effect could be seen in MYC-expressing A549 cells (Fig. 4.11). After MYC expression, the occupancy of Pol II at the *GATA4* promoter of A549 cells was significantly elevated. Altogether, these data corroborate the hypothesis that *GATA4* is transcriptionally active

in MYC expressing cells. Moreover, the present data suggest a significant change in the epigenetic landscape of the *GATA4* promoter upon MYC expression: DNA hypomethylation of a region encompassing CpG islands 13-22, which is accompanied by an epigenetic switch from repressive to active histone marks.

### **5.5. MYC induces changes in protein occupancy at GATA4 promoter**

Changes in protein occupancy levels at *GATA4* promoter in MYC-expressing A549 cells were mentioned above. Briefly, the disenrichment of EZH2 at *GATA4* promoter of A549 J5-1 cells suggests that *GATA4* transcription has been repressed by the PcG proteins in wild-type A549 cells, and the enrichment of Pol II supports the evidence of active transcription of *GATA4* in MYC-expressing A549 cells. Among other proteins tested in this work, GATA4 markedly bound to its own promoter upon MYC expression. On the other hand, the HDAC and DNMTs recruiter - MAZ<sup>66</sup> - and the already mentioned EZH2 protein were displaced from *GATA4* promoter in MYC-expressing A549 cells (Fig. 4.11). MAZ displacement from the region which became hypomethylated after MYC expression, suggests that its role as HDAC and DNMTs recruiter might be a key event for the *GATA4* repression before MYC expression, either by recruitment of DNMTs and subsequent methylation of that promoter region, or by recruitment of HDACs, deacetylating the histones and therefore maintaining the nucleosomes in a transcriptionally silent state<sup>97</sup>. The late hypothesis was excluded by inhibition of HDACs activity in A49 cells. Trichostatin (TSA) treatment of A549 cells, a potent inhibitor of HDACs activity<sup>50</sup> did not result in the activation of the hypermethylated *GATA4* gene (Fig. 4.13). Therefore, MAZ seems to repress *GATA4* expression in A549 cells by DNMTs recruitment, while HDACs might not be involved. MAZ displacement might prevent *de novo* methylation by absence of DNMT

recruitment and therefore provoke promoter site-specific hypomethylation. In this work, the knock-down of MAZ in A549 cells led to *GATA4* activation and overexpression of its functional target, mucin2 (Figs. 4.12.C-D). Moreover, the cells lacking MAZ expression mimic the behavior of MYC expressing A549 cells in soft agar proposing MAZ as a key-player in MYC induced metastasis via *GATA4* activation (Figs. 4.12.A-B).

These findings suggest the scenario that *GATA4* is usually kept repressed by MAZ, DNMT1 and PcG containing complexes. Upon MYC expression, chk-MYC interacts with its binding site (E-box) near the *GATA4* promoter which leads to DNA hypomethylation of the region containing the MAZ binding site and the E-box and subsequent MAZ and EZH2 displacement. Activated transcription of *GATA4* is then self-sustained by *GATA4* interacting with its own promoter (Fig. 5.1).

### ***5.6. Epigenetic changes induced by MYC are genome-wide***

Candidate gene approaches are not sufficient to evaluate the amount of epigenetic alteration in a cancer / metastasis genome<sup>98</sup>. This is just possible using a genome-wide approach, which discloses methylation signatures and opens up novel treatment options that include epigenetic therapeutic strategies<sup>98</sup>. Taking advantage of recent technological advances, it is possible to obtain a better picture from the cancer transcriptome and from genome-wide epigenetic changes that occur in a cancer genome<sup>99,98</sup>. In this work, the whole-genome analysis of methylation levels in A549 and metastatic MYC expressing A549 cells revealed that MYC induced epigenetic changes are not limited to *GATA4*, yet they were observed in a wide range of genes among the genome. Indeed, many genes showed differential methylation upon MYC ectopic expression in

A549 cells (Fig. 4.14.A). This is not surprising since several studies have previously connected MYC with reprogramming events<sup>100</sup>. The broad range of genes differentially methylated upon ectopic MYC expression did not show only hypomethylation but also hypermethylation of many genes (Fig. 4.14.A).

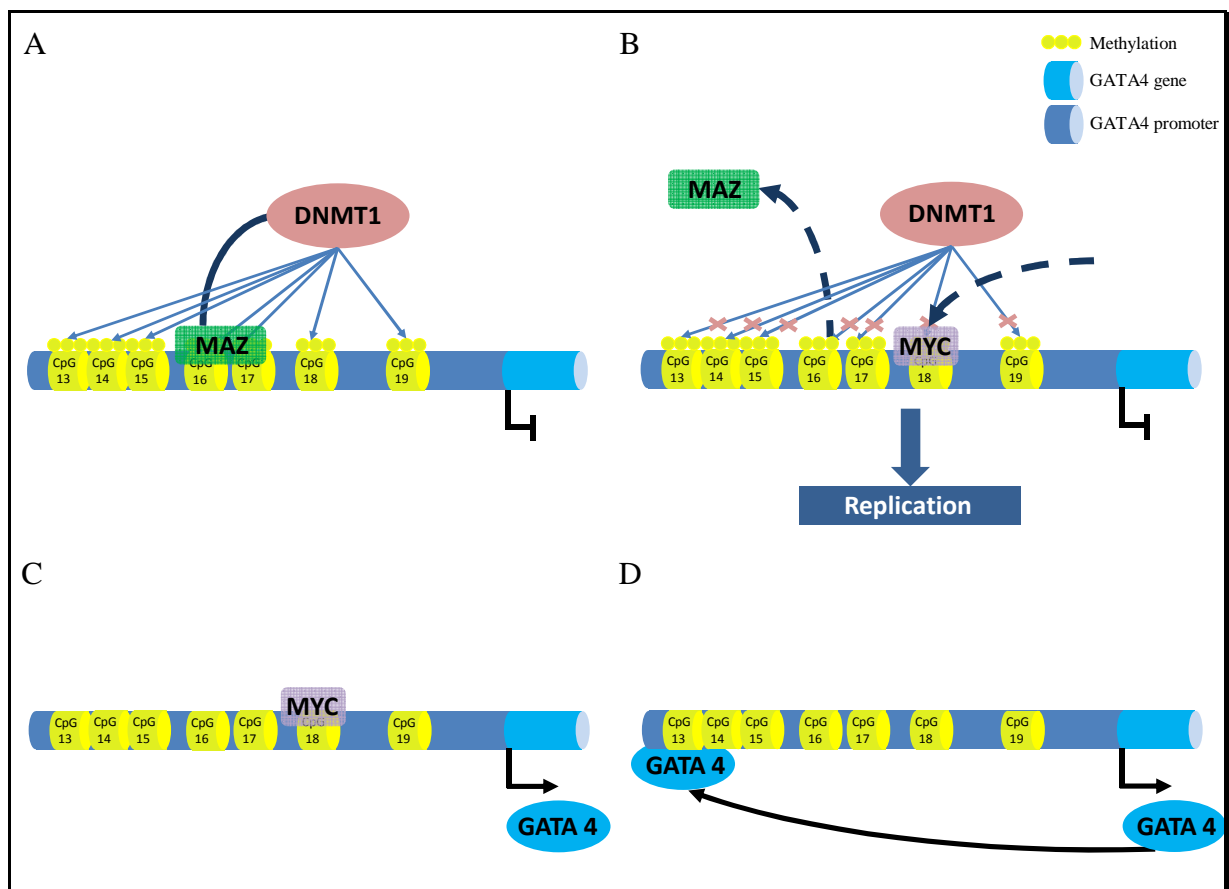


**Figure 5.1. Locked switch model of self-perpetuating GATA4-expression induced by MYC.**

(A) Under physiological conditions MAZ binds to the *GATA4* promoter. Sitting on the *GATA4* promoter MAZ recruits DNMTs, which in turn methylate the CpG-sites. (B) When MYC expression rises above a given threshold, MYC binds to the *GATA4* promoter displacing MAZ. As a consequence DNMTs are not recruited to the DNA-region anymore. (C) After replication CpG-sites remain unmethylated due to the absence of DNMT-recruitment. (D) The expression of GATA4 is now maintained even in the absence of MYC by GATA4 binding to its own promoter.

---

Actually, hypermethylation at CpG islands is prevalent in basically every human cancer<sup>101</sup> with emphasis on tumor or metastasis suppressor genes, like p16<sup>INK4a</sup> in lung cancer, in which methylation is accompanied with poor prognosis<sup>102</sup>. Consistently, the results from the Infinium-chip in the present work show hypermethylation of p16<sup>INK4a</sup> tumor suppressor gene in the metastatic MYC-expressing A549 cells (data not shown). Indeed, hypermethylation exceeds hypomethylation in cancer<sup>1</sup>, but little is known about this phenomena distinguishing benign from malignant tumors.

In this work, the number of aberrant hypermethylated genes prevailed over the number of genes aberrantly hypomethylated in MYC expressing A549 cells. The number of genes aberrantly hypermethylated (in this case considered as methylation of A549 < 20% and methylation of A549 J5-1 > 80%) reached the number of 49, while genes methylated more than 80% in A549 and less than 20% in A549 J5-1 cells did not exceed 18. Data from a gene expression microarray analysis of A549 and A549 J5-1 cells performed by Ellen Leich was combined with the data from the Infinium-chip, and the correlation between the 2 events was calculated by Tobias Müller using mathematical approaches. The combined data from methylation and expression showed that there are much more genes in which downregulation is correlated with promoter hypermethylation (41 genes) than genes in which upregulation is correlated with promoter hypomethylation (9 genes) (Figs. 4.14.B-C).

Among the 41 genes silenced in MYC expressing cells by promoter hypermethylation, 11 were previously described as tumor or metastasis suppressors, and their downregulation was reported to be involved in tumor progression or poor prognosis. These known tumor suppressor genes, such as PXDN in lymphocytic and myeloid leukemia<sup>103,104</sup>, FOXL2 in ovarian cancer<sup>105</sup>, ADAMTS18 in esophageal, nasopharyngeal, gastric, colorectal and pancreatic cancers<sup>106,107</sup>,

---

H19 in colorectal cancer and hepatocarcinoma<sup>108</sup>, RBP4 in gastric, ovarian and esophageal cancer<sup>109,110,111</sup>, PCDH9 in nephro and glioblastoma<sup>112,113</sup>, EPHA5 in breast, colorectal, brain and lung cancers<sup>114,115,116</sup>, IGFBP3 in breast, prostate, endometrial, esophageal and Non-Small-Cell Lung Cancers<sup>117,118,119,120,121</sup>, DAPK1 in brain, renal, oral and Non-Small-Cell Lung cancers<sup>122,123,124,125</sup>, DKK1 in meduloblastoma, myeloid leukemia, breast, renal and lung cancers<sup>126,127,128,129,130</sup> and SFRP1 in hepatocellular carcinoma, esophageal, thyroid, colorectal, lung cancers and specifically NSCLC<sup>131,132,133,134,135,136</sup> were previously found to be downregulated and in most of the cases, epigenetically repressed by hypermethylation.

Interestingly, the association between reduced lung cancer and metastasis risk and high Insulin-like Growth Factor Binding Protein (IGFBP)-3 - the major IGF carrier protein in the serum<sup>117</sup> - in the plasma was reported years ago<sup>137,119</sup>. The re-expression of IGFBP-3 in NSCLC significantly decreases the migration, invasion and metastatic potential of the tumors, *in vivo* and *in vitro*<sup>138</sup>. Reportedly, antiproliferative and pro-apoptotic IGFBP-3 effectively blocks uPA- and matrix metalloproteinase-2-stimulated invasion pathways reducing lung cancer cell metastasis<sup>119</sup>. In general, the tumor-suppressive properties of IGFBP-3 include sequestration of the IGFs<sup>139</sup>, senescence association<sup>140</sup>, and inhibition of cell adhesion to extracellular matrix components<sup>141</sup>. Moreover, the cooperation between MYC overexpression and IGFBP-3 deletion was previously associated with greater risk of aggressive, metastatic prostate cancer<sup>118</sup>. Besides IGFBP-3, some other tumor or metastasis suppressors silenced by hypermethylation in the present study piqued my interest for further discussion, namely EPHA5, DAPK1, SFRP1 and DKK1.

Consistently with the present data, the receptors for Ephrin family ligands (EPH) have been described as important players in oncogenesis and progression of many types of cancer,

including lung cancer<sup>142</sup>. Ephrin/EPH signaling pathway networks with the Wnt signaling pathway during embryogenesis, tissue regeneration, and carcinogenesis<sup>143</sup>. This fact is of special interest since Wnt pathway was recently implicated in lung adenocarcinoma metastasis<sup>144</sup> and its aberrant activation often correlates with overexpression or amplification of *c-MYC* oncogene<sup>145</sup>. The EPH receptor tyrosine kinase family member EPHA5 plays a critical role in the regulation of carcinogenesis<sup>114</sup>. Recent studies showed that the silencing of this gene by hypermethylation is correlated with progression of breast cancer from a noninvasive to an invasive phenotype<sup>114</sup> and that the decrease of EPHA5 levels in plasma of mice is associated with angiogenic fast growing glioblastoma<sup>116</sup>, which together with the results from the present work suggest the involvement of EPHA5 silencing in progression to metastasis.

Also the Death-associated protein (DAP) kinase, a positive mediator of apoptosis<sup>146</sup>, has been described as a metastasis suppressor not only in lung cancer metastasis but also in mesothelioma, clear cell renal cell carcinoma and neuroblastoma metastasis<sup>123,147,122,124</sup>. In the later, the molecular pathology was related with several genomic alterations including amplification of the *N-MYC* oncogen<sup>122</sup>. Aggressiveness of malignant tumors and poor survival rates have been associated with the methylation of the promoter region of the DAPK gene and the loss of DAPK expression<sup>148</sup>. Therefore, the epigenetic aberration found in the present work for this gene promoter seems to be supported by previously published studies.

Consistently with the present data, the downregulation of the secreted frizzled-related protein 1 (SFRP1) gene by promoter hypermethylation suppressing tumor growth of lung cancer cells has been described some years ago<sup>136,131</sup>. SFRP1 hypermethylation was found to be associated with lymph node metastasis and progression from lung cancer<sup>149</sup>. Hereupon, the interest for SFRP1 increased, especially after evidences for its role as Wnt antagonist<sup>150</sup>. Interestingly, another Wnt



antagonist – Dickkopf-related protein 1 (DKK1) - revealed in the present study to be downregulated by promoter hypermethylation upon ectopic MYC expression in NSCLC cells<sup>150</sup>. The poor prognosis associated to DKK1 downregulation due to epigenetic changes has been reported in several types of cancer, including lung cancer<sup>126,127,128</sup>. The silencing of DKK1 was found to coincide with polycomb-mediated repression in lung cancer<sup>126</sup>. Reportedly, the metastatic suppression through DKK1 silencing includes anti-apoptotic activity, proliferation induction and inhibition of anchorage independent growth *in vitro*<sup>129,128</sup>.

Unrestrained Wnt signaling is found in many tumors and experimentally activated Wnt is oncogenic<sup>151</sup>. Moreover, the oncoprotein c-MYC, which is upregulated by Wnt signaling activity, participates in a positive feedback loop of canonical Wnt signaling through repression of Wnt antagonists DKK1 and SFRP1<sup>150,151</sup>. The downregulation of these 2 metastasis repressors - SFRP1 and DKK1 - upon MYC expression in A549 cells is convincingly supported by the revised literature.

As previously discussed, hypomethylated promoters related with upregulation of the corresponding gene occurred at lower frequency than hypermethylation/downregulation events. The upregulation of those genes in MYC-expressing A549 cells was individually validated by mRNA levels measurement: HKDC1, LAMC2, KCNAB2 and SLC6A15 (Fig. 4.15).

HKDC1 is a hexokinase which catalyzes the conversion of glucose to glucose-6-phosphate in the glycolytic pathway<sup>152</sup> and is frequently overexpressed in rapidly growing tumors<sup>153</sup>. This is not surprising since the well known Warburg effect describes the energy production in tumor cells by a high rate of glycolysis, regardless of the availability of oxygen<sup>154</sup>. Consistently with the present data, c-MYC overexpression was previously associated with the regulation of glucose

metabolism by regulating glycolysis-associated genes like Lactate dehydrogenase-A (LDH-A), GluT1, hexokinase 2 (HK2), phosphofructokinase (PFK) and enolase 1 (ENO 1)<sup>155</sup>. This suggests that MYC might regulate HKDC1, and induce a metabolic switch in NSCLC which accompanied by progression to malignancy.

LAMC2 is one of the 3 components of Laminin-5, an essential component of the basement membrane<sup>156</sup>. Diverse biological functions attributed to laminin include stimulation of cell growth and differentiation, cell adhesion, and locomotion<sup>157</sup> and it has been implicated in a number of stages in tumor invasion and metastasis<sup>158</sup>. Additionally to its roles in cell adhesion and migration, laminin was described to mediate interactions of tumor cells with the immune system and to have more subtle roles in controlling metastatic behavior being proposed as an antimetastatic molecule suitable for therapy<sup>158</sup>. In the case of lung cancer, LAMC2, which was upregulated / demethylated in the metastatic cell line A549 J5-1 in the present work, was reported to accumulate around tumor clusters and this event was suggested as being significant for the spread and growth of malignant tumors<sup>159</sup>. Moreover, the upregulation of this gene due to promoter demethylation was earlier associated with metastasis with origin in bladder and gastric cancers<sup>160,161</sup>. Altogether, previous reports and the present data suggest that the epigenetic activation of LAMC2 by MYC might be important for the acquired metastatic behavior of A549 J5-1 cells.

Finally, epigenetic changes induced by MYC have an important effect in expression of both metastasis-suppressing and metastasis-inducing genes, altering the proteomic and epigenomic landscape of the tumor cells in a manner which is strongly supported by previous publications.

### **5.7. *GATA4* alone is not enough to induce angiogenesis in vitro**

Along with few studies reporting overexpression of *GATA4* in metastasis from other types of cancer, the present work also shows the upregulation of *GATA4* in metastatic NSCLC (Figs. 4.3.C and 4.4.D). *GATA4* expression was previously associated with aggressive behavior of Ovarian Granulosa Cell Tumors and infiltrating pancreatic cancers<sup>77,162</sup>. In the latter, the overexpression of *GATA4* was even correlated with infrequent methylation<sup>163</sup> like it was found in the present work. Here, the *GATA4* transcription factor showed to be involved in the metastatic behavior induced by *MYC* since, as discussed above, the knockdown of *GATA4* in A549 J5-1 cells withdrew their acquired ability to grow anchorage independent (Fig. 4.5). Although not altering proliferation rates in adherent culture, the overexpression of *GATA4* in A549 cells led to an increased ability to grow anchorage independently in soft agar when compared with A549 wild type cells, mimicking the behavior of *MYC* expressing cells (Figs. 4.17.A-C). This supports the evidence that *GATA4* is needed to the metastatic behavior induced by *MYC* in NSCLC. Moreover, the introduction of human *GATA4* in A549 cells led to morphological changes and conferred a tendency to detach from adherent plates (Fig. 4.16.D). As expected, immunocytochemistry analysis of A549 *GATA4*-11 cells showed localization of *GATA4* transcription factor in the nucleus (Fig. 4.16.C).

Unexpectedly, upon *GATA4* expression, A549 cells showed a decrease in migration ability while performing a wound-healing assay (Fig. 4.17.D). A possible explanation for this is the limitation of the assay itself. The ability of this approach to simulate biological processes in human tissues is limited, since it is known that signaling pathways function optimally when cells are spatially organized in three-dimensional tissues, but are uncoupled and lost in rudimentary monolayer culture systems<sup>164</sup>. Indeed, three-dimensional migration assays were recently reported

to correlate better the wound healing and migration of breast cancer cells lines with their metastatic capacity, in contrast to monolayer assays, which correlated inversely the migration capacity of the cancer cells with their metastatic capacity<sup>165</sup>. Therefore, a three-dimensional migration assay might be necessary to give a better insight about the migration ability of NSCLC cells upon GATA4 expression, simulating more authentically the conditions *in vivo* like cell–cell and cell–extracellular matrix contacts<sup>166</sup>.

Angiogenesis is the recruitment of new blood vessels induced by solid tumor growth and is an essential component of the metastatic pathway. These vessels are the principal path by which tumor cells exit the primary tumor site and enter the circulation<sup>167</sup>.

The best characterized angiogenic factor – VEGF - is the main driving force behind angiogenesis and blood vessel formation by induction of proteases secretion, migration and proliferation<sup>68</sup>. In cancer patients, high levels of VEGF expression are closely related with the development of metastasis<sup>168</sup>. When a tumor grows beyond a certain size (usually 2mm), the cells in the center of the tumor have restricted access to nutrients and oxygen, leading to quiescence and hypoxia, respectively<sup>169</sup>. Hypoxia activates the expression of VEGF gene via the HIF-1 response element in its promoter<sup>170</sup>.

Also the transcription factor NFkB has been shown to rapidly transduce hypoxic signals by increasing its DNA binding activity to promoters of several genes including genes encoding cytokines implicated in angiogenesis like VEGF, basic fibroblast growth factor (bFGF), and tumor necrosis factor (TNF)<sup>171</sup>. ANG-1, a member of angiopoietin family has also been described as an important regulator of angiogenesis governing the transition between quiescence and angiogenic growth<sup>68</sup>. The lately pro-angiogenic factors are expected to be upregulated in

metastatic cells. The assumption that GATA4 is a limiting step for metastasis induced by MYC in NSCLC led to the interest about regulation of these angiogenic factors in A549 GATA4-11 cells (Fig. 4. 20). Surprisingly, none of the mentioned factors showed elevated levels of mRNA compared with the parental cell line A549. These results are not so surprising after a closer look at the tumor-induced angiogenesis mechanism. As mentioned above, hypoxia is required for VEGF production. Since the cells used in the present work were growing in monolayer, hypoxic conditions were absent and this might explain the current observations. Indeed, stromal environment is absolutely needed to induce angiogenesis, and such environment is difficult to reproduce *in vitro*. Cancers are not autonomous neoplastic cells but also include fibroblasts, immune cells, endothelial cells and specialized mesenchymal cells. These different cell types in the tumor stroma can be recruited by the malignant cells to produce angiogenic factors, support tumor growth and facilitate metastatic dissemination<sup>172</sup>.

Still in the context of angiogenesis, TGF- $\beta$  has been reported as a pro and anti-angiogenic factor<sup>173,174</sup>. In this work, mRNA levels of TGF- $\beta$  were impaired upon GATA4 expression in A549 cells (Fig. 4.20.D). This could indicate angiogenesis progression by downregulation of this anti-angiogenic factor, but considering the absence of stromal environment within the cells during the experiment, no statement can be made about its pro or anti-angiogenic properties in A549 GATA4-11 cells.

To overcome the discussed experimental limitations, *in vivo* analyses are required. Alternatively, A549 GATA4-11 cells can be cocultured with normal pulmonary fibroblasts, given that the crosstalk between the 2 cell types might be of great importance for the signaling between tumor cells and normal neighboring fibroblasts<sup>175</sup>.

### **5.8. GATA4 induces accelerated tumor growth in vivo**

The central question of the present work is whether GATA4 is able to induce metastasis from NSCLC *in vivo*. To answer this question, A549 cells overexpressing GATA4 in addition to GFP were transplanted in nude mice, and the appearance of metastasis was screened weekly using a laser-capture microscope to dissect GFP positive cells. The time frame of the transplantation experiment was 38 days, due to the fast growth of the tumors with origin in GATA4 expressing A549 cells, and no metastasis could be seen by whole mice or organs imaging (Figs. 4.18 and 4.19). This result does not exclude that GATA4 is sufficient to induce metastasis, considering that the time frame of the experiment was too short for the development of tumors in adjacent organs (animals had to be sacrificed as soon as the tumors were bleeding or reached 2 cm of diameter). In a previous work where Rag-/- mice were transplanted with chk-MYC expressing A549 cells, metastasis to liver and lung could be observed at low frequency and it was suggested that a higher metastasis frequency could be achieved in a longer time frame<sup>2</sup>. To clarify if GATA4 is sufficient to induce metastasis from NSCLC using the xenograft model presented in this work, the primary tumor should be removed surgically when bleeding starts or 2 cm are reached, increasing the life time of the animals and therefore increasing the chance of metastasis development. Despite GATA4 failed to induce metastasis *in vivo*, the accelerated tumor growth induced by A549 cells expressing this transcription factor was clear and suggests a much more aggressive phenotype (Figs. 4.18.A-B). In contrast to the *in vitro* data, the accelerated tumor growth induced by GATA4 indicates that cell proliferation is increased and therefore dependent on the presence of other cell types from the tumor stroma. The differences in the tumor sizes from mice transplanted with A549 GATA4-11 or control cells can also be attributed to the recruitment of different cell types by the malignant cells. In addition to neoplastic cells, also

fibroblasts, immune cells, endothelial and specialized mesenchymal cells might account to tumor enlargement. Moreover, these cells can produce angiogenic factors to recruit blood vessels<sup>67</sup>. The induction of angiogenesis *in vivo* by GATA4 is suggested by the observation of blood vessels with the necked eye in the tumors constituted of GATA4 expressing cells, and the fact that 12 out of 15 tumors started to bleed before the achievement of 2 cm of diameter (Fig. 4.19.A).

### **5.9. GATA4 might induce pluripotency in NSCLC cells**

The reported lineage switch induced by MYC led to the question whether GATA4 expression induces reprogramming to pluripotency, conferring to the cells an unlimited potential to grow which is characteristic from cancer and metastatic cells. This hypothesis was tested in the present work, by measuring the mRNA levels of 3 pluripotent stem cell markers in A549 cells upon expression of GATA4, namely, BMP4, HNF4A and CD30<sup>70,71,72</sup>. The current data showed upregulation of the latter but not of the 2 former markers in A549 cells upon GATA4 expression (Fig. 4.21). The upregulation of CD30 suggests that GATA4 might induce pluripotency in NSCLC. CD30 is a member of the tumor necrosis factor receptor superfamily whose upregulation was related to anaplastic large cell lymphoma, Hodgkin lymphoma cells and human transformed pluripotent stem cells<sup>72</sup>. Moreover, it was shown that CD30 expression provides a significant survival advantage to the pluripotent stem cells expressing it<sup>72</sup>. In addition, induced pluripotency might be important for metastasis dissemination, because of loss of organ-identity of the cells, which makes possible that they proliferate in a different organ from its origin<sup>30</sup>. This suggests that NSCLC cells overexpressing GATA4 might reprogram into pluripotency acquiring a survival advantage to become metastatic.

To conclude, in the present work it was possible to show that MYC induces a wide broad of epigenetic changes in NSCLC conferring metastatic potential, and GATA4 was identified as a potential target for anti-metastatic therapy, although further investigations are required to validate it.



---

## 6. References

1. Risch A, Plass C. Lung cancer epigenetics and genetics. *International Journal of Cancer*. 2008 Jul;123(1):1-7.
2. Rapp UR, Korn C, Ceteci F, et al. Myc Is a Metastasis Gene for Non-Small-Cell Lung Cancer. *PLoS ONE*. 2009 Jun;4(6):e6029.
3. Shi W, Bellusci S, Warburton D. Lung Development and Adult Lung Diseases. *Chest*. 2007 Aug;132(2):651-6.
4. Cardoso WV, Lü J. Regulation of Early Lung Morphogenesis: Questions, Facts and Controversies. *Development*. 2006 May; 133(9):1611-24.
5. Jeffery PK. The Development of Large and Small Airways. *American Journal of Respiratory and Critical Care Medicine*. 1998 May; 157(5 Pt 2):S174-80.
6. Effros RM. Anatomy, development, and physiology of the lungs. *GI Motility online*. 2006 May; doi:10.1038/gimo73.
7. Anon. Malformations of the respiratory system. *Centre de référence des maladies respiratoires rares*. 2012. Available at: [www.respirare.fr](http://www.respirare.fr).
8. Itoh H, Nishino M, Hatabu H. Architecture of the lung: morphology and function. *Journal of Thoracic Imaging*. 2004 Oct; 19(4):221-7.
9. Bellusci S. Lung stem cells in the balance. *Nature Genetics*. 2008 Jul; 40(7):822–823.
10. Kim CFB, Jackson EL, Woolfenden AE, et al. Identification of Bronchioalveolar Stem Cells in Normal Lung and Lung Cancer. *Cell*. 2005 Jun; 121(6):823-35.
11. Pheesse TJ, Clarke AR. Normal stem cells in cancer prone epithelial tissues. *British Journal of Cancer*. 2009 Jan; 100(2): 221–227.
12. Anand P, Kunnumakara AB, Sundaram C, et al. Cancer is a Preventable Disease that Requires Major Lifestyle Changes. *Pharmaceutical Research*. 2008 Sep; 25(9): 2097–2116.
13. Anon. Cancer - PubMed Health. Available at: <http://www.ncbi.nlm.nih.gov/pubmedhealth/PMH0002267/>. Accessed April 17, 2012.
14. Stagg J, Johnstone RW, Smyth MJ. From cancer immunosurveillance to cancer immunotherapy. *Immunological Reviews*. 2007 Dec; 220:82-101.
15. Garnis C, Buys TP, Lam WL. Genetic alteration and gene expression modulation during cancer progression. *Molecular Cancer*. 2004 Mar; 3:9.

- 
16. Fedorov LM, Papadopoulos T, Tyrsin OY, et al. Loss of p53 in craf-induced transgenic lung adenoma leads to tumor acceleration and phenotypic switch. *Cancer Research*. 2003 May; 63(9):2268-77.
  17. Roberts PJ, Der CJ. Targeting the Raf-MEK-ERK mitogen-activated protein kinase cascade for the treatment of cancer. *Oncogene*. 2007 May; 26(22):3291-310.
  18. Kerkhoff E, Fedorov LM, Siefken R, et al. Lung-targeted expression of the c-Raf-1 kinase in transgenic mice exposes a novel oncogenic character of the wild-type protein. *Cell Growth & Differentiation*. 2000 Apr; 11(4):185-90.
  19. Soucek L, Whitfield J, Martins CP, et al. Modelling Myc inhibition as a cancer therapy. *Nature*. 2008 Oct; 455(7213):679-83.
  20. Birrer MJ, Segal S, DeGreve JS, et al. L-myc cooperates with ras to transform primary rat embryo fibroblasts. *Molecular and Cellular Biology*. 1988 Jun; 8(6):2668-73.
  21. Larsson LG, Henriksson MA. The Yin and Yang functions of the Myc oncoprotein in cancer development and as targets for therapy. *Experimental Cell Research*. 2010 May; 316(8):1429-37.
  22. Meuwissen R, Berns A. Mouse Models for Human Lung Cancer. *Genes & Development*. 2005; 19(6):643–664.
  23. Cole MD, McMahon SB. The Myc oncoprotein: a critical evaluation of transactivation and target gene regulation. *Oncogene*. 1999 May; 18(19):2916-24.
  24. Ponzelli R, Katz S, Barsyte-Lovejoy D, et al. Cancer therapeutics: Targeting the dark side of Myc. *European Journal of Cancer*. 2005 Nov; 41(16):2485-501.
  25. Cowling VH, Chandriani S, Whitfield ML, et al. A Conserved Myc Protein Domain, MBIV, Regulates DNA Binding, Apoptosis, Transformation, and G2 Arrest. *Molecular Cell Biology*. 2006 Jun; 26(11):4226-39.
  26. Adhikary S, Eilers M. Transcriptional regulation and transformation by Myc proteins. *Nature Reviews Molecular Cell Biology*. 2005 Aug; 6(8):635-45.
  27. Murphy DJ, Junttila MR, Pouyet L, et al. Distinct thresholds govern Myc's biological output in vivo. *Cancer Cell*. 2008 Dec; 14(6):447-57.
  28. Schreck R, Rapp UR, Schreck R, et al. Raf kinases: Oncogenesis and drug discovery, Raf kinases: Oncogenesis and drug discovery. *International Journal of Cancer*. 2006 Nov; 119(10):2261-71.
  29. Rapp UR. Metastasis as a faulty recapitulation of ontogeny. *Nature Precedings*. 2007 Aug; doi:10.1038/npre.2007.805.1.
  30. Rapp UR, Ceteci F, Schreck R. Oncogene-induced plasticity and cancer stem cells. *Cell Cycle*. 2008 Jan; 7(1):45-51.

- 
31. Krivtsov AV, Twomey D, Feng Z, et al. Transformation from committed progenitor to leukaemia stem cell initiated by MLL-AF9. *Nature*. 2006 Aug; 442(7104):818-22.
32. Leber MF, Efferth T. Molecular principles of cancer invasion and metastasis (review). *International Journal of Oncology*. 2009 Apr; 34(4):881-95.
33. Hanahan D, Weinberg RA. Hallmarks of Cancer: The Next Generation. *Cell*. 2011 Mar; 144(5):646-74.
34. Pantel K, Brakenhoff RH. Dissecting the metastatic cascade. *Nature Reviews Cancer*. 2004 Jun; 4(6):448-56.
35. Van Zijl F, Krupitza G, Mikulits W. Initial steps of metastasis: Cell invasion and endothelial transmigration. *Mutation Research/Reviews in Mutation Research*. 2011 Jul-Oct; 728(1-2):23-34.
36. Zijlstra A, Mellor R, Panzarella G, et al. A Quantitative Analysis of Rate-Limiting Steps in the Metastatic Cascade Using Human-Specific Real-Time Polymerase Chain Reaction. *Cancer Research*. 2002 Dec; 62(23):7083-92.
37. Plank MJ, Sleeman, BD. Tumor-Induced Angiogenesis: A Review. *Journal of Theoretical Medicine*. 2003 Sep–Dec; 5(3–4):137–153.
38. Koop S, Schmidt EE, MacDonald IC, et al. Independence of metastatic ability and extravasation: metastatic ras-transformed and control fibroblasts extravasate equally well. *Proceedings of the National Academy of Sciences*. 1996 Oct; 93(20):11080-4.
39. Cameron MD, Schmidt EE, Kerkvliet N, et al. Temporal Progression of Metastasis in Lung: Cell Survival, Dormancy, and Location Dependence of Metastatic Inefficiency. *Cancer Research*. 2000 May; 60(9):2541-6.
40. Zheng R, Blobel GA. GATA Transcription Factors and Cancer. *Genes Cancer*. 2010 Dec; 1(12):1178-88.
41. Viger RS, Guittot SM, Anttonen M, et al. Role of the GATA Family of Transcription Factors in Endocrine Development, Function, and Disease. *Molecular Endocrinology*. 2008 Apr; 22(4):781-98.
42. Viger RS, Taniguchi H, Robert NM, et al. Role of the GATA family of transcription factors in andrology. *Journal of Andrology*. 2004 Jul-Aug; 25(4):441-52.
43. Belaguli NS, Zhang M, Rigi M, et al. Cooperation between GATA4 and TGF-beta signaling regulates intestinal epithelial gene expression. *American Journal of Physiology - Gastrointestinal and Liver Physiology*. 2007 Jun; 292(6):G1520-33.
44. Rojas A, Kong SW, Agarwal P, et al. GATA4 Is a Direct Transcriptional Activator of Cyclin D2 and Cdk4 and Is Required for Cardiomyocyte Proliferation in Anterior Heart Field-Derived Myocardium. *Molecular and Cellular Biology*. 2008 Sep; 28(17):5420-31.

- 
45. Bosse T, Piaseckyj CM, Burghard E, et al. Gata4 is essential for the maintenance of jejunal-ileal identities in the adult mouse small intestine. *Molecular and Cellular Biology*. 2006 Dec; 26(23):9060-70.
46. Kyrönlahti A, Rämö M, Tamminen M, et al. GATA-4 regulates Bcl-2 expression in ovarian granulosa cell tumors. *Endocrinology*. 2008 Nov; 149(11):5635-42.
47. He A, Shen X, Ma Q, et al. PRC2 directly methylates GATA4 and represses its transcriptional activity. *Genes & Development*. 2012 Jan; 26(1):37-42.
48. Jones PA, Baylin SB. The epigenomics of cancer. *Cell*. 2007 Feb; 128(4):683-92.
49. Rodenhiser D, Mann M. Epigenetics and Human Disease: Translating Basic Biology into Clinical Applications. *Canadian Medical Association Journal*. 2006 Jan; 174(3):341-8.
50. Jones PA, Baylin SB. The fundamental role of epigenetic events in cancer. *Nature Reviews Genetics*. 2002 Jun; 3(6):415-28.
51. Gal-Yam EN, Saito Y, Egger G, et al. Cancer Epigenetics: Modifications, Screening, and Therapy. *The Annual Review of Medicine*. 2008 Oct; 59:267-80
52. Fraga MF, Ballestar E, Villar-Garea A, et al. Loss of acetylation at Lys16 and trimethylation at Lys20 of histone H4 is a common hallmark of human cancer. *Nature Genetics*. 2005 Apr; 37(4):391-400.
53. Seligson DB, Horvath S, Shi T, et al. Global histone modification patterns predict risk of prostate cancer recurrence. *Nature*. 2005 Jun; 435(7046):1262-6.
54. Esteller M, Herman JG. Cancer as an epigenetic disease: DNA methylation and chromatin alterations in human tumours. *The Journal of Pathology*. 2002 Jan; 196(1):1-7.
55. Littlewood TD, Hancock DC, Danielian PS, et al. A modified oestrogen receptor ligand-binding domain as an improved switch for the regulation of heterologous proteins. *Nucleic Acids Research*. 1995 May; 23(10):1686-90.
56. Sessa L, Breiling A, Lavorgna G, et al. Noncoding RNA synthesis and loss of Polycomb group repression accompanies the colinear activation of the human HOXA cluster. *RNA*. 2007 Feb; 13(2):223-39.
57. Fang R, Olds LC, Santiago NA, et al. GATA family transcription factors activate lactase gene promoter in intestinal Caco-2 cells. *American Journal of Physiology - Gastrointestinal and Liver Physiology*. 2001 Jan; 280(1):G58-67.
58. Wang Y, Yu YA, Shabahang S, et al. Renilla luciferase- Aequorea GFP (Ruc-GFP) fusion protein, a novel dual reporter for real-time imaging of gene expression in cell cultures and in live animals. *Molecular Genetics & Genomics*. 2002 Oct; 268(2):160-8.

- 
59. Zhu Z, Zheng T, Lee CG, et al. Tetracycline-controlled transcriptional regulation systems: advances and application in transgenic animal modeling. *Seminars in Cell & Developmental Biology*. 2002 Apr;13(2):121-8.
60. Weinstein IB. Cancer. Addiction to oncogenes--the Achilles heel of cancer. *Science*. 2002 Jul; 297(5578):63-4.
61. Zhang Y, Goss AM, Cohen ED, et al. A Gata6-Wnt pathway required for epithelial stem cell development and airway regeneration. *Nature Genetics*. 2008 Jul;40(7):862-70.
62. Van der Sluis M, Melis MHM, Jonckheere N, et al. The murine Muc2 mucin gene is transcriptionally regulated by the zinc-finger GATA-4 transcription factor in intestinal cells. *Biochemical and Biophysical Research Communications*. 2004 Dec; 325(3):952-60.
63. Ohara Y, Atarashi T, Ishibashi T, et al. GATA-4 gene organization and analysis of its promoter. *Biological and Pharmaceutical Bulletin*. 2006 Mar; 29(3):410-9.
64. Kent WJ, Sugnet CW, Furey TS, et al. The human genome browser at UCSC. *Genome Research*. 2002 Jun; 12(6):996-1006.
65. Werner T. Computer-assisted analysis of transcription control regions. MatInspector and other programs. *Methods in Molecular Biology*. 1999 Aug; 132:337-49.
66. Song J, Ugai H, Kanazawa I, et al. Independent repression of a GC-rich housekeeping gene by Sp1 and MAZ involves the same cis-elements. *The Journal of Biological Chemistry*. 2001 Jun; 276(23):19897-904.
67. Entschladen F, Drell TL 4th, Lang K, et al. Tumour-cell migration, invasion, and metastasis: navigation by neurotransmitters. *The Lancet Oncology*. 2004 Apr; 5(4):254-8.
68. Plank MJ, Sleeman, BD. Tumour-induced angiogenesis: a review. *Journal of Theoretical Medicine*. 2003 Sep-Dec; 5(3-4):137-153.
69. Takahashi K, Yamanaka S. Induction of pluripotent stem cells from mouse embryonic and adult fibroblast cultures by defined factors. *Cell*. 2006 Aug; 126(4):663-76.
70. Zhang J, Li L. BMP signaling and stem cell regulation. *Developmental Biology*. 2005 Aug; 284(1):1-11.
71. DeLaForest A, Nagaoka M, Si-Tayeb K, et al. HNF4A is essential for specification of hepatic progenitors from human pluripotent stem cells. *Development*. 2011 Oct; 138(19):4143-53.
72. Herszfeld D, Wolvetang E, Langton-Bunker E, et al. CD30 is a survival factor and a biomarker for transformed human pluripotent stem cells. *Nature Biotechnology*. 2006 Mar; 24(3):351-7.

- 
73. Ho JS, Ma W, Mao DY, et al. p53-Dependent transcriptional repression of c-myc is required for G1 cell cycle arrest. *Molecular and Cellular Biology*. 2005 Sep; 25(17):7423-31.
74. Nakamura T, Nakagawa M, Ichisaka T, et al. Essential roles of ECAT15-2/Dppa2 in functional lung development. *Molecular and Cellular Biology*. 2011 Nov; 31(21):4366-78.
75. Tremblay JJ, Viger RS. Transcription factor GATA-4 is activated by phosphorylation of serine 261 via the cAMP/protein kinase a signaling pathway in gonadal cells. *The Journal of Biological Chemistry*. 2003 Jun; 278(24):22128-35.
76. Mori S, Chang JT, Andrechek ER, et al. Anchorage-independent cell growth signature identifies tumors with metastatic potential. *Oncogene*. 2009 Aug; 28(31):2796-805.
77. Anttonen M, Unkila-Kallio L, Leminen A, et al. High GATA-4 expression associates with aggressive behavior, whereas low anti-Müllerian hormone expression associates with growth potential of ovarian granulosa cell tumors. *The Journal of Clinical Endocrinology & Metabolism*. 2005 Dec; 90(12):6529-35.
78. Walhout AJ, Gubbels JM, Bernards R, et al. c-Myc/Max heterodimers bind cooperatively to the E-box sequences located in the first intron of the rat ornithine decarboxylase (ODC) gene. *Nucleic Acids Research*. 1997 Apr; 25(8):1493-501.
79. Zeller KI, Zhao X, Lee CW, et al. Global mapping of c-Myc binding sites and target gene networks in human B cells. *Proceedings of the National Academy of Sciences*. 2006 Nov; 103(47):17834-9.
80. Mazaud Guittot S, Tétu A, Legault E, et al. The proximal Gata4 promoter directs reporter gene expression to sertoli cells during mouse gonadal development. *Biology of Reproduction*. 2007 Jan; 76(1):85-95.
81. Boulende Sab A, Bouchard MF, Béland M, et al. An ebox element in the proximal gata4 promoter is required for gata4 expression in vivo. *PLoS ONE*. 2011;6(12):e29038.
82. Lyabin DN, Eliseeva IA, Skabkina OV, et al. Interplay between Y-box-binding protein 1 (YB-1) and poly(A) binding protein (PABP) in specific regulation of YB-1 mRNA translation. *RNA Biology*. 2011 Sep-Oct; 8(5):883-92.
83. Wu Y, Yamada S, Izumi H, et al. Strong YB-1 expression is associated with liver metastasis progression and predicts shorter disease-free survival in advanced gastric cancer. *Journal of Surgical Oncology*. 2012 Jun; 105(7):724-30.
84. Feinberg AP, Vogelstein B. Hypomethylation distinguishes genes of some human cancers from their normal counterparts. *Nature*. 1983 Jan; 301(5895):89-92.
85. James G, Herman ME. Detection of Aberrant Promoter Hypermethylation of Tumor Suppressor Genes in Serum DNA from Non-Small Cell Lung Cancer Patient. *Cancer Research*. 1999 Jan; 59(1):67-70.

- 
86. Guo M, Akiyama Y, House MG, et al. Hypermethylation of the GATA genes in lung cancer. *Clinical Cancer Research*. 2004 Dec; 10(23):7917-24.
87. Montavon C, Gloss BS, Warton K, et al. Prognostic and diagnostic significance of DNA methylation patterns in high grade serous ovarian cancer. *Gynecologic Oncology*. 2012 Mar; 124(3):582-8.
88. Esteller M. Cancer epigenomics: DNA methylomes and histone-modification maps. *Nature Reviews Genetics*. 2007 Apr; 8(4):286-98.
89. Wang Y, Fischle W, Cheung W, et al. Beyond the double helix: writing and reading the histone code. *Novartis Foundation Symposia*. 2004; 259:3-17; discussion 17-21, 163-9.
90. Dahl JA, Reiner AH, Klungland A, et al. Histone H3 lysine 27 methylation asymmetry on developmentally-regulated promoters distinguish the first two lineages in mouse preimplantation embryos. *PLoS ONE*. 2010 Feb; 5(2):e9150.
91. Zhang Y, Reinberg D. Transcription regulation by histone methylation: interplay between different covalent modifications of the core histone tails. *Genes & Development*. 2001 Sep; 15(18):2343-60.
92. Cao R, Wang L, Wang H, et al. Role of histone H3 lysine 27 methylation in Polycomb-group silencing. *Science*. 2002 Nov; 298(5595):1039-43.
93. Kuzmichev A, Nishioka K, Erdjument-Bromage H, et al. Histone methyltransferase activity associated with a human multiprotein complex containing the Enhancer of Zeste protein. *Genes & Development*. 2002 Nov; 16(22):2893-905.
94. Takaya T, Kawamura T, Morimoto T, et al. Identification of p300-targeted acetylated residues in GATA4 during hypertrophic responses in cardiac myocytes. *The Journal of Biological Chemistry*. 2008 Apr; 283(15):9828-35.
95. Ptashne M. Regulation of transcription: from lambda to eukaryotes. *Trends in Biochemical Sciences*. 2005 Jun; 30(6):275-9.
96. Chen Y, Jørgensen M, Kolde R, et al. Prediction of RNA Polymerase II recruitment, elongation and stalling from histone modification data. *BMC Genomics*. 2011 Nov; 12:544.
97. Struhl K. Histone acetylation and transcriptional regulatory mechanisms. *Genes & Development*. 1998 Mar; 12(5):599-606.
98. Park YJ, Claus R, Weichenhan D, et al. Genome-wide epigenetic modifications in cancer. *Progress in Drug Research*. 2011 Dec; 67:25-49.
99. Rhodes DR, Chinnaiyan AM. Integrative analysis of the cancer transcriptome. *Nature Genetics*. 2005 Jun; 37 Suppl:S31-7.

- 
100. Papp B, Plath K. Reprogramming to pluripotency: stepwise resetting of the epigenetic landscape. *Cell Research*. 2011 Mar; 21(3):486-501.
101. Costello JF, Frühwald MC, Smiraglia DJ, et al. Aberrant CpG-island methylation has non-random and tumour-type-specific patterns. *Nature Genetics*. 2000 Feb; 24(2):132-8.
102. Otterson GA, Khleif SN, Chen W, et al. CDKN2 gene silencing in lung cancer by DNA hypermethylation and kinetics of p16INK4 protein induction by 5-aza 2'deoxyctidine. *Oncogene*. 1995 Sep; 11(6):1211-6.
103. Santanam U, Zanesi N, Efanov A, et al. Chronic lymphocytic leukemia modeled in mouse by targeted miR-29 expression. *Proceedings of the National Academy of Sciences*. 2010 Jul; 107(27):12210-5.
104. Desmond JC, Raynaud S, Tung E, et al. Discovery of epigenetically silenced genes in acute myeloid leukemias. *Leukemia*. 2007 May; 21(5):1026-34.
105. Benayoun BA, Kalfa N, Sultan C, et al. The forkhead factor FOXL2: a novel tumor suppressor?. *Biochimica et Biophysica Acta*. 2010 Jan; 1805(1):1-5.
106. Jin H, Wang X, Ying J, et al. Epigenetic identification of ADAMTS18 as a novel 16q23.1 tumor suppressor frequently silenced in esophageal, nasopharyngeal and multiple other carcinomas. *Oncogene*. 2007 Nov; 26(53):7490-8.
107. Li Z, Zhang W, Shao Y, et al. High-resolution melting analysis of ADAMTS18 methylation levels in gastric, colorectal and pancreatic cancers. *Medical Oncology*. 2010 Sep; 27(3):998-1004.
108. Yoshimizu T, Miroglio A, Ripoche MA, et al. The H19 locus acts in vivo as a tumor suppressor. *Proceedings of the National Academy of Sciences*. 2008 Aug; 105(34):12417-22.
109. Yamashita S, Tsujino Y, Moriguchi K, et al. Chemical genomic screening for methylation-silenced genes in gastric cancer cell lines using 5-aza-2'-deoxycytidine treatment and oligonucleotide microarray. *Cancer Science*. 2006 Jan; 97(1):64-71.
110. Lorkova L, Pospisilova J, Lacheta J, et al. Decreased concentrations of retinol-binding protein 4 in sera of epithelial ovarian cancer patients: a potential biomarker identified by proteomics. *Oncology Reports*. 2012 Feb; 27(2):318-24.
111. Tsunoda S, Smith E, De Young NJ, et al. Methylation of CLDN6, FBN2, RBP1, RBP4, TFPI2, and TMEFF2 in esophageal squamous cell carcinoma. *Oncology Reports*. 2009 Apr; 21(4):1067-73.
112. Dallosso AR, Hancock AL, Szemes M, et al. Frequent long-range epigenetic silencing of protocadherin gene clusters on chromosome 5q31 in Wilms' tumor. *PLOS Genetics*. 2009 Nov; 5(11):e1000745.



- 
113. De Tayrac M, Etcheverry A, Aubry M, et al. Integrative genome-wide analysis reveals a robust genomic glioblastoma signature associated with copy number driving changes in gene expression. *Genes, Chromosomes and Cancer*. 2009 Jan; 48(1):55-68.
114. Fu DY, Wang ZM, Wang BL, et al. Frequent epigenetic inactivation of the receptor tyrosine kinase EphA5 by promoter methylation in human breast cancer. *Human Pathology*. 2010 Jan; 41(1):48-58.
115. Kober P, Bujko M, Olędzki J, et al. Methyl-CpG binding column-based identification of nine genes hypermethylated in colorectal cancer. *Molecular Carcinogenesis*. 2011 Nov; 50(11):846-56.
116. Almog N, Ma L, Raychowdhury R, et al. Transcriptional switch of dormant tumors to fast-growing angiogenic phenotype. *Cancer Research*. 2009 Feb; 69(3):836-44.
117. Kim WY, Kim MJ, Moon H, et al. Differential impacts of insulin-like growth factor-binding protein-3 (IGFBP-3) in epithelial IGF-induced lung cancer development. *Endocrinology*. 2011 Jun; 152(6):2164-73.
118. Mehta HH, Gao Q, Galet C, et al. IGFBP-3 is a metastasis suppression gene in prostate cancer. *Cancer Research*. 2011 Aug; 71(15):5154-63.
119. Oh SH, Lee OH, Schroeder CP, et al. Antimetastatic activity of insulin-like growth factor binding protein-3 in lung cancer is mediated by insulin-like growth factor-independent urokinase-type plasminogen activator inhibition. *Molecular Cancer Therapeutics*. 2006 Nov; 5(11):2685-95.
120. Gribben L, Baxter RC, Marsh DJ. Insulin-like growth factor binding protein-3 inhibits migration of endometrial cancer cells. *Cancer Letters*. 2012 Apr; 317(1):41-8.
121. Zhao L, He LR, Zhang R, et al. Low expression of IGFBP-3 predicts poor prognosis in patients with esophageal squamous cell carcinoma. *Medical Oncology*. 2012 Dec; 29(4):2669-76.
122. Gonzalez-Gomez P, Bello MJ, Lomas J, et al. Aberrant methylation of multiple genes in neuroblastic tumours. relationship with MYCN amplification and allelic status at 1p. *European Journal of Cancer*. 2003 Jul; 39(10):1478-85.
123. Tang X, Khuri FR, Lee JJ, et al. Hypermethylation of the death-associated protein (DAP) kinase promoter and aggressiveness in stage I non-small-cell lung cancer. *Journal of the National Cancer Institute*. 2000 Sep; 92(18):1511-6.
124. Christoph F, Hinz S, Kempkensteffen C, et al. mRNA expression profiles of methylated APAF-1 and DAPK-1 tumor suppressor genes uncover clear cell renal cell carcinomas with aggressive phenotype. *Journal of Urology*. 2007 Dec; 178(6):2655-9.

- 
125. Supic G, Kozomara R, Jovic N, et al. Prognostic significance of tumor-related genes hypermethylation detected in cancer-free surgical margins of oral squamous cell carcinomas. *Oral Oncology*. 2011 Aug; 47(8):702-8.
126. Hussain M, Rao M, Humphries AE, et al. Tobacco smoke induces polycomb-mediated repression of Dickkopf-1 in lung cancer cells. *Cancer Research*. 2009 Apr; 69(8):3570-8.
127. Vibhakar R, Foltz G, Yoon J-G, et al. Dickkopf-1 is an epigenetically silenced candidate tumor suppressor gene in medulloblastoma. *Neuro-oncology*. 2007 Apr; 9(2):135-44.
128. Mikheev AM, Mikheeva SA, Maxwell JP, et al. Dickkopf-1 mediated tumor suppression in human breast carcinoma cells. *Breast Cancer Research and Treatment*. 2008 Nov; 112(2):263-73.
129. Hirata H, Hinoda Y, Nakajima K, et al. Wnt antagonist DKK1 acts as a tumor suppressor gene that induces apoptosis and inhibits proliferation in human renal cell carcinoma. *International Journal of Cancer*. 2011 Apr; 128(8):1793-803.
130. Valencia A, Román-Gómez J, Cervera J, et al. Wnt signaling pathway is epigenetically regulated by methylation of Wnt antagonists in acute myeloid leukemia. *Leukemia*. 2009 Sep; 23(9):1658-66.
131. Selamat SA, Galler JS, Joshi AD, et al. DNA methylation changes in atypical adenomatous hyperplasia, adenocarcinoma in situ, and lung adenocarcinoma. *PLoS ONE*. 2011 Jun; 6(6):e21443.
132. Huang J, Zhang YL, Teng XM, et al. Down-regulation of SFRP1 as a putative tumor suppressor gene can contribute to human hepatocellular carcinoma. *BMC Cancer*. 2007 Jul; 7:126.
133. Meng Y, Wang QG, Wang JX, et al. Epigenetic inactivation of the SFRP1 gene in esophageal squamous cell carcinoma. *Digestive Diseases and Sciences*. 2011 Nov; 56(11):3195-203.
134. Starker LF, Svedlund J, Udelsman R, et al. The DNA methylome of benign and malignant parathyroid tumors. *Genes, Chromosomes and Cancer*. 2011 Sep; 50(9):735-45.
135. Caldwell GM, Jones C, Gensberg K, et al. The Wnt antagonist sFRP1 in colorectal tumorigenesis. *Cancer Research*. 2004 Feb; 64(3):883-8.
136. Fukui T, Kondo M, Ito G, et al. Transcriptional silencing of secreted frizzled related protein 1 (SFRP 1) by promoter hypermethylation in non-small-cell lung cancer. *Oncogene*. 2005 Sep; 24(41):6323-7.
137. Yu H, Rohan T. Role of the insulin-like growth factor family in cancer development and progression. *Journal of the National Cancer Institute*. 2000 Sep; 92(18):1472-89.

- 
138. Paharkova-Vatchkova V, Lee KW. Nuclear export and mitochondrial and endoplasmic reticulum localization of IGF-binding protein 3 regulate its apoptotic properties. *Endocrine Related Cancer*. 2010 Mar; 17(2):293-302.
139. Nickerson T, Huynh H, Pollak M. Insulin-like growth factor binding protein-3 induces apoptosis in MCF7 breast cancer cells. *Biochemical and Biophysical Research Communications*. 1997 Aug; 237(3):690-3.
140. Schwarze SR, DePrimo SE, Grabert LM, et al. Novel pathways associated with bypassing cellular senescence in human prostate epithelial cells. *Journal of Biological Chemistry*. 2002 Apr; 277(17):14877-83.
141. Massoner P, Colleselli D, Matscheski A, et al. Novel mechanism of IGF-binding protein-3 action on prostate cancer cells: inhibition of proliferation, adhesion, and motility. *Endocrine Related Cancer*. 2009 Sep; 16(3):795-808.
142. Kinch MS, Moore MB, Harpole DH Jr. Predictive value of the EphA2 receptor tyrosine kinase in lung cancer recurrence and survival. *Clinical Cancer Research*. 2003 Feb; 9(2):613-8.
143. Katoh M, Katoh M. Comparative integromics on Eph family. *International Journal of Oncology*. 2006 May; 28(5):1243-7.
144. Nguyen DX, Chiang AC, Zhang XH, et al. WNT/TCF signaling through LEF1 and HOXB9 mediates lung adenocarcinoma metastasis. *Cell*. 2009 Jul; 138(1):51-62.
145. You Z, Saims D, Chen S, et al. Wnt signaling promotes oncogenic transformation by inhibiting c-Myc-induced apoptosis. *The Journal of Cell Biology*. 2002 Apr; 157(3):429-40.
146. Sanchez-Cespedes M, Esteller M, Wu L, et al. Gene promoter hypermethylation in tumors and serum of head and neck cancer patients. *Cancer Research*. 2000 Feb; 60(4):892-5.
147. Fischer JR, Ohnmacht U, Rieger N, et al. Promoter methylation of RASSF1A, RARBeta and DAPK predict poor prognosis of patients with malignant mesothelioma. *Lung Cancer*. 2006 Oct; 54(1):109-16.
148. Shaw RJ, Hall GL, Woolgar JA, et al. Quantitative methylation analysis of resection margins and lymph nodes in oral squamous cell carcinoma. *British Journal of Oral and Maxillofacial Surgery*. 2007 Dec; 45(8):617-22.
149. Zhang YW, Miao YF, Yi J, et al. Transcriptional inactivation of secreted frizzled-related protein 1 by promoter hypermethylation as a potential biomarker for non-small cell lung cancer. *Neoplasma*. 2010; 57(3):228-33.
150. Licchesi JD, Van Neste L, Tiwari VK, et al. Transcriptional regulation of Wnt inhibitory factor-1 by Miz-1/c-Myc. *Oncogene*. 2010 Nov; 29(44):5923-34

- 
151. Cowling VH, D’Cruz CM, Chodosh LA, et al. c-Myc transforms human mammary epithelial cells through repression of the Wnt inhibitors DKK1 and SFRP1. *Molecular and Cellular Biology*. 2007 Jul; 27(14):5135-46.
152. Zhao Y, Liu H, Riker AI, et al. Emerging metabolic targets in cancer therapy. *Frontiers in Bioscience*. 2011 Jan; 16:1844-60.
153. Archer MC. Role of sp transcription factors in the regulation of cancer cell metabolism. *Genes & Cancer*. 2011 Jul; 2(7):712-9.
154. Warburg O, Posener K, Negelein E. On the metabolism of carcinoma cells. *Biochem Z*. 1924; 152:309–44.
155. Noch E, Khalili K. Oncogenic viruses and tumor glucose metabolism: like kids in a candy store. *Molecular Cancer Therapeutics*. 2012 Jan; 11(1):14-23.
156. Sathyanarayana UG, Padar A, Suzuki M, et al. Aberrant promoter methylation of laminin-5-encoding genes in prostate cancers and its relationship to clinicopathological features. *Clinical Cancer Research*. 2003 Dec; 9(17):6395-400.
157. Kallunki P, Sainio K, Eddy R, et al. A truncated laminin chain homologous to the B2 chain: structure, spatial expression, and chromosomal assignment. *The Journal of Cell Biology*. 1992 Nov; 119(3):679-93.
158. Hunt G. The role of laminin in cancer invasion and metastasis. *Experimental Cell Biology*. 1989; 57(3):165-76.
159. Määttä M, Soini Y, Pääkkö P, et al. Expression of the laminin gamma2 chain in different histological types of lung carcinoma. A study by immunohistochemistry and in situ hybridization. *The Journal of Pathology*. 1999 Aug ;188(4):361-8.
160. Ii M, Yamamoto H, Taniguchi H, et al. Co-expression of laminin  $\beta$ 3 and  $\gamma$ 2 chains and epigenetic inactivation of laminin  $\alpha$ 3 chain in gastric cancer. *International Journal of Oncology*. 2011 Sep; 39(3):593-9.
161. Smith SC, Nicholson B, Nitz M, et al. Profiling bladder cancer organ site-specific metastasis identifies LAMC2 as a novel biomarker of hematogenous dissemination. *American Journal of Pathology*. 2009 Feb; 174(2):371-9.
162. Karafin MS, Cummings CT, Fu B, et al. The developmental transcription factor Gata4 is overexpressed in pancreatic ductal adenocarcinoma. *International Journal of Clinical and Experimental Pathology*. 2010 Jan; 3(1): 47–55.
163. Fu B, Guo M, Wang S, et al. Evaluation of GATA-4 and GATA-5 methylation profiles in human pancreatic cancers indicate promoter methylation patterns distinct from other human tumor types. *Cancer Biology and Therapy*. 2007 Oct; 6(10):1546-52.

- 
164. Egles C, Huet HA, Dogan F, et al. Integrin-blocking antibodies delay keratinocyte re-epithelialization in a human three-dimensional wound healing model. *PLoS ONE*. 2010 May; 5(5):e10528.
165. Indra I, Undyala V, Kadow C, et al. An in vitro correlation of mechanical forces and metastatic capacity. *Physical Biology*. 2011 Feb; 8(1):015015.
166. An Z, Gluck CB, Choy ML, et al. Suberoylanilide hydroxamic acid limits migration and invasion of glioma cells in two and three dimensional culture. *Cancer Letters*. 2010 Jun; 292(2):215-27.
167. Zetter BR. Angiogenesis and tumor metastasis. *Annual Review of Medicine*. 1998 Feb; 49:407-24.
168. Rosen LS. Clinical experience with angiogenesis signaling inhibitors: focus on vascular endothelial growth factor (VEGF) blockers. *Cancer Control*. 2002 Mar-Apr; 9(2 Suppl):36-44.
169. Sutherland RM. Cell and environment interactions in tumor microregions: the multicell spheroid model. *Science*. 1988 Apr; 240(4849):177-84.
170. Tsuzuki Y, Fukumura D, Oosthuyse B, et al. Vascular endothelial growth factor (VEGF) modulation by targeting hypoxia-inducible factor-1alpha--> hypoxia response element--> VEGF cascade differentially regulates vascular response and growth rate in tumors. *Cancer Research*. 2000 Nov; 60(22):6248-52.
171. Royds JA, Dower SK, Qwarnstrom EE, et al. Response of tumour cells to hypoxia: role of p53 and NFkB. *Molecular Pathology*. 1998 Apr; 51(2):55-61.
172. Bremnes RM, Dønnem T, Al-Saad S, et al. The role of tumor stroma in cancer progression and prognosis: emphasis on carcinoma-associated fibroblasts and non-small cell lung cancer. *Journal of Thoracic Oncology*. 2011 Jan; 6(1):209-17.
173. Bikfalvi A. Significance of angiogenesis in tumour progression and metastasis. *European Journal of Cancer*. 1995 Jul-Aug; 31A(7-8):1101-4.
174. Pepper MS, Vassalli JD, Orci L, et al. Proteolytic balance and capillary morphogenesis in vitro. *EXS*. 1992; 61:137-45.
175. Fromigué O, Louis K, Dayem M, et al. Gene expression profiling of normal human pulmonary fibroblasts following coculture with non-small-cell lung cancer cells reveals alterations related to matrix degradation, angiogenesis, cell growth and survival. *Oncogene*. 2003 Nov; 22(52):8487-97.

## 7. Appendix

### 7.1. List of abbreviations

APEC – Alveolar Papillary Columnar Epithelial cells

BASCs – Bronchioalveolar stem cells

cDNA – complementary DNA

ChIP – Chromatin immunoprecipitation

CIAP – Calf Intestinal Alkaline Phosphatase

chk-MYC – Chicken v-MYC

cm – centimeter

DAB – 3,3'-Diaminobenzidine

DMSO – Dimethyl sulfoxide

DNA – Deoxyribonucleic acid

DNMTs – DNA methyltransferase

dNTP – Deoxynucleotide Triphosphates

DOX – Doxycycline

E. coli – Escherichia coli

ECM – Extracellular matrix

EGFP – Enhanced Green Fluorescent Protein

GFP – Green Fluorescent Protein

GG – Gallus gallus

g – gram

h – hour

HDACs – Histone deacetylase

HE – Hematoxylin and Eosin

hs – *Homo sapiens*

i.p. – intraperitoneal

kg – kilogram

kV – kilovolt

LB – Luria Bertani

min – minute

ml – milliliter

mM – millimolar

ms – millisecond

MTT – 3-(4,5-Dimethylthiazol-2-yl)-2,5-diphenyltetrazolium bromide

ng – nanogram

nm – nanometer

ns – nanosecond

NSCLC – Non-Small-Cell Lung Cancer

OD – Optical Density

OHT – 4-hydroxy-tamoxifen

P.A. – pro analysis

PBS – Phosphate buffered saline

PcG – Polycomb group complexes

PCR – Polymerase chain reaction

PFA – Paraformaldehyde

pM – picomolar

POL II – RNA-polymerase II

PRC – Polycomb-repressive complex

RNA – Ribonucleic acid

rpm – Revolutions Per Minute

SD – Standard Deviation

sec – second

TSA – Trichostatin A

UV – Ultraviolet

w – week

V – volt

$\mu$ F – microfarad

$\mu$ g – microgram

$\mu$ l – microliter



## Curriculum Vitae

### Personal Information

---

Name: Inês Sofia Cardoso e Castro  
Date and place of birthday: 24<sup>th</sup> of April 1982 in Paredes, Portugal  
Nationality: Portuguese

### PhD Thesis

---

since 09/2008 PhD-thesis at the Institut für Medizinische Strahlenkunde und Zellforschung (first year) and later at the Department of Microbiology, University of Würzburg (Titel: “Epigenetic switch induced by MYC in Non-Small-Cell Lung Cancer”)

### Professions

---

05/2007 – 08/2008 Quality, health and safety manager at STB, Lda, Vila do Conde, Portugal (Sector: Civil Engineering)  
06/2006 – 02/2007 Quality manager at Maia Ferreira, Lda, Paços de Ferreira, Portugal (Sector: Furniture Industry)

### Education

---

09/2001 - 11/2005 Diploma in Biology at the University of Minho, Braga, Portugal  
03/2005 – 07/2005 Diploma thesis at the Department of Food Microbiology at The Royal Veterinary and Agricultural University, Copenhagen, Denmark under the supervision of Prof. Dr. Mogens Jakobsen (Title: “Binding of Probiotic *Lactobacillus* strains and pathogens (*Escherichia coli*) to the porcine intestinal epithelium: Investigation of a competitive interaction “)  
09/1994 – 07/2000 High School of Paredes, Portugal

### Publications

---

“**Myc is a Metastasis Gene for Non-Small-Cell Lung Cancer.**” Ulf R. Rapp, Christian Korn, Fatih Ceteci, Christiaan Karreman, Katharina Luetkenhaus, Valentina Serafin, Emanuele Zanucco, Inês Castro and Tamara Potapenko. *PLoS ONE*, June 2009.

“**MYC-induced epigenetic activation of GATA4 in lung adenocarcinoma.**” Inês C. Castro, Achim Breiling, Katharina Luetkenhaus, Fatih Ceteci, Simone Hausmann, Sebastian Kress, Frank Lyko, Thomas Rudel, Ulf R. Rapp. Accepted for publication in *Molecular Cancer Research*, on 04/12/2012.